PROCESSABILITY AND INSTABILITIES OF POLYOLEFIN-ORGANOCLAY NANOCOMPOSITES IN A SINGLE SCREW EXTRUDER

BY

AYUBA ADEGOKE ADESINA

A Dissertation Presented to the

DEANSHIP OF GRADUATE STUDIES

KING FAHD UNIVERSITY OF PETROLEUM & MINERALS

DHAHRAN, SAUDI ARABIA

In Partial Fulfillment of the
Requirements for the Degree of

DOCTOR OF PHILOSOPHY

In

CHEMICAL ENGINEERING

MAY 2011

KING FAHD UNIVERSITY OF PETROLEUM & MINERALS
DHAHRAN 31261, SAUDI ARABIA

DEANSHIP OF GRADUATES STUDIES

This dissertation, written by **AYUBA ADEGOKE ADESINA** under the direction of his dissertation advisor and approved by his dissertation committee, has been presented to and accepted by the Dean of Graduate Studies, in partial fulfillment of the requirements for the degree of **DOCTOR OF PHILOSOPHY IN CHEMICAL ENGINEERING.**

Dissertation Committee

Prof. Ibnelwaleed A. Hussein
(Dissertation Advisor)

Prof. Nouar Tabet
(Member)

Dr. Usamah A. Al-Mubaiyedh
(Member)

Dr. Usamah A. Al-Mubaiyedh
(Department Chairman)

Dr. Abdulhadi A. Al-Juhani
(Member)

Dr. Salam A. Zummo
(Dean of Graduate Studies)

Prof. Jose A. Covas
(Member)

11/9/11
Date

DEDICATION

This work is dedicated to my dearest Mum- Saalimah Bello who died on Sunday, 2nd Jumada Thanni 1431 AH (16th May 2010)

I pray to Allah to forgive her and admit her in Jannat Firdaus.

We all love you Mum.

ACKNOWLEDGEMENTS

In the name of Allah, the most Beneficent, the most Merciful.

All praises be to Allah, and the peace and blessings of Allah be upon his prophet, Muhammad (S.A.W).

I thank King Fahd University of Petroleum & Minerals (KFUPM) for the opportunity given to me to come for PhD program through the Lecturer-B scheme. I am grateful to King Abdul Aziz City for Science and Technology (KACST) for providing financial support for this research under research Grant # AT-27-107.

With heartfelt appreciation, I express my sincere thanks to my thesis advisor, Dr. Ibnelwaleed A. Hussein for his consistent mentorship, guidance, support and cooperation towards completion of this research. You are indeed more than academic supervisor to me. I am very grateful to all my thesis committee members: Professor Noah Thabit, Dr. Abdulhadi A. Al-Juhani, Dr. Usamah A. Al-Mubaiyedh, and Professor Jose A. Covas. I gained immensely from my interaction with you all. Notably, my 2-time visit to the laboratory of Professor Jose A. Covas in Portugal made a turning point in my research work. It left an everlasting positive impact in my life. The advanced numerical methods thought by Dr Al-Mubaiyedh helped me in all my simulation problems in this work. Your efforts during that time were indeed very rewarding. I also thank you as the Chairman of the Chemical Engineering Department for your entire supportive role towards me. My first teacher in Polymer Science and Engineering was my respected Dr Al-Juhani. Thank you for introducing mto the world of Polymer. I never regretted you introduced me to it. I will not forget my contact with Professor Nouar Tabet. His in-depth understanding of

surface science assisted a lot in analyzing the XRD results from his laboratory. I am indeed very grateful for making his laboratory available for me at all time.

Special thanks are due to Professor Wilhelm and his group in Germany especially Dr. Ingo F. C. Naue for his visit to our laboratory in KFUPM. I gained a lot from him. I also thank Dr. Loic Hilloiu, Pedro Marquis and Paulo Texeira of University of Minho Portugal for your efforts during the velocimetry measurement in your lab. I agree you are all smart and dedicated to excellence.

I am grateful to Dr Anwar Ul-Hamid of the Research Institute at KFUPM for his tremendous assistance towards SEM testing. I am grateful to Mr Saeed of Physics Department for his efforts in analyzing my XRD results. My special thanks are to Mr. Mofiz-ul-Islam for his selfless assistance in many aspects in rheology and polymer lab. Mr Awwal Suleiman can't be forgotten for his brotherly and moral support. Thank you for being there for me at all time.

My appreciation is also extended to Saudi Arabia Basic Industries Corporation (SABIC) for providing polymer samples for this work. Dyneon also supplied the fluoropolymer at no cost. Thank you for this.

I am also thankful to the entire faculty and staff members of the Department of Chemical Engineering, KFUPM especially Mr. Taher H. Al-Helaili (a.k.a Abu Maaher), Abdullah Al-Khalaf, Thaniyullah Shaji and Comedia Jefrey for their cooperation and support.

I will not forget to thank my caring and enduring dad, mother in law and father in law for their constant prayer for me. I pray to Allah to preserve your lives to enjoy the fruit of your progenies. I also offer my sincere thanks to my siblings and all other members of the family for their encouragements.

Finally, my deepest appreciation goes to my loving, caring, enduring darling. You are wonderful. Thank you for being there for me always. Also, I thank my children for their patience throughout my PhD program. I love you all. You are the joy of my life.

TABLE OF CONTENTS

LIST OF FIGURES

LIST OF TABLES

THESIS ABSTRACT (ENGLISH)

Name: ADESINA, AYUBA ADEGOKE

Title: PROCESSABILITY AND INSTABILITIES OF POLYOLEFIN-ORGANOCLAY NANOCOMPOSITES IN A SINGLE SCREW EXTRUDER

Major Field: CHEMICAL ENGINEERING.

Date of degree: MAY, 2011

The impact of organoclay on the rheology and extrusion of polyethylenes was studied. Organoclay effect was studied at very low clay loading (≤ 0.1 wt %) while serving as a processing aid. The polyethylenes used in this work were high density polyethylene (HDPE) and linear low density polyethylenes of different branch content. A special design single screw extruder was used in the study of the extrusion melt instabilities. The slit die attached to the extruder has three highly sensitive piezoelectric transducers mounted along its length. Particle Image Velocimetry (PIV) was used in the study to measure wall slip during extrusion of polyethylene while organoclay served as a processing aid. The morphological characterization with X-ray diffractometer (XRD) and Scanning Electron Microscopy (SEM) showed that good dispersion was obtained with master batch-dilution method of polyolefin-organoclay nanocomposites. The rheological results showed that shear-rate dependent viscosity, normal stress difference, extensional strain and stress growth of HDPE were reduced with the addition of organoclay. So, organoclay (≤ 0.1 wt %) has an effect on the shear and extensional rheology of HDPE. The reduction is more pronounced in linear polyethylene. Such effects gradually decrease as the branch content increases. The trend is independent of the type of flow (shear and extensional). It is striking to note that FT-rheology is not effective in explaining the impact of organoclay on polyethylene. The intensity of the melt instability was characterized with both a moment analyses and a distortion factor (DF) from an advanced Fourier transform analysis. Both showed the same trends in the characterization of the pressure fluctuations in the die. Generally, addition of organoclay (≤ 0.1 wt %) to HDPE led to the reduction in DF. The ratio of first and

second moment analyses became reduced as well. The results quantified the extent of elimination of gross melt fracture in HDPE by organoclay. Also, the extrusion pressure was reduced with organoclay (≤ 0.1 wt %) inclusion hence more throughput. There was a good correlation between rheology and extrusion. However, the maleated polyethylene added as a compatibilizer did not give substantial synergistic effect. To further understand the mechanism involved during polyethylene-organoclay extrusion, the effect of organoclay on the wall slip of high density polyethylene (HDPE) was investigated with the aid of particle image velocimetry (PIV). The study showed that organoclay did not cause wall slip during low shear testing in a parallel plate rheometer. PIV measurements during continuous extrusion of HDPE showed that organoclay induced more wall slip. So, it was suggested based on these results that in the presence of high shear flow, organoclay aligned in the flow direction and migrated towards the die wall. The alignment and migration affect the bulk properties (like shear thinning) and surface properties (like wall slip) of HDPE. Such effects contributed to the reduction in the extrusion pressure of HDPE and possibly elimination/postponement of melt instabilities in HDPE during continuous extrusion. Furthermore, the rheological tests on the HDPE containing organoclay, boron nitride and fluoropolymer showed that the phase angle of HDPE during frequency sweep reduced below the cross over frequency. All the processing aids eliminated the weak sharkskin-like instability. However, the fluoropolymer did not succeed in eliminating the stick-slip fracture. The gross melt fracture in HDPE was not eliminated by boron nitride and organoclay at apparent shear rate of 114 s^{-1}. The combined organoclay and fluoropolymer did not as well. However, both moment and distortion factor analyzes were able to quantify the visual trends in the extrudates. The quantifying tools indicated that combined organoclay and fluoropolymer as processing aids acted better in the reduction of the pressure fluctuation compared to when both were used individually.

DOCTOR OF PHILOSOPHY
KING FAHD UNIVERSITY OF PETROLEUM & MINERALS
DHAHRAN, SAUDI ARABIA.

THESIS ABSTRACT (ARABIC)

الإســـــــــــم: **أيوب أدى جوك أديسينا**

عنوان الرسالة: **تقليل تقلبات البثق في مركبات البولي أولفين بإستخدام الصلصال متناهي الصغر**

تاريخ التخرج: **مايو 2011م**

تم في هذا البحـــث دراسة تأثير إستخدام الصلصال متناهي الصغـــر في تسهيـــل عملية البثـــق للبولي أوليفينات وذلـــك بإستخدام كميات قليلة من الصلصال لا تتجاوز الـــ 1000 جزء في المليون وتم إستخدام طرق الريولوجيا، الأشعة الســـينية ومجهـــر المسح الإلكتروني وعدة طرق لبثق البولمرات بإستخدام البثـــق المتصل، أما بالنسبة لطـــرق تحليل المعلـــومات فتم إستخـــدام طـــرق الـــ Fourier Transform المتقدمة وقد خلصت الدراسة إلى أن استخدام 500–1000 جزء من المليون مـــن الصلصـــال يؤجل ظهور هذه التقلبات وينتج عنه بولمر ذا سطح أملس ويؤدي لزيادة إنتاج البولمر دون ظهور خشونة على سطحه. كذلك فـــإن الضغط عند البثق يقل عند إستخدام الصلصال كما أن التضخم في حجم البومر المنتج يقل كذلك. أستخدمت في هذه الدراسة طرق مختلفة من تحاليل الريولوجي وقد تطابقت جميعها في دعم النتائج أعلاه. كذلك تم إستخدام البولمر الذي يحتـــوي علـــى الفلـــور مـــع الصلصال معاً ووجد أنها تعمل بصورة أحسن من أي منهما منفرداً. تم دعم هذه الدراسة من مدينة الملك عبدالعزيز للعلوم والتقنية.

جامعة الملك فهد للبترول والمعادن

قسم الهندسة الكيميائية

CHAPTER ONE

General Introduction

1.1 Preamble

Plastic industry is a rapidly growing sector among the manufacturing companies. Some important factors that determine the growth in the use of plastics are: barrier, thermal and mechanical properties, colorability and UV resistance among others. The low production cost is another important consideration. Recently, a new area of polymer composites emerged in which the reinforcing material has nanometric dimensions [1]. These new composites, nanocomposites, have high performances due the high aspect ratio and the high surface area of the dispersed nanosized particles. The reinforcement efficiency of nanocomposites with 2 to 6% of anisotropic nanoparticles can in some situations match that of conventional composites with 40–50% of loading with classical fillers. Various nano reinforcements are currently being developed; however, layered silicate clay minerals are popular due to their availability (natural source), low cost and more importantly environmentally friendly [2].

Various nano reinforcements currently being developed are nanoclay layered silicates [3, 4]; cellulose nanowhiskers [5], ultra fine layered titanate [6], and carbon nanotubes [7]. Of particular interest is an organically modified layered silicate (organoclay) polymer nanocomposite. Organoclay showed significant enhancement of a large number of physical properties, including gas barrier properties, flammability resistance, thermal and environmental stability of polymers [2]. These improvements

were generally attained at lower silicate content (≤6 wt %) compared to that of conventionally filled systems. For these reasons, polymer-organoclay nanocomposites are far lighter in weight than conventional composites, which make them competitive with other materials for specific applications such as packaging and automotive parts. The main reason for these improved properties in polymer-organoclay nanocomposites is the high surface area of the organoclay as opposed to conventional fillers [4]. Organoclays generally have layer thickness in the order of 1 nm and very high aspect ratios (10–1000).

On the basis of the strength of the polymer- organoclay interaction, two different types of nancomposites are thermodynamically achievable (Figure 1.1, from [8]): (i) intercalated nanocomposites, where insertion of polymer chains into the silicate structure occurs in a crystallographically regular fashion, regardless of polymer to organoclay ratio, and a repeat distance of few nanometer, and (ii) exfoliated nanocomposites, in which the individual silicate layers are separated in polymer matrix by average distances that totally depend on the organoclay loading.

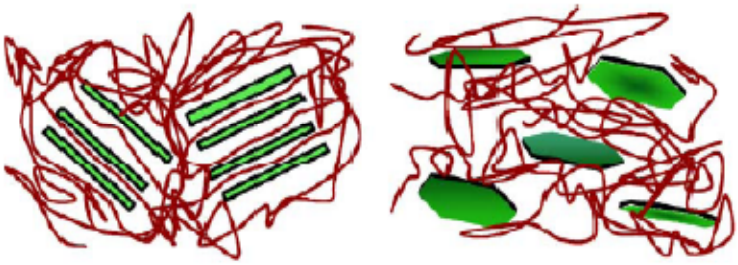

(b) intercalated (a) exfoliated

Figure 1.1: Schematic illustration of two different types of thermodynamically achievable polymer-organoclay nanocomposites

Dispersion of organoclay in the polyolefins is so important that the enhanced properties would not be achieved without it. One successful method to prepare polyolefin-organoclay nanocomposites is to intercalate polymers into the silicate galleries. Generally, intercalation of polymer chains into the silicate galleries is done by using one of the following two approaches: insertion of suitable monomers in the silicate galleries and subsequent polymerization or direct insertion of polymer chains into the silicate galleries from either solution [9] or the melt [3]. Recently, the melt intercalation technique [10] has become a main stream for the preparation of polymer-organoclay nanocomposites because it does not require the use of solvent and therefore industrially more convenient. So, melt intercalation was used in this work.

In brief, the addition of organoclays to polymers to form polymer nanocomposites impacted the following properties:

1. Polymer nanocomposites generally exhibit improved mechanical properties (For example, [11]).
2. They show much improved gas barrier properties towards small gases, e.g. oxygen, water vapor, carbon dioxide (for example [12]).
3. Thermal stability of polymer nanocomposites is expected to increase because clay acts as a heat barrier, which enhances the overall thermal stability of the system ([12, 13]. However, recent research [14] has shown that degradation of the organic modifier may lead to poor dispersion of the inorganic clay in the polymer.
4. Shear thinning of pure polymer will likely increase after nanocomposites formation [8].

Most of the above mentioned enhanced properties were achieved with organoclay loading above 6 % as earlier mentioned. In this work, organoclay is used as a processing aid with very low organoclay loading (less than 1000 ppm). The motivation came from the recent work of Hatzikiriakos et al. [15] studied which showed that addition of organoclays to polyolefins eliminates the sharkskin and stick-slip fracture behaviors and postpones the onset of gross melt fracture; hence improve processability of polymers [15]. This is critically important for the industrial applications that look for increased production but limited by the melt instabilities.

1.2 Thesis Outline

This section gives general outlook of this manuscript-based thesis.

CHAPTER TWO

This chapter discussed the rheology and processing of a typical polyolefin, high density polyethylene (HDPE) using different concentration of organoclay. The effect of a compatibilizer on the dispersion of organoclay in HDPE was also considered. Specially designed slit die containing highly sensitive pressure transducers were used in the characterization of the developed melt instabilities. At the end, the observed trend in rheology was linked to the extrusion result to suggest a mechanism through which organoclay interacted with HDPE.

CHAPTER THREE

This chapter considered wall slip effect in HDPE-organoclay nanocomposites. Particle Image Velocimetry (PIV) was used in this study. In addition to the PIV study,

rheology was used to investigate whether the nature of the effect of organoclay on HDPE is bulk or surface.

CHAPTER FOUR

This chapter extended the work on HDPE to include other polyethylenes such as Ziegler Natta based and metallocene-based polyethylenes. Rheology and extrusion in a mini twin screw extruder containing a backflow channel were used in the characterization of the effect of organoclay on the linear low density polyethylenes (LLDPEs). With such study, the chapter was able to systematically discuss the relationship between branch content in polyethylene and low organoclay loading.

CHAPTER FIVE

The interaction between organoclay and other conventional processing aids like fluoropolymers and boron nitride was investigated in this chapter. The different processing aids were compared in term of effectiveness using the specially developed slit die attached to a single screw extruder. The chapter would also consider if any synergistic effect exist between the different processing aids especially organoclay and fluoropolymers. Also, rheology was used as a tool to understand the phenomena occurring during processing.

CHAPTER SIX

Brief conclusions of the work in this thesis were presented. In addition, the anticipated significance of this work was discussed.

1.3 References

1 Giannelis, E.P. Polymer Layered Silicate Nanocomposites. *Advanced Materials*, 1996, **8**(1), 29-35.

2 Sinha Ray, S. and Okamoto, M. Polymer/layered silicate nanocomposites: a review from preparation to processing. *Progress in Polymer Science*, 2003, **28**(11), 1539-1641.

3 Vaia, R.A., Ishii, H. and Giannelis, E.P. Synthesis and properties of two-dimensional nanostructures by direct intercalation of polymer melts in layered silicates. *Chemistry of Materials*, 1993, **5**(12), 1694-1696.

4 Chen, J.-S., Poliks, M.D., Ober, C.K., Zhang, Y., Wiesner, U. and Giannelis, E. Study of the interlayer expansion mechanism and thermal-mechanical properties of surface-initiated epoxy nanocomposites. *Polymer*, 2002, **43**(18), 4895-4904.

5 Mohanty, A.K., Wibowo, A., Misra, M. and Drzal, L.T. Development of renewable resource–based cellulose acetate bioplastic: Effect of process engineering on the performance of cellulosic plastics. *Polymer Engineering & Science*, 2003, **43**(5), 1151-1161.

6 Hiroi, R., Ray, S.S., Okamoto, M. and Shiroi, T. Organically Modified Layered Titanate: A New Nanofiller to Improve the Performance of Biodegradable Polylactide. *Macromolecular Rapid Communications*, 2004, **25**(15), 1359-1364.

7 Mitchell, C.A., Bahr, J.L., Arepalli, S., Tour, J.M. and Krishnamoorti, R. Dispersion of Functionalized Carbon Nanotubes in Polystyrene. *Macromolecules*, 2002, **35**(23), 8825-8830.

8 Sinha Ray, S. and Bousmina, M. Biodegradable polymers and their layered silicate nanocomposites: In greening the 21st century materials world. *Progress in Materials Science*, 2005, **50**(8), 962-1079.

9 Aranda, P. and Ruiz-Hitzky, E. Poly(ethylene oxide)-silicate intercalation materials. *Chemistry of Materials*, 1992, **4**(6), 1395-1403.

10 Vaia, R.A. and Giannelis, E.P. Polymer Melt Intercalation in Organically-Modified Layered Silicates:â€‰ Model Predictions and Experiment. *Macromolecules*, 1997, **30**(25), 8000-8009.

11 Hotta, S. and Paul, D.R. Nanocomposites formed from linear low density polyethylene and organoclays. *Polymer*, 2004, **45**(22), 7639-7654.

12 Chang, J.-H., An, Y.U., Cho, D. and Giannelis, E.P. Poly(lactic acid) nanocomposites: comparison of their properties with montmorillonite and synthetic mica (II). *Polymer*, 2003, **44**(13), 3715-3720.

13 Paul, M.-A., Alexandre, M., Degée, P., Henrist, C., Rulmont, A. and Dubois, P. New nanocomposite materials based on plasticized poly(-lactide) and organo-modified montmorillonites: thermal and morphological study. *Polymer*, 2003, **44**(2), 443-450.

14 Shah, R.K. and Paul, D.R. Organoclay degradation in melt processed polyethylene nanocomposites. *Polymer*, 2006, **47**(11), 4075-4084.

15 Hatzikiriakos, S.G., Rathod, N. and Muliawan, E.B. The effect of nanoclays on the processibility of polyolefins. *Polymer Engineering & Science*, 2005, **45**(8), 1098-1107.

CHAPTER TWO

Impact of Organoclay and Maleated Polyethylene on the Rheology and Instabilities in the Extrusion of High Density Polyethylene

Ayuba A. Adesina, Ibnelwaleed A. Hussein

Abstract

The impact of organoclay on the rheology and extrusion of high density polyethylene (HDPE) using maleated polyethylene as a compatibilizer was studied. Organoclay effect was studied at very low clay loading (≤ 0.1 wt %) while serving as a processing aid. A special design single screw extruder was used in the study of the extrusion melt instabilities. The slit die attached to the extruder has three highly sensitive piezoelectric transducers mounted along its length. The rheological results showed that normal stress difference of HDPE was reduced during steady shear rate and stress growth tests when organoclay (≤ 0.1 wt %) was added. The extensional strain and stress growth of HDPE reduced with the addition of organoclay. So, organoclay (≤ 0.1 wt %) has an effect on the shear and extensional rheology of HDPE. The intensity of the melt instability was characterized with both a moment analyses and a distortion factor (DF) from an advanced Fourier transform analysis. Both showed the same trends in the characterization of the pressure fluctuations in the die. Generally, addition of organoclay (≤ 0.1 wt %) to HDPE led to the reduction in DF. The ratio of first and second moment analyses became reduced as well. The results quantified the extent of elimination of gross melt fracture in HDPE by organoclay. Also, the extrusion pressure was reduced with organoclay (≤ 0.1 wt %) inclusion hence more throughput. There was

a good correlation between rheology and extrusion. Both showed that the platy-like organoclay streamlined the melt flow. However, the maleated polyethylene added as a compatibilizer did not give substantial synergistic effect.

Keywords: organoclay, melt instability, extrusion, polyethylene, distortion factor, processing aid

2.1 Introduction

In polymer processing, the continuous increase in the production rate at low power consumption during the extrusion process is limited by the onset of polymer melt fractures. The onset of surface and/or gross melt instabilities at relatively high shear rates made the glossy polymer surface rough. Many studies had been carried out in the past to understand the causes, effects and ways to eliminate or postpone these instabilities [1-3]. Methods used to solve these instabilities, among others, include modification of the extruder especially the die head [4-7], conditioning the die surface [8-12], modification of the polymer [13-16] and addition of processing additives [17]. The processing additives often added, depending on the types of instabilities, include fluoropolymers [18-20], stearates [17], silicon-based additives and boron nitride [21-24]. Other materials such as carbon nanotube [25, 26] also have indirect improvement on the polymer melt instabilities. Recently, it was proposed that organoclays [27] can also be a very good processing additive for polyolefins. Researchers, at times, combine several additives to tackle different stages of melt fractures [27, 28].

Gross melt fracture is a bulk instability which occurs in polymers at high shear rates. This type of melt fracture becomes important and underscores the other types of instabilities in processes like extrusion with post pelletization. Parts of the major efforts being adopted to eliminate or postpone gross melt fracture include the addition of platy-like boron nitride and very recently, organoclay. It was also reported that dicumyl peroxide [29, 30] and carbon nanotube [25] can also postpone the occurrence of melt fracture in polyethylene to higher shear rate. Boron nitride can eliminate both sharkskin and gross melt fracture depending on the ratio of the dispersive and non-dispersive

components of the surface energy of the boron nitride [23, 31-33]. Generally, the addition of boron nitride to the host polymer did not result in the decrease of the extrusion pressure but enhanced the temperature effect [33] during the extrusion to eliminate the melt fracture. It was observed that as the concentration of boron nitride in fluoropolymer processing decreased, the critical shear rates at which melt fracture set-in decreased [21, 22]. The reverse was the case when boron nitride was used as a processing additive in polyolefin processing [22]. Recently, the single–walled and double-walled carbon nanotubes effects on the processing of polyolefins were studied. They modified the sharkskin and spurt instabilities of the parent polyolefins at low shear rates and completely eliminated the gross melt fracture at high shear rates [25]. It was observed that there was a complex interaction between the types of branching and the carbon nanotubes. Similar to what was observed in the use of the boron nitride, the critical stress threshold was not affected by the addition of carbon nanotubes [25]. Low carbon nanotube loading less than 0.1 wt % can eliminate low shear rate instability-sharkskin. However, a carbon nanotube loading more that 3 wt% must be used to see its effectiveness in eliminating or postponing high shear rate instability - gross melt fracture. Palza et al. further observed that the addition of a carbon nanotube reduced the die swell of the parent polymer due to its impact on first normal stresses and such effect may influence the morphology changes in the polymer melt instabilities [25]. The carbon nanotube loading was relatively high so it may not be a good processing aid when compared to the quantity of other processing nano-additives, which are often far less than 0.5 wt % [27].

There appears to be little published literatures on the subject of organoclay as a processing aid in polymers [27, 34]. In their works, capillary rheometer was used during the processing. It was observed that organoclay eliminated surface melt fracture-sharkskin and postponed the critical shear rate at which the gross melt fracture occurred. The organoclay was able to postpone the bulk fracture because it reduced the extensional stresses which often caused such instability in polyolefins [27]. These effects were observed in the capillary and crosshead dies attached to the capillary rheometer. Impact of organoclay on the extrusion pressure was characterized by a complex relationship between the parent polymers and types of dies. After careful observation of the Hatzikiriakos et al. work, we noticed that the addition of 0.1 wt % organoclay to HDPE had no effect on the extrusion pressure regardless of the types of dies [27].

In this work, the effect of organoclay on the continuous extrusion of HDPE in a single screw extruder with a specially designed slit die as a head is studied. The slit die has three highly sensitive piezoelectric pressure transducers along its length. This type of system has not been used before to study the impact of organoclay on melt instabilities. Another key point in the effective elimination or postponement of melt instabilities is the dispersion of organoclay in the polyolefin matrix. Two different mixing techniques are examined in this work. The effect of compositions ($\leq$ 0.1 wt %) of organoclay in the polymer matrix on shear and extensional rheology is further investigated and correlated to instabilities in the extrusion process. It should be noted it would be redundant to study higher compositions because organoclay is being proposed as a new processing aid for polyolefin extrusion.

2.2 Experimental

2.2.1 Materials

Commercial grade HDPE (relative density= 0.952, melting point = 132^{o}C and melt flow rate=0.05g/10mins at 190^{o}C and 2.16 kg load) used in this work was supplied by Saudi Basic Industries Corporation (SABIC). It has an average-weight molecular weight (M_w) of 285 kg/mol with molecular weight distribution of 26.5. Organoclay used in this work was Cloisite$^{(R)}$ 15A (C15A) obtained from Southern Clay. The surfactant modifier in C15A was dimethyl, dehydrogenated tallow, quaternary ammonium salt. The concentration of the modifier was 125 meq / 100g clay (i.e. the concentration modifier is 0.125g per 100g clay). According to the supplier, the d_{001} spacing of C15A was 31.5 Angstrom. C15A was chosen for this work because it is one of the most easily dispersed organoclay in polyolefin [35]. Polyethylene grafted maleic anhydride (PE-g-MA) from Aldrich was used as a compatibilizer. This was used in the received form without any modification. The maleic anhydride as a co-monomer in PE-g-MA was approximately 3 wt%. The compatibilizer viscosity was 4.5 Pa.s at 140^{o}C with relative density of 0.925. Its melting point and saponification value were 105^{o}C and 33mg KOH/g respectively. Various researchers had previously used PE-g-MA to facilitate the dispersion of organoclay in polyethylene [36-40] . The antioxidant used in this work was a 50/50 weight blend of Irganox 1010 and Irgafos 168 from Ciba- Geigy Speciality.

2.2.2 Melt Blending and Morphology Characterization

The Brabender 50 EHT mixer supplied with a Plastograph was used in the preparation of the nanocomposites. The organoclays were first heated in a vacuum oven at 108^{o}C for more than 24 hours to remove physico adsorbed water. HDPE was grinded

and physically pre-mixed with organoclay and antioxidant. Then, a master batch with and without compatibilizer was prepared in the Brabender mixer. A desired final concentration of a particular blend was obtained by mixing additional virgin HDPE to the master batch using the same mixer. The blending was done at a temperature of 200^{o}C and screw speed of 50 rpm for 10 minutes. 0.1 wt % of antioxidant was added to avoid degradation of the nanocomposite during the melt blending.

The amount of PE-g-MA in the blends was fixed such that its ratio to C15A content was 3:1. The compositions of the prepared HDPE-C15A nanocomposites (HDPE-x) were as listed in Table 2.1. HDPE-1000 represented a nanocomposite based on HPDE with 0.1 wt% C15A without a compatibilizer. HDPE-1000w represented a nanocomposite based on HPDE containing 0.1 wt% C15A and 0.3 wt% PE-g-MA.

The structures of the HDPE-C15A nanocomposites were characterized by FE-SEM and XRD. The XRD analysis was performed on XRD-6000 Shimadzu diffractometer with CuKα radiation (λ=0.154nm) in a reflection mode, operating at 40 kV and 30 mA. Scanning speed of 1^{o}/min was used. The scan range was 2-10^{o} at room temperature.

Table 2.1: HDPE containing different compositions of C15A and compatibilizer

Sample	HDPE (wt%)	PE-g-MA (wt%)	C15A (wt %)
Pure-HDPE	100	0	0
HDPE+Compatibilizer	99.7	0.3	0
HDPE-500	100	0	0.05
HDPE-1000	100	0	0.1
HDPE-1000w	99.7	0.3	0.1

Scanning electron micrographs were obtained with FE-SEM Nova^{TM} Nanosem 230. It is possible to achieve ultra-high resolution on non-conductive nano-materials with

Nova^{TM} Nanosem 230. The SEM samples were made into thin films and etched for 4 hours. The etching solution was made from a solution of $H_2SO_4/H_3PO_4/H_2O$ (10/4/1) and 0.01 g/ml $KMnO_4$ as described by Szadi et al. [36]. The etched samples were then covered with gold to make them conductive.

2.2.3 Rheological Measurement

The samples for the shear experiments were prepared from melt blended samples at a temperature of 200^{o}C and a pressure of up to 30Pa was applied in a Carver press. The disc samples with dimensions of 25 mm diameter and 2 mm thickness were prepared for shear rheology. An ARES rheometer was used for all the rheological measurements, namely a controlled strain rheometer equipped with heavy transducer (range 0.02-20 N for normal force; 2 x 10^{-5}-2 x 10^{-1} Nm for torque). The linear and non-linear viscoelastic experiments were performed using 25 mm parallel plates. The plates were heated for at least 20 minutes to equilibrate the temperature. For reproducibility of results, a pre-steady shear rate of 0.1 s^{-1} was applied for 20 s for all the tests in the parallel plates and time delay of 100 s before the actual tests. Different rheological tests were conducted to study the material properties under different rheological conditions.

Strain sweep tests were conducted for all the samples to determine the linear viscoelastic region. A Strain range of 10-400% with shear amplitude of 1rad/s was used. Frequency sweep experiments were performed in the frequency range between 0.01 rad/s and 100 rad/s. The applied strain was 20%. The strain was within the linear regime as determined by the strain sweep test. Auto tension was applied during the test to keep the upper plate in contact with the sample throughout the experiment. Steady shear rate sweep tests were conducted between 0.001 and 1 s^{-1}. The maximum shear rate

was limited by the secondary flow-induced instabilities generated at the melt sample periphery edges [37]. The delay and measurement time for each strain rate was 30 s. A Rosand RH7 twin bore capillary rheometer was used at high shear rates to get more rheological viscosity data. The diameter (D) and entrance angle of the long and short capillary dies were 2mm and 180^o respectively. The lengths of the long (L_l) and short dies (L_s) were 16mm and 4mm respectively. If P_L is the pressure drop across the long die and P_s is the pressure drop across the short die, the orifice pressure drop (P_o) was calculated by interpolation using:

$$P_o = P_s - \frac{P_L - P_s}{L_l - L_s} L_s \tag{1}$$

The true wall shear stress (σ_w) was determined via:

$$\sigma_w = \frac{(P_l - P_o)D}{4L_l} \tag{2}$$

The apparent wall shear rate ($\dot{\gamma}_a$) and true wall shear rate ($\dot{\gamma}_w$) were:

$$\dot{\gamma}_a = \frac{32Q}{\pi D^3} \quad and \quad \dot{\gamma}_w = \frac{1+3n}{4n} \tag{3}$$

where Q is the volume flow rate and n is the power law index.

The responses of the samples during stress growth were conducted to study the effect of organoclay on the non-linear shear material function of HDPE. The imposed shear rate was $0.8\ s^{-1}$. Low shear rate was used due to the limitation of the parallel plate geometry as mentioned earlier. An Extensional Viscosity Fixture (EVF) from ARES was used for the study of extensional rheology. The sample was pre-stretched with a strain rate of $0.4\ s^{-1}$ to remove sagging. The sample was left in the fixture for 3 minutes to relax any accumulated stress before the start of the experiment. A Hencky

strain rate of 10 s^{-1} and a temperature of 145^{o}C were used for these experiments. Such a high Hencky strain rate and low temperature were necessary to observe the effect of organoclay on the extensional rheology of HDPE.

2.2.4 Set-up for Melt Flow Instabilities

Extrusion was carried out in a single screw extruder 19/25D from a Brabender equipped with a specially developed slit die. The slit die has a dimension of 0.8 mm height, 20 mm width and 160 mm length. The slit die has highly sensitive piezoelectric transducers located at three different positions. The positions of the transducers along the slit die were 30mm, 80mm and 140mm from the entrance of the die. The pressure and time resolutions of these transducers are of the order of 10^{-1} mbar and 1ms respectively. Details about the die were reported elsewhere [7, 14 and 38]. However, this set-up was different from those reported earlier in 2 ways: First, the slit die in this work was attached to a single screw extruder; second, the die has larger dimensions as shown in Figure 2.1.It was developed with the help of Prof. Manfred Wilhelm of Karlsruhe Institute of Technology, Germany.

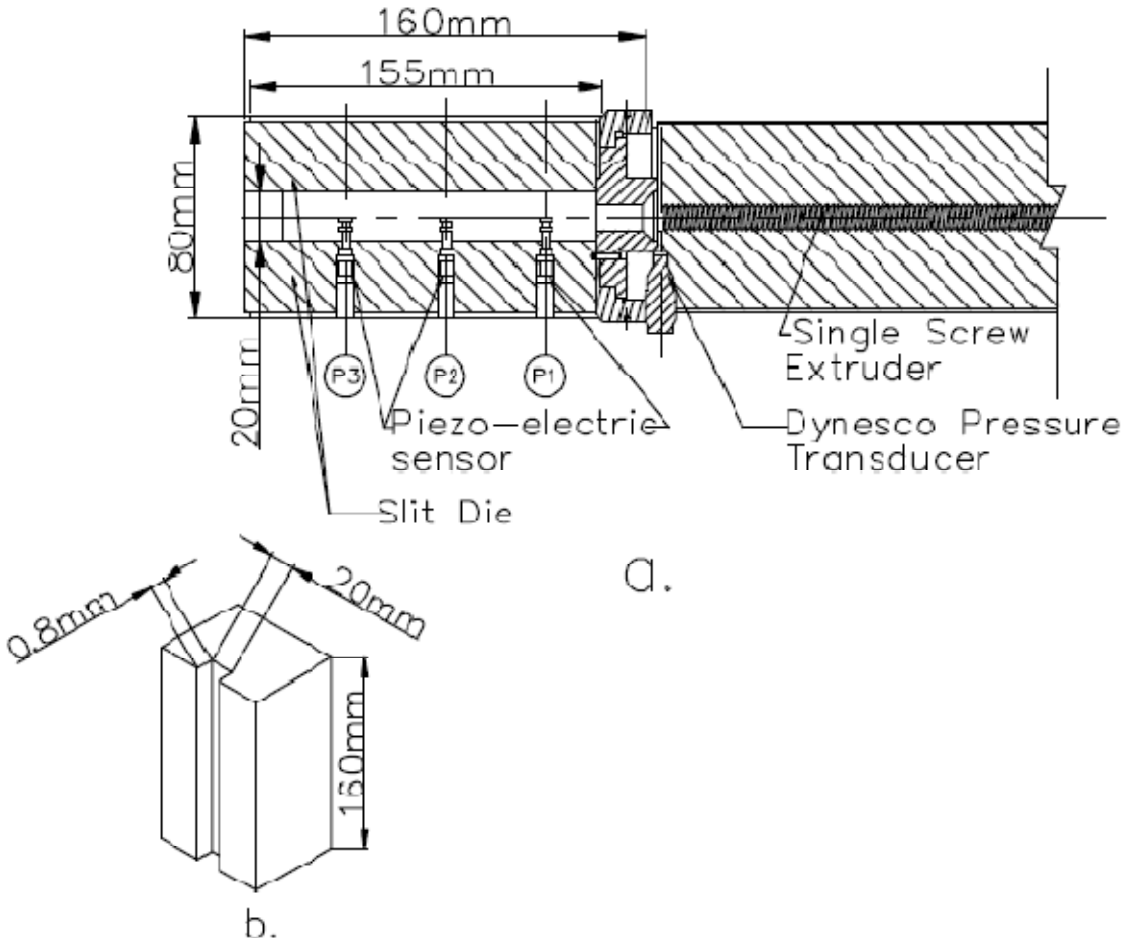

Figure 2.1: (a) Longitudinal section of the single screw extruder with slit die head having 3 highly sensitive piezoelectric pressure transducers along the die. This is the set-up for the study of melt instabilities during polymer extrusion. (b) The slit die

The measurements with the three highly sensitive piezoelectric transducers were done to specifically identify and analyze the time dependent pressure fluctuations associated with smooth polymer flow and melt flow instabilities. The time dependent pressure oscillations were collected by the use of these fast acquisition piezoelectric transducers combined with an oversampling technique to increase the noise to signal ratio. So, the 30,000 data points/channel was reduced to 100 data points/s using an oversampling rate of 300 data points/s. The oversampled time dependent pressure was

further analyzed using a Fourier transformation. This resulted in a spectrum with a maximum intensity at a frequency of 0 Hz. This intensity corresponds directly to the mean value of the pressure. The pressure oscillation during melt flow instabilities can be observed as additional peaks, located at higher frequencies. Details of these advanced mathematical analyzes can be seen elsewhere [14]. In this work, both moment analyses and a distortion factor from a Fourier transform analysis were used in our analyses.

The moment analysis is often used to characterize the time dependent data. Generally, k-moment

$$m_k = \frac{1}{t_f - t_o} \int_{t_o}^{t_f} (p(t) - \bar{p})^k dt \qquad (4)$$

where m_k is the kth moment of the pressure, $\bar{p}$ is the mean value which is the first moment around zero and $p(t)$ is the time dependent pressure signal. The second moment is the variance and its square root is the standard deviation. In this work, the ratio of the standard deviation divided by the mean of the pressure fluctuation will be used in the characterization of the melt instability.

A Fourier transform analysis (FT) is another alternative and growing advanced mathematical tool in the analysis of the inherent periodic contributions from the time dependent variables like pressure fluctuation along the die. The time dependent pressure can be analyzed as being a combination of different harmonic contributions as shown below:

$$p(t) = \bar{p} + \sum_{i\geq 1} l_i \cos(w_i t + \emptyset_i) \quad (5)$$

Where $\bar{p}$ is the pressure mean value at $\frac{w}{2\pi} = 0$; $\frac{w_i}{2\pi}$, $\emptyset_i$ and l_i are the characteristic frequencies, phases, and amplitudes of the pressure fluctuation as quantified from the Fourier analysis of the processed signals, respectively. It is assumed that all the information related to the melt instability is included in these parameters. Details of the FT analysis can be seen in the work of Palza et al. [7, 25]. One of the most important parameters from the FT analysis in quantifying melt instabilities is the distortion factor (DF). This is a measure of the relative pressure fluctuation (RPF) as defined in equation (6).

$$DF = \frac{\sum_{i\geq 1} l_i}{l_0} \quad (6)$$

l_0 represents the peak value at w=0 and it is related to the pressure mean value. It should be noted that the summation of harmonics (amplitudes of the pressure fluctuations) is retained because there are higher harmonics with a magnitude of the same order as l_1.

There are three heating zones along the single screw extruder with a separate heating element for the slit die. The extrusion was done at temperature program 160-160-160-145^{o}C where the screw and slit die were maintained at 160 and 145^{o}C respectively. The screw speed was varied up to the limit of the extruder. The piezoelectric transducer can only be used to obtain pressure fluctuation and not absolute

pressure. Hence, the pressure drop (ΔP) across the slit die was measured with the Dynisco pressure transducer placed at the entrance of the slit die (see Figure 2.1). The maximum allowable pressure in the transducer was 70 MPa. The pressure data was collected via the acquisition program provided by the Brabender. The acquisition rate was 1 data per 20s. The volumetric flow rate ($\dot{Q}$) was determined by collecting and measuring the ejected mass as a function of time. From the data, the wall shear stress (τ_{app}) and the apparent shear rate ($\dot{\gamma}_{app}$) were calculated using:

$$\tau_{app} = \Delta P \frac{h}{2l} \tag{7}$$

$$\dot{\gamma}_{app} = 6\frac{\dot{Q}}{bh^2} \tag{8}$$

$where$ h, l and b and b are the height, length and width of the slit die, respectively.

2.3 Results and Discussion

In this section, the outcomes of the morphological characterization, rheological tests and extrusion experiments on HDPE-C15A with and without a compatibilizer were discussed. The relationships between rheology and extrusion were combined to propose a mechanism through which the organoclay possibly influenced the HDPE extrusion in the wake of melt instabilities.

2.3.1 Morphological Characterization

Figure 2.2 showed the wide-angle x-ray diffraction (WAXD) chromatogram for different composition of C15A in HDPE. It was observed that the C15A peaks at 2.99^{o}

(d_{001}=2.953nm) and 7.13° (d_{002}=1.239nm) disappeared. While one might infer that there was exfoliation of organoclay in all the nanocomposites, the dilution procedure might have also caused the disappearance. The addition of a compatibilizer did not lead to any difference in the chromatogram. The implications of these will be discussed during rheological testing and extrusion of the nanocomposites.

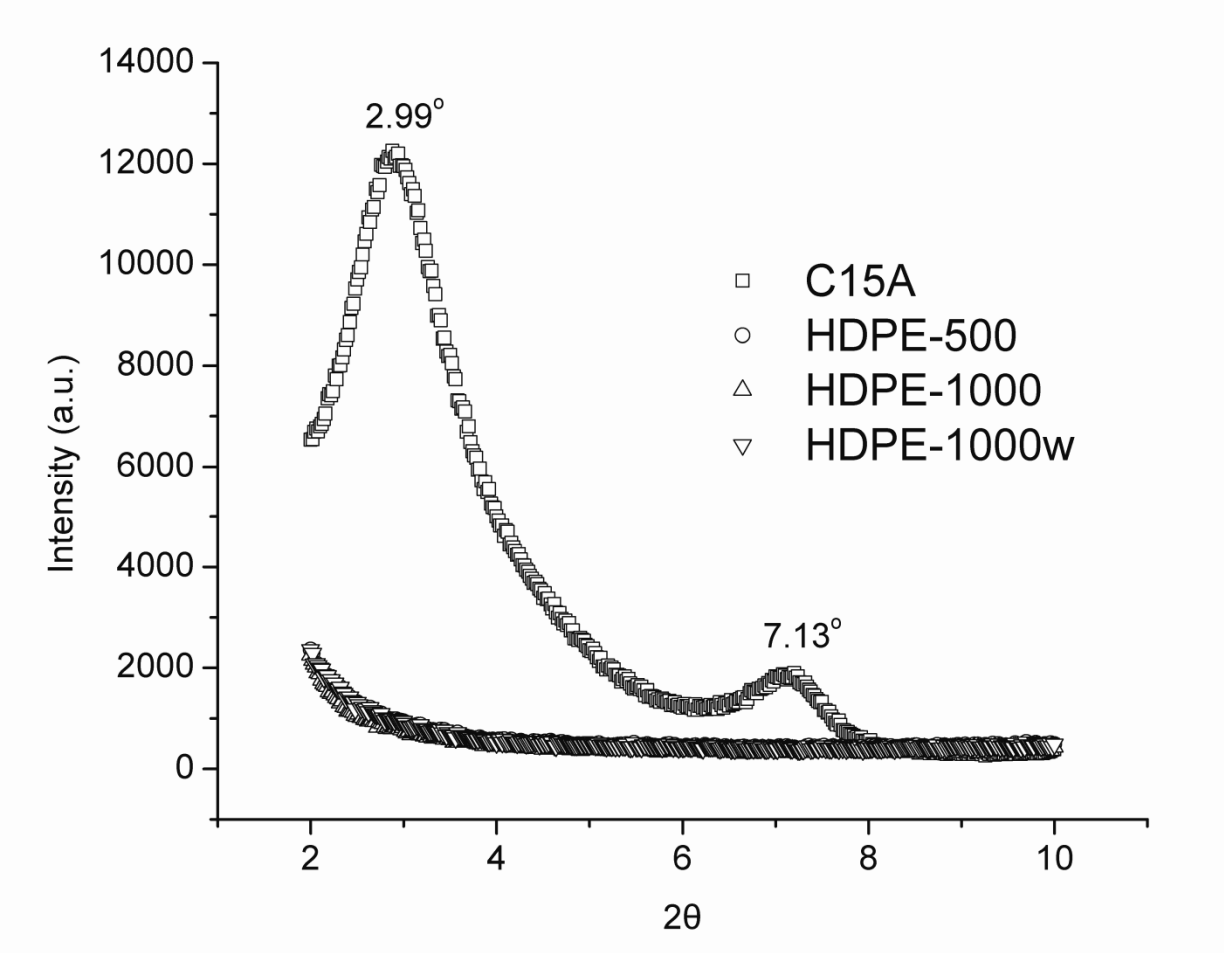

Figure 2.2: WAXD for HDPE, organoclay (C15A) and HDPE containing different clay loadings + compatibilizer

The SEM images of HDPE containing 0.1 wt % of organoclay with/without a compatibilizer were as shown in Figure 2.3a and 2.3b. These results were obtained after

etching. The figures showed that C15A was present and dispersed in both samples (HDPE-1000 and HDPE-1000w respectively). Transmission electron microscopy was not carried out on the sample because it is too time consuming and costly for routine characterization. Moreover, we are not interested in the type of dispersion since the instability study would be carried out in an extruder at high shear rates. Such extrusion will further lead to the dispersion of the organoclay. These images supported the XRD results. However, the surface impact of the etching solution was very obvious in the chromatograms.

Figure 2.3:Scanning Electron Micrograph for (a) HDPE with 0.1 wt % C15A and (b) HDPE with 0.1 wt % C15A +0.3 wt % compatibilizer

2.3.2 Rheological Characterization

In the rheological characterization, both shear and extensional rheology were conducted. The tests were designed to comprehensively examine whether organoclay truly impacts the rheology of HDPE. The influence of the compatibilizer on the linear and non-linear material properties of HDPE were discussed as well.

2.3.2.1 Shear Rheology

The addition of organoclay and a compatibilizer to HDPE reduced the stress responsible for HDPE deformation during strain sweep tests. The inclusion of 0.1 wt % of C15A to HDPE (HDPE-1000) caused a very small decrease of 5 % in the relaxation modulus of HDPE (figure not shown). Such a decrease might be neglected because it was discovered that $\tan(\delta)$ for the plots were well reproducible with ± 2 % difference. However, as the clay loading decreased, the relaxation modulus also decreased both at linear and non-linear regimes. The reduction caused by the addition of 0.05 wt % C15A was as shown in Figure 2.4. The reduction was approximately 21 % throughout the strain range considered in this work. The inclusion of a 0.3 wt % compatibilizer alone to HDPE also decreased the relaxation modulus of HDPE up to 20 % (figure not shown).

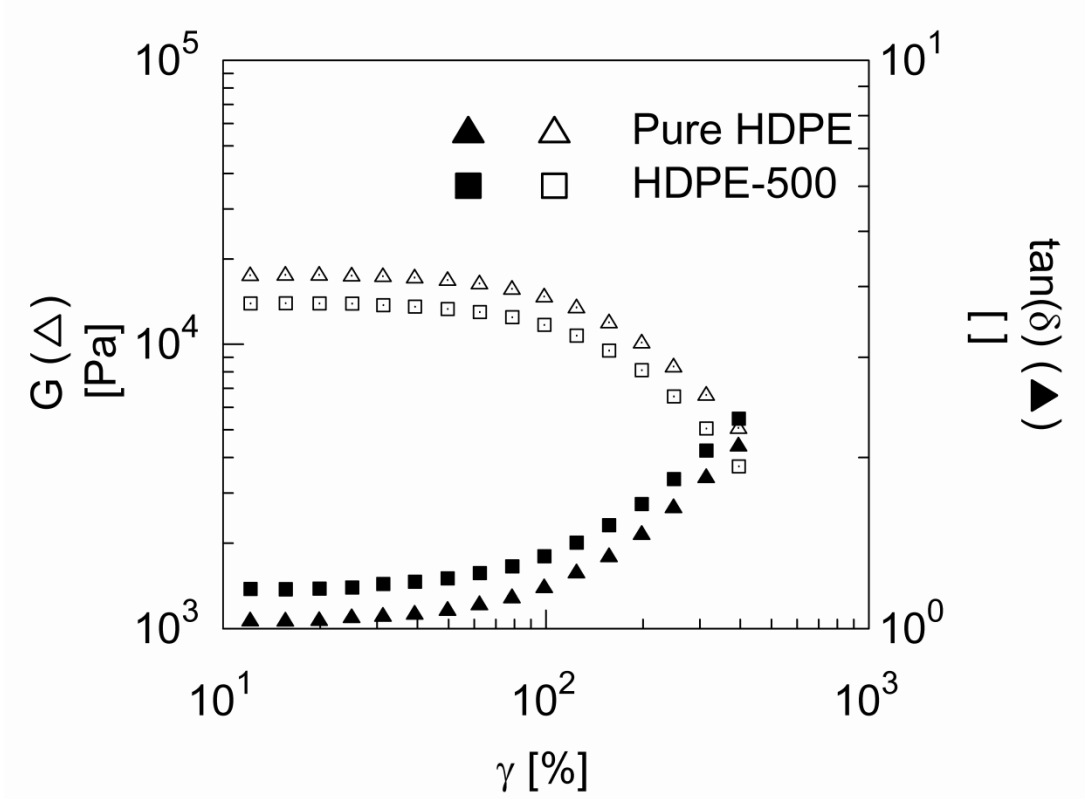

Figure 2.4: Relaxation modulus and tan(δ) versus strain during strain sweep test for Pure HDPE and HDPE with 0.05 wt % organoclay

A representative frequency sweep plot for virgin HDPE and addition of low amount of C15A was as shown in Figure 2.5. The crossover frequencies for all the samples were of the same order. At high frequencies above the crossover frequency, the elastic and viscous moduli were the same for all samples. Below the crossover frequency, the effect of organoclay began to appear as in Figure 2.5 for HDPE-500. With the addition of 0.1 wt % C15A to HDPE (HDPE-1000), the decrease in the moduli was not pronounced (figure not shown). The decrease was within the range of data reproducibility, namely 6 %. This was in agreement with the result reported in the work of Hatzikiriakos et al. when they used 0.1 wt % of organoclay [27]. They concluded based on the result that a small addition of organoclay into polyolefins has no effect on

the shear rheological properties of the polymers [27]. However, Figure 2.5 showed that as the clay loading was decreased to 0.05 wt % the elastic modulus decreased.

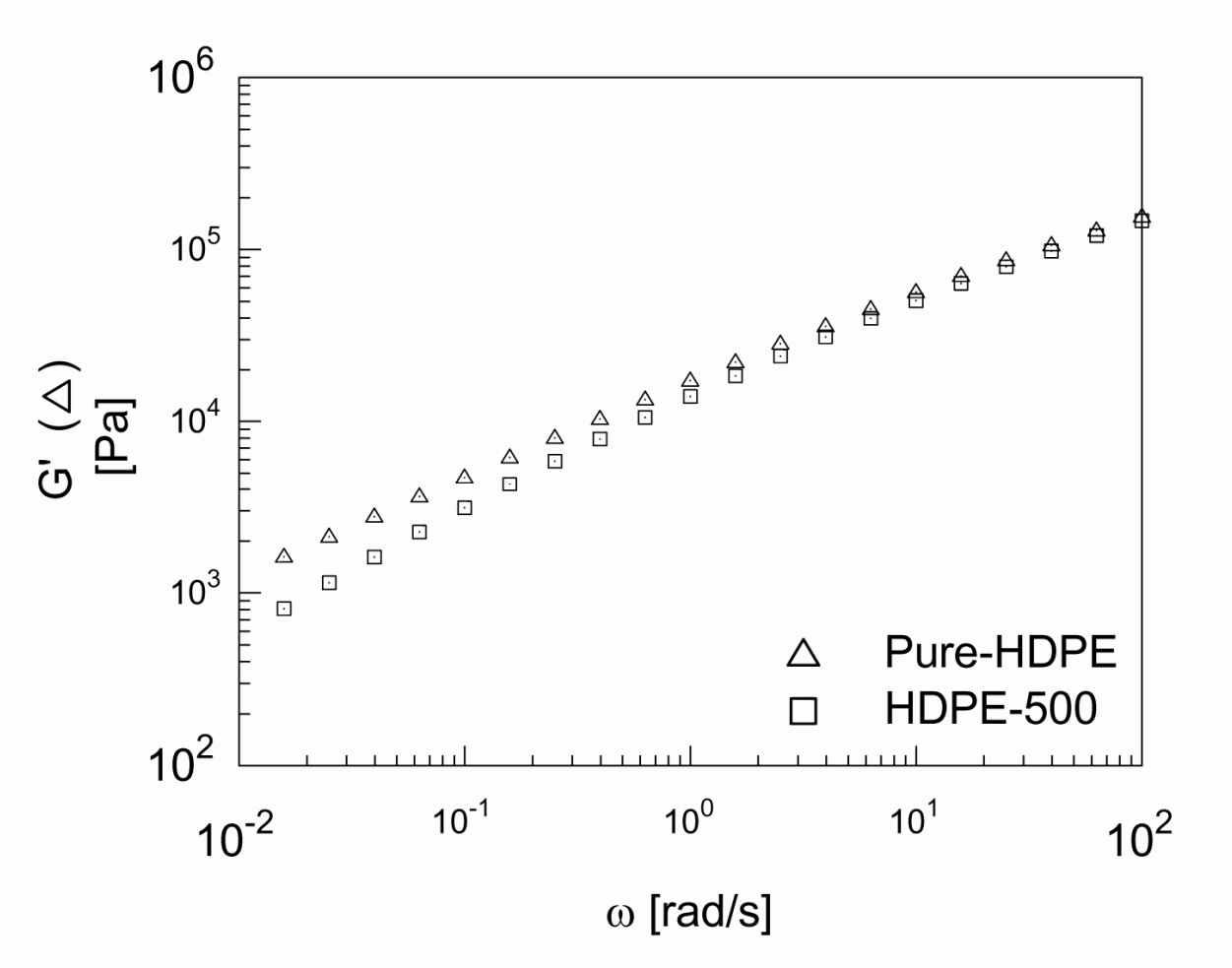

Figure 2.5: Dynamic frequency sweep of pure HDPE and HDPE with 0.05 wt % organoclay

At a frequency of 5 rad/s, the elastic modulus of HDPE decreased by 15% while it was 50% at a frequency of 0.015 rad/s. This was an indication that the linear viscoelastic properties of the polymers were affected by the addition of small amounts of C15A less that 0.1 wt %. An Addition of 0.3 wt % compatibilizer to HDPE also lowered the moduli at low frequencies. Hence, there was a further slight decrease in the

elastic modulus of HDPE-1000 with the addition of a compatibilizer (figure not shown). Terminal plateau was not detected in Figure 5 because the use of HDPE was highly linear. Percolation threshold was absent in all the rheological plots because the amount of clay (less than 0.1 wt %) added to HDPE was very small to lead to a percolation network.

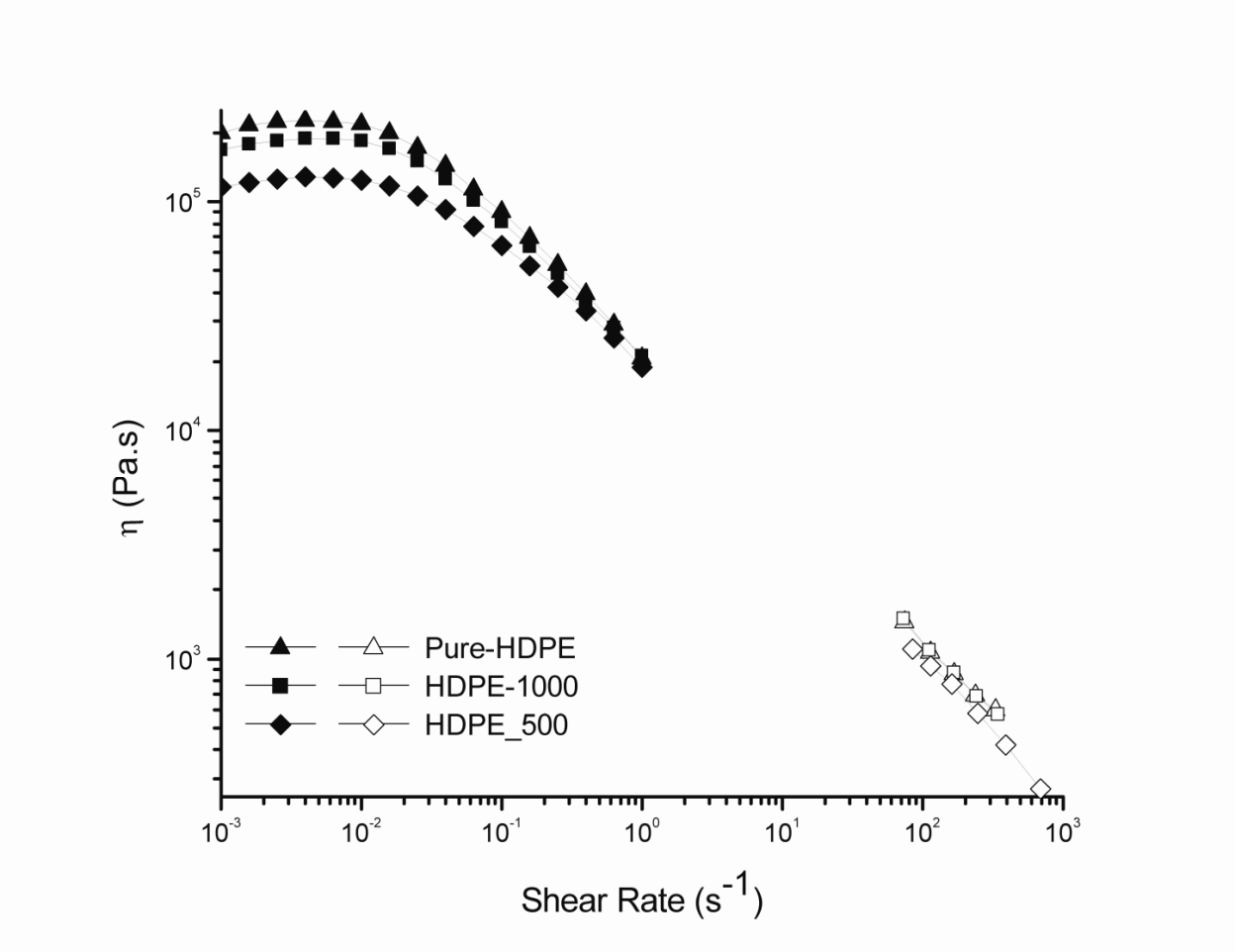

Figure 2.6: Effect of different clay loadings on the viscosity (η) of HDPE during steady shear rate sweep test in parallel plates (filled legend) and capillary rheometry (open legend)

The severe impediment to the lateral motion of HDPE molecules during steady shear rate test led to the high zero-shear rate viscosity shown in Figure 2.6. A Cross model as defined in equation 9 was used in the fitness of shear rate dependent viscosity.

$$\eta = \frac{\eta_o}{1 + (C\dot{\gamma})^m} \tag{9}$$

η_o is the zero shear viscosity in Pa.s, m is the (Cross) rate constant (dimensionless) and C is the Cross time constant (or Consistency) in second. C^{-1} is the inverse of Cross time constant. It is the critical shear rate that shows the onset shear rate for shear thinning.

Table 2.2: Cross model parameters for Pure-HDPE and its C15A nanocomposites

Cross Model Parameters	Pure-HDPE	HDPE-Compatibilizer	HDPE-1000	HDPE-1000w	HDPE-500
η_o (Pa.s)	236180.0	146740.0	197010.0	133610.0	132290.0
m	0.87	0.83	0.84	0.79	0.81
C (s)	10.99	7.07	9.08	6.05	6.26
C^{-1} (s^{-1})	0.09	0.14	0.11	0.17	0.16
% Diff*	0.0	37.9	16.6	43.4	44.0
Correlation	0.9878	0.9893	0.9844	0.9902	0.9883
Variance	0.0028	0.0019	0.0035	0.0017	0.0019

Note:$* \%\ Diff = \frac{\eta_{o,pure-HDPE} - \eta_o}{\eta_{o,pure-HDPE}}$

Table 2.2 gave the summary of the Cross model parameters for all the samples. From the table, the zero-shear viscosity reduced with the addition of organoclay and a compatibilizer. For instance, at clay loading of 0.1 wt %, the zero-shear viscosity of HDPE reduced by 16 %. There was a further decrease of up to 44 % when the clay loading was reduced to 0.05 wt %. The observed trends became important when it was noticed that the experimental data was reproducible within error margin less than 6 %. At the shear thinning region, the Cross rate constant and critical shear rate for the onset of the shear thinning were of the same order for all the samples. The capillary rheometer results (open legends in Figure 2.6) showed that at higher shear rate, there was a slight decrease in the shear viscosity due to the addition organoclay especially with 0.05 wt % clay loading. Another observable trend at the shear-thinning region was the effect of organoclay on normal stress differences in Figure 2.7.

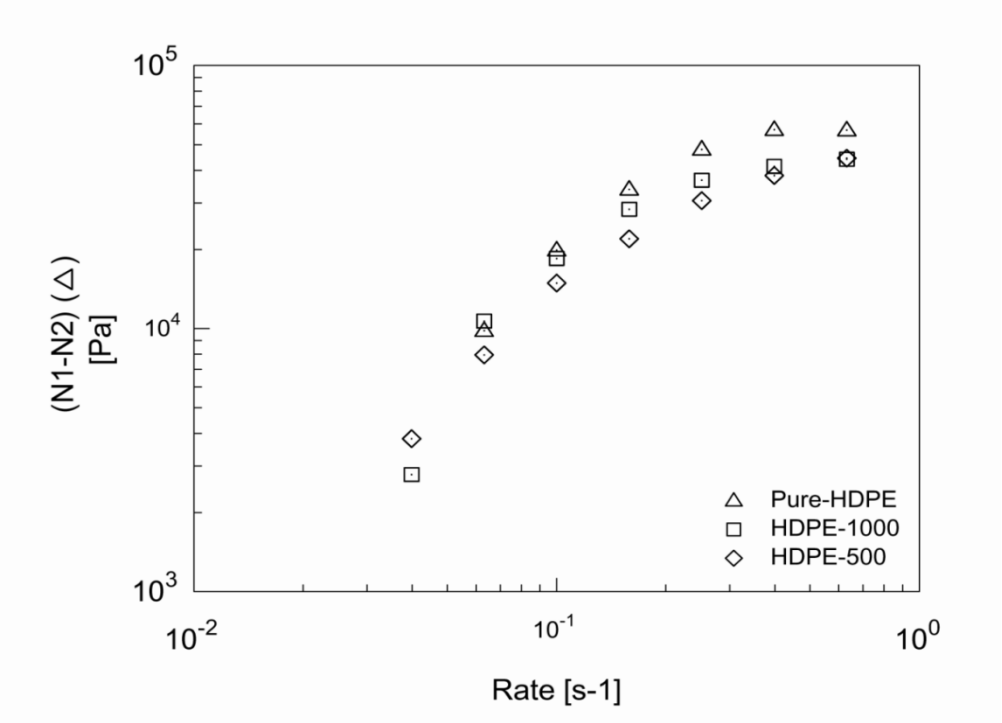

Figure 2.7: Effect of different clay loadings on the normal stress differences (N1-N2) of HDPE

The data reproducibility for the experiment was within 10%. Despite the high experimental error, the organoclay reduced the normal stress differences in HDPE. For instance, the normal stress difference in HDPE was reduced by 27 % (at shear rate=0.04 s^{-1}) when 0.1 wt % organoclay was added. There was a further decrease of up to 33 % when the clay loading was decreased to 0.05 wt %. The reason for the reduction in the normal stress difference might likely be as a result of the decrease in the elastic component of the polymer as previously discussed. The compatibilizer had an effect on the zero-shear and shear thinning viscosities of HDPE (Table 2.2). The compatibilizer interaction with organoclay led to a 43.4 % decrease in the zero-shear viscosity of HDPE. It should be noted that the compatibilizer alone caused a decrease of 37% in the zero shear viscosity of HDPE.

It is known that polymer extrusion involves a transient flow at high shear rates. So, a stress growth experiment was conducted to monitor the effect of organoclay on the normal stress differences of HDPE. Figure 2.8 showed that as the clay loading decreased from 0.1 wt % to 0.05 wt %, the normal stress differences decreased. Hence, the lower the clay loading used in HDPE, the better the performance of the clay in the reduction of the normal force. Similar results as in the case of the steady shear rate tests were experienced when the compatibilizer was added during the growth test.

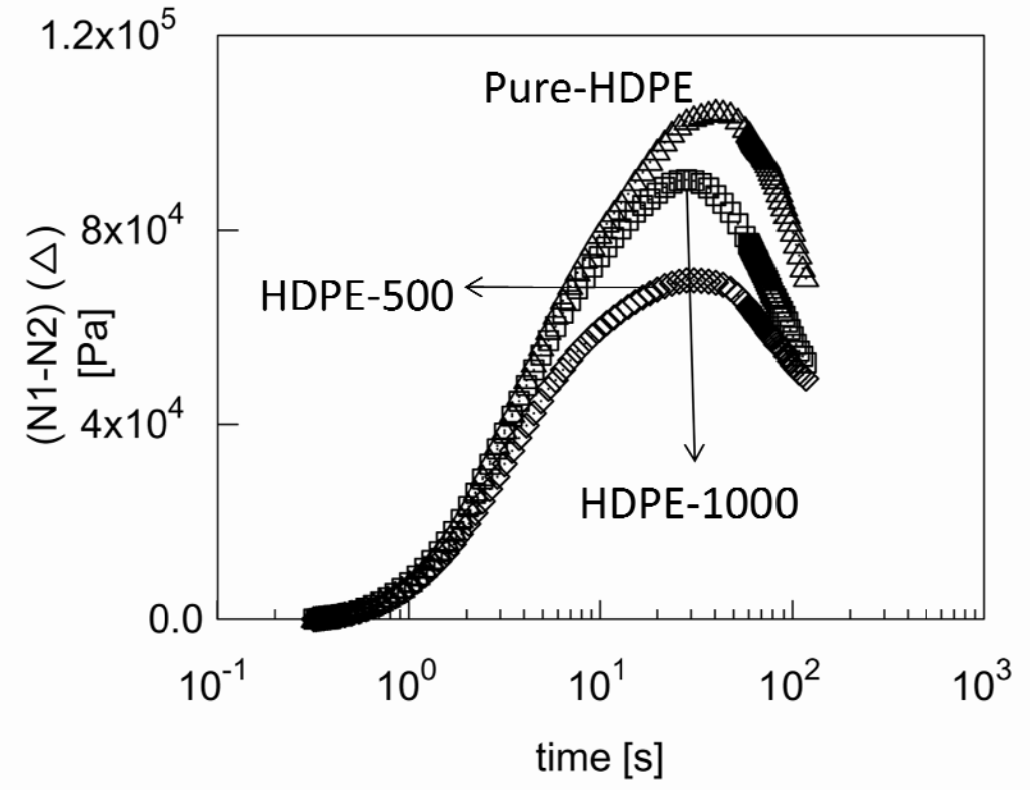

Figure 2.8: Effect of different clay loadings on the normal stress differences (N1-N2) of HDPE

An abundance of experimental discussion was offered on shear rheology to arrive at a reasonable conclusion that organoclay had an effect on the linear and non-linear shear rheology of HDPE. The results showed that the addition of organoclay reduced the linear viscoelastic behavior of HDPE especially after the cross over frequency. Also, the shear viscosity and normal stress difference of HDPE decreased when organoclay was added to it. The same trend was observed during stress growth test. However, no synergistic effect was noticed between the organoclay and PE-g-MA in the reduction of the shear behavior of HDPE.

2.3.2.2 Extensional Rheology

The extensional effect of the organoclay and the compatibilizer on HDPE at 145^{o}C and Hencky strain rate 10s^{-1} was as shown in Figure 2.9. Strain hardening was observed in the plot of HDPE at this high Hencky strain rate. This is typical of linear polymer when subjected to high strain deformation near the polymer melt state. Both the organoclay and the compatibilizer reduced the extensional stress and strain within the polymer. For clay loading of 0.1 wt %, the maximum extensional stress developed in HDPE (at extensional strain of 4) decreased by 68%. When the clay loading was further decreased to 0.05 wt %, a decrease of up to 89% was observed in the maximum extensional stress developed in HDPE. Such a decrease in extensional stress and strain indicated that organoclay was able to dissipate energy within the polymer as in the case of boron nitride [39]. It seemed the compatibilizer also assisted the organoclay to further decrease the maximum extensional stress in HDPE by 88%.

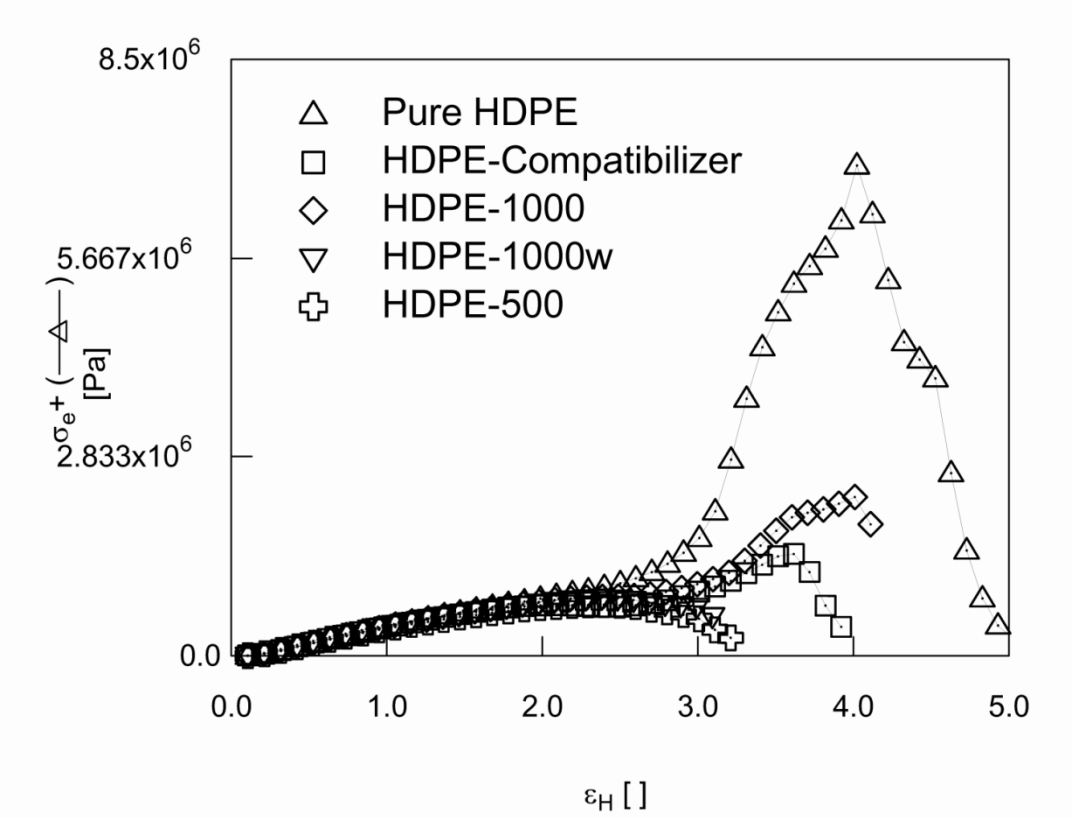

Figure 2.9: Effect of compatibilizer and different clay loadings on the extensional stress growth

The results from the shear and extensional rheology indicated that both the organoclay and the compatibilizer had effects on the rheology of HDPE. However, their effects on extensional rheology were more than their impacts on shear rheology. It should be noted that the shear and extensional rheology were conducted at 200^{o}C and 145^{o}C, respectively. This might be the reason for the larger reduction in extensional rheology as compared to shear rheology.

Since materials during continuous extrusion undergo shearing and elongation processes, the correlation between the rheology and extrusion should be studied. Therefore, the next section will discuss how the compatibilizer and the organoclay effect extrusion of HDPE especially at the onset of melt instability, gross melt fracture.

2.3.3 Extrusion Processing

As earlier mentioned, the melt instability in HDPE during extrusion was studied in a single screw extruder with a slit die. At the processing temperature of 160^{o}C, the extruded HDPE had gross melt fracture at all the attainable apparent shear rates. Figure 2.10 shows the flow curve for the HDPE and its organoclay nanocomposites.

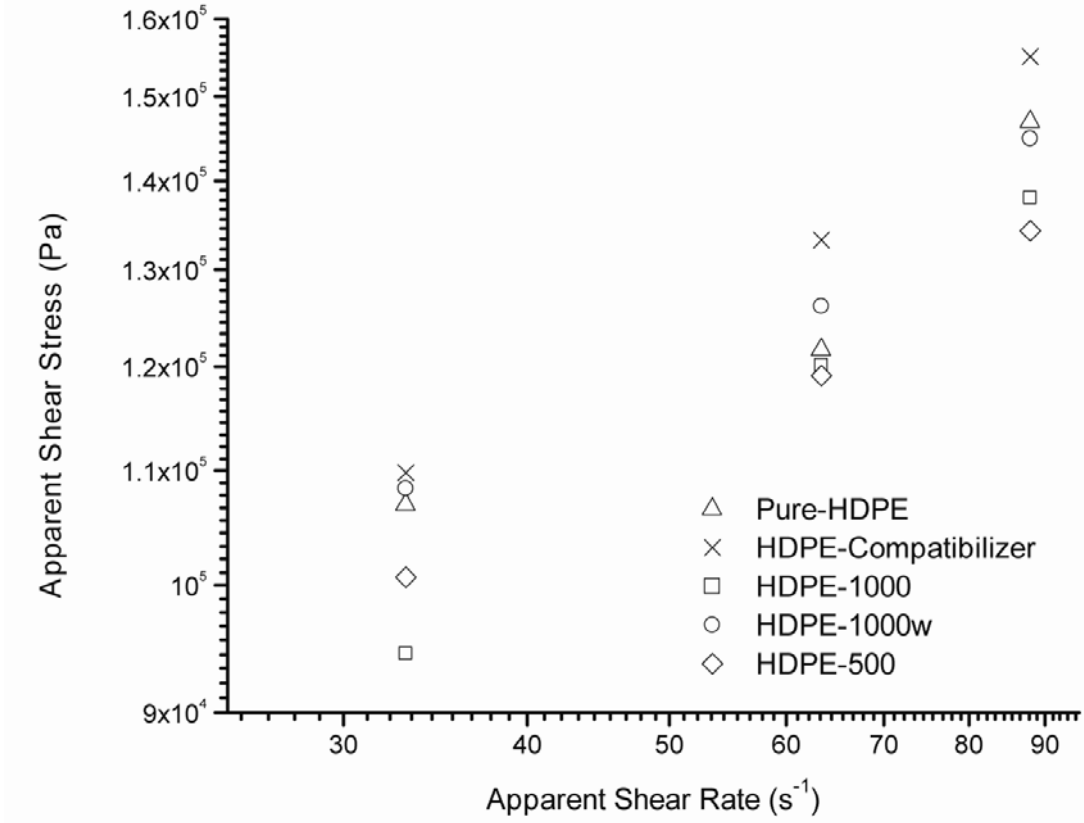

Figure 2.10: Flow curves for Pure-HDPE, HDPE-Compatibilizer and HDPE containing organoclay of different loadings

At the same apparent shear rate, the stress of HDPE became reduced in the presence of organoclay. This showed that organoclay as a processing aid in HDPE led to reduction in extrusion pressure. The intensity of the melt fracture in HDPE increased as the shear rate increased. The addition of organoclay (C15A) eliminated the melt fracture in HDPE. The elimination occurred at all the attainable shear rates in this experiment. High pressure fluctuation was an indication of gross melt fracture. For example, at a shear rate of $33s^{-1}$, typical recorded pressure fluctuations along the die with piezoelectric transducers were as shown in Figure 2.11. The corresponding visual observation of the extruded samples (Pure-HDPE and HDPE-500) was as presented in Figure 2.12.

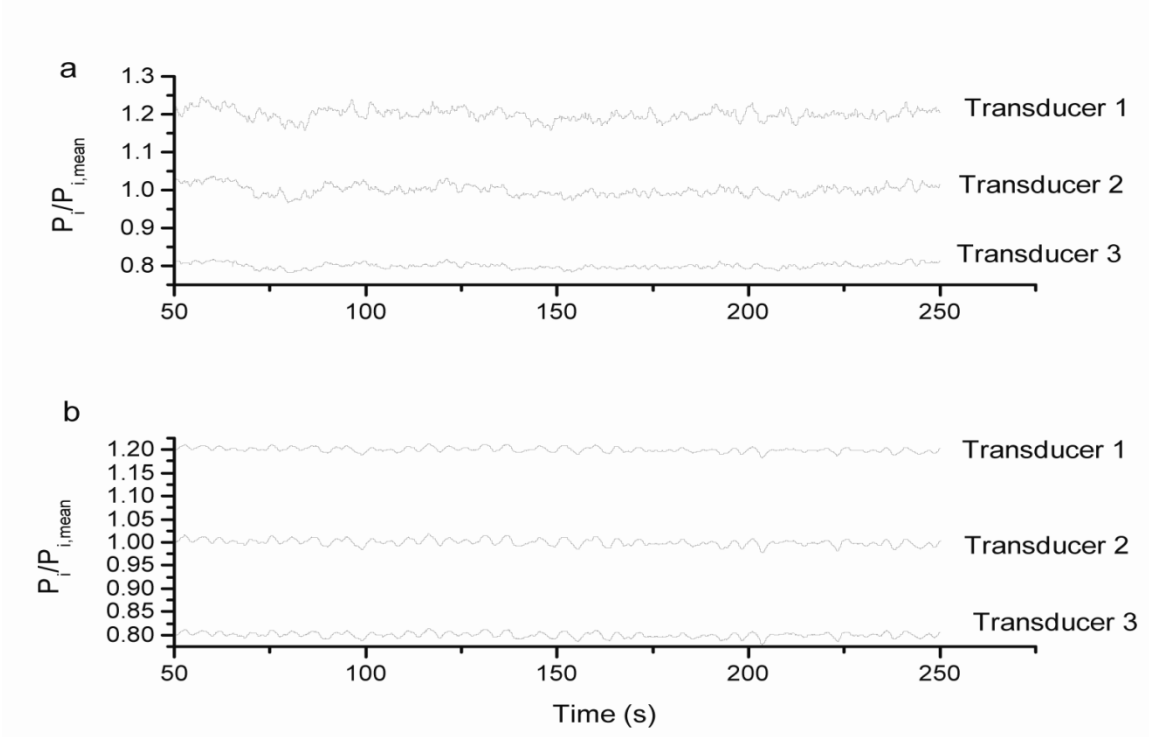

Figure 2.11: The associated normalized pressure fluctuations along the slit die at a shear rate of $33s^{-1}$ (a) For HDPE where gross melt fracture developed. (b) For HDPE-500 where 0.05 wt % addition of organoclay to HDPE eliminated the melt instability. Curves were shifted by ±0.2 in the vertical axes for better representation.

We observed that with the addition of organoclay, the pressure fluctuation along the die became reduced. Another striking point in Figure 11 was that these fluctuations occurred simultaneously. The in-phase between the pressure signals was confirmed with cross correlation analysis. The maximum in the cross correlation was at zero-time lag regardless of the pair of transducers analyzed. This implied that the gross melt fracture possibly originated from the entrance of the die producing a continuous fluctuating signal inside the die. To characterize the pressure fluctuations during the melt fracture and its attenuation, both moment analysis and distortion factor were used.

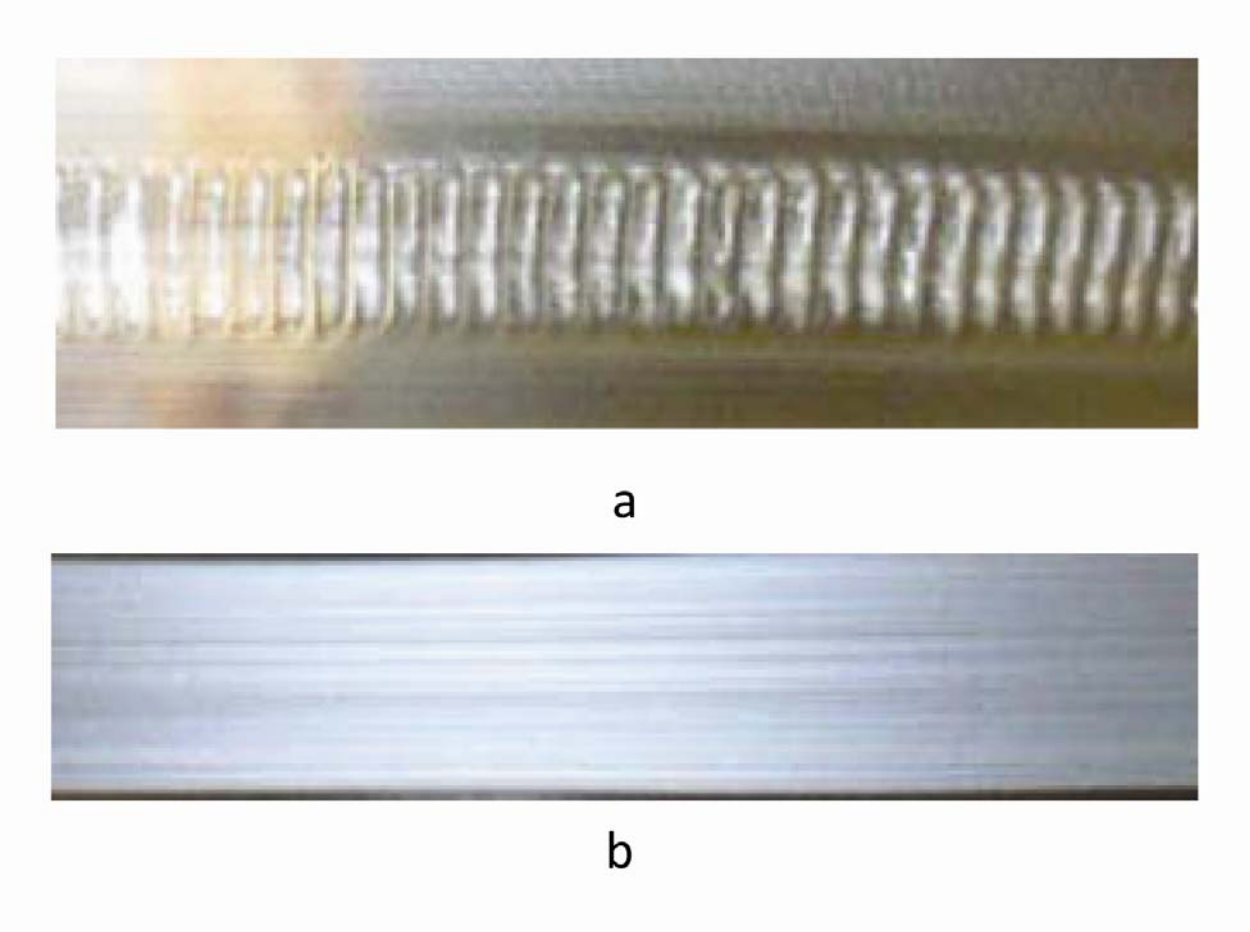

Figure 2.12: Visual Observation of (a) HDPE with gross melt fracture and (b) HDPE-500

Figure 2.13 presented the effect of organoclay and the compatibilizer on the relative pressure fluctuations as measured by the ratio between standard deviation of the pressure signals and its mean value (SD/MV). It can be seen from the figure that an addition of 0.05 wt % organoclay to HDPE (HDPE-500) was most effective in reducing the intensity of the pressure fluctuations both at the entrance and exit of the die. The visual observation confirmed the trend showed in the figure. The addition of the compatibilizer alone did not help in the improvement of the extrusion of HDPE. As a result no reduction was seen in the SD/MV values of HDPE both at the entrance and exit of the die. Even though 0.1 wt % organoclay improved the glossiness of the HDPE extrudate, the addition of compatibilizer to it had no additional synergistic effect on the extrudate as confirmed in Figure 2.13.

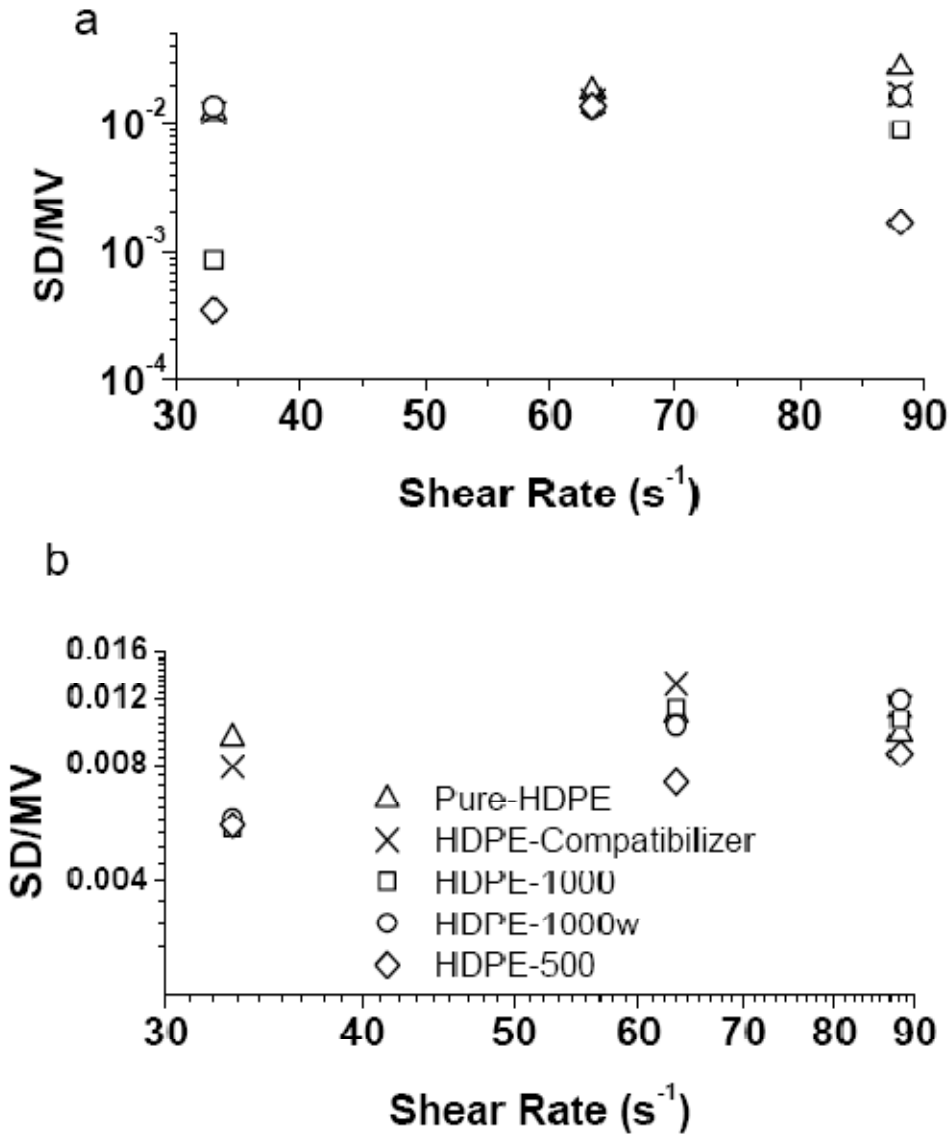

Figure 2.13: The effect of different clay loadings and compatibilizer on the pressure fluctuation measured as the ratio between the standard deviation of the pressure signal (SD) and its mean value (MV). (a) SD/MV versus shear rates at the entrance of the die. (b) SD/MV versus shear rates at the position P3 from the exit of the die.

A distortion factor (DF) was used as defined in Equation 6 to further quantify the generated pressure fluctuation. Generally, the DF decreased downwardly along the die as shown in Figure 2:14. The decrease indicated that HDPE became relaxed as it moved towards the die exit. This DF plot also confirmed that 0.05 wt % organoclay acted best in the attenuation of the pressure fluctuation.

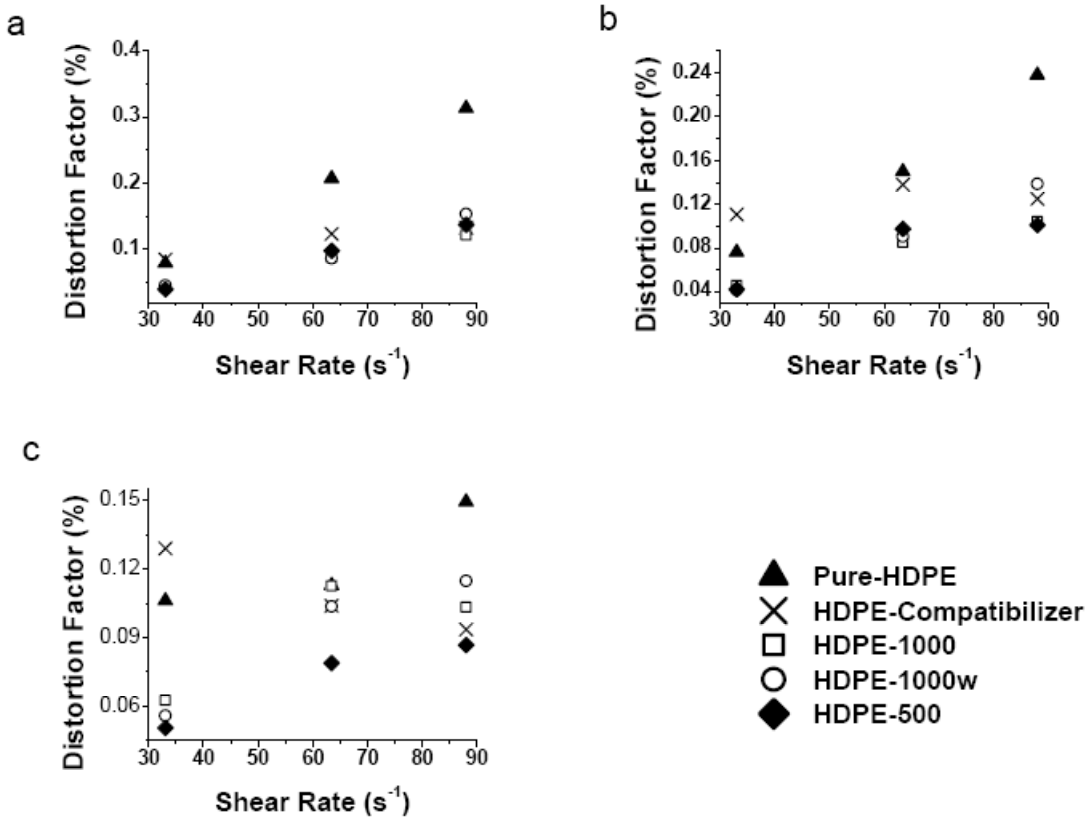

Figure 2.14: The effect of different clay loadings and compatibilizer on the pressure fluctuation measured with distortion factor (DF). (a) DF versus shear rate for transducer 1 at position P1. (b) DF versus shear rate for transducer 2 at position P2. (c) DF versus shear rate for transducer 3 at position P3.

The reduction caused by 0.05 wt % organoclay was 2 decades less at low shear rate and a decade less at high shear rate (compare the DF values at shear rates 33 s^{-1} and 88s^{-1} respectively). Both 0.1 wt % (HDPE-1000) and 0.05 wt % (HDPE-500) organoclay acted equally at the upstream of the die, hence similar DF values. However, at the die exit the DF of HDPE-500 was less than that of HDPE-1000. This difference might have contributed to the smoother surface of HDPE-500. This result could be expected because at the die exit there were other complicated phenomena such as a swelling phenomena and normal forces which could contribute to melt instability. But with a reduction in the pressure fluctuation, such complications could possibly be reduced and hence eliminate or postpone gross melt fracture. Figure 2.14 also confirmed that the compatibilizer did not improve the action of organoclay - as a processing additive - in HDPE.

The observed improvement during the extrusion of HDPE was due to the effect of organoclay and not degradation due to processing. This was confirmed by conducting further dynamic frequency sweeps on the extrudates. The elastic and loss moduli of the samples before and after extrusion were found to be the same within the allowable error margins, which were less than 3%.

2.3.4 Relationship between Rheology and Processing of HDPE and its organoclay nanocomposites

The linear and non-linear shear rheological studies showed that the elastic behavior of HDPE reduced with the addition of organoclay. This led to the decrease in non-linear material properties like normal stress differences in steady shear and stress growth tests. Also, the extensional rheology showed that the extensional stress growth

and strain in pure HDPE were reduced with the addition of organoclay and compatibilizer. All these rheological results showed why organoclay enhanced the HDPE processing during extrusion. The organoclay was able to streamline the polymer flow and hence its alignment in the flow direction. This alignment aided the elastic energy dissipation in HDPE. So, the addition of organoclay eliminated the gross melt fracture in the extruded HDPE and reduced the extrusion pressure. According to Larson [40] and Kissi et al. [41], large normal stress differences are responsible for the solid-like fracture of molten polymers-gross melt fracture. Our work confirmed this proposition because the organoclay was able to reduce the normal stress differences and hence eliminated the gross melt fracture. This work confirmed the proven fact that an addition of organoclay leads to a reduction of extensional stress growth [27]. However, based on the new results of this study, it can be argued that the elimination or postponement of melt instabilities especially gross melt fracture was not only due to the decrease of extensional stress alone. The reduction of large normal stress differences due to pre-shearing of the samples at the upstream of the die entrance contributed to the elimination or postponement of the gross melt fracture as well. It is also possible that organoclay is playing the role of a plasticizer in HDPE.

Further dispersion of clay using a compatibilizer had no synergistic effect at low clay loading of 0.1 wt %. The observed reduction in the presence of compatibilizer was solely due to the dominant effect of PE-g-MA alone. Therefore, it can be concluded that master batching followed by the dilution of the organoclay in the HDPE caused the required amount of dispersion. Thus, it is enough to use the organoclay as a processing aid without a compatibilizer. This finding is of important industrial implications and can

be implemented by adding small amounts of clay (approximately 0.05 wt %) as an additive in the extrusion of polymer especially HDPE. The effectiveness of 0.05 wt% clay loading as compared to 0.1 wt % might be because of a difference in the size of the organoclay during its dispersion in HDPE. It is more likely that there was more agglomeration in HDPE-1000 when compared to HDPE-500.

2.4 Conclusion

The effect of organoclay on the rheology and extrusion of HDPE was studied. It was found that at clay loadings between 0.05-0.1 wt percent, the shear and extensional rheology of HDPE were impacted. The elasticity of HDPE was reduced with the addition of organoclay as suggested by the data collected on the reduction of the normal stress differences of the polymer. Also, the organoclay was able to reduce the extensional stress growth and strain in HDPE. All these contributed to the ability of the organoclay to act as a good processing aid during HDPE extrusion. The gross melt fracture was eliminated with organoclay in a single-screw extruder. The intensity of the melt instabilities were characterized by both moment analysis and distortion factor. Both analyses showed that the organoclay reduced the intensity of pressure fluctuations along the die. Furthermore, this work showed that, at a low clay loading, the addition of a compatibilizer may not be necessary in the dispersion of organoclay when using a combination of master batching and dilution. Finally, this work concluded with the assertion that both shear and extensional rheology contributed to the melt instabilities observed in the extrusion of HDPE and such instabilities could be delayed by using small amounts of organoclay.

2.5 References

1. Carreras E., N. Kissi, J.-M. Piau, F. Toussaint, and S. Nigen, *Rheologica Acta*, **45,** 209 (2006).
2. Evdokia A., C. G. Georgios, and S. G. Hatzikiriakos, *Applied Rheology* 88 (2002).
3. Hatzikiriakos S. G. and K. B. Migler, *Polymer Processing Instabilities Control and Understanding*, Marcel Dekker, New York (2005).
4. Delgadillo-Velázquez O., G. Georgiou, M. Sentmanat, and S. G. Hatzikiriakos, *Polymer Engineering & Science*, **48,** 405 (2008).
5. Mitsuyoshi F. and I. Hitoshi, *Journal of Applied Polymer Science*, **84,** 2111 (2002).
6. Mitsuyoshi F. and I. Hitoshi, *Journal of Applied Polymer Science*, **84,** 2120 (2002).
7. Palza H., S. Filipe, I. F. C. Naue, and M. Wilhelm, *Polymer*, **51,** 522 (2010).
8. Anastasiadis S. H. and S. G. Hatzikiriakos, *Journal of Rheology*, **42,** 795 (1998).
9. Kolnaar J. W. H. and A. Keller, *Journal of Non-Newtonian Fluid Mechanics*, **69,** 71 (1997).
10. Pudjijanto S. and M. M. Denn, *Journal of Rheology*, **38,** 1735 (1994).
11. Perez-Gonzalez J. and M. M. Denn, *Industrial & Engineering Chemistry Research*, **40,** 4309 (2001).
12. Hatzikiriakos S. G., H. Peter, H. Wally, and W. S. Charles, *Journal of Applied Polymer Science*, **55,** 595 (1995).

13. Kazatchkov I. B., S. G. Hatzikiriakos, N. Bohnet, and S. K. Goyal, *Polymer Engineering & Science*, **39,** 804 (1999).

14. Filipe S., A. Becker, C. V. Barroso, and M. Wilhelm, *Appl. Rheology* 12 (2009).

15. Hong Y., J. J. Cooper-White, M. E. Mackay, C. J. Hawker, E. Malmstrom, and N. Rehnberg, *Journal of Rheology*, **43,** 781 (1999).

16. Hong Y., S. J. Coombs, J. J. Cooper-White, M. E. Mackay, C. J. Hawker, E. Malmström, and N. Rehnberg, *Polymer*, **41,** 7705 (2000).

17. Hatzikiriakos S. G., I. B. Kazatchkov, and D. Vlassopoulos, *Journal of Rheology*, **41,** 1299 (1997).

18. Xing K. C. and H. P. Schreiber, *Polymer Engineering & Science*, **36,** 387 (1996).

19. Migler K. B., C. Lavallee, M. P. Dillon, S. S. Woods, and C. L. Gettinger, *Journal of Rheology*, **45,** 565 (2001).

20. Kharchenko S. B., P. M. McGuiggan, and K. B. Migler, *Journal of Rheology*, **47,** 1523 (2003).

21. Franky Y., S. G. Hatzikiriakos, and M. C. Thomas, *Journal of Vinyl and Additive Technology*, **6,** 113 (2000).

22. Eugene E. R., K. R. Stuart, S. G. Hatzikiriakos, W. S. Charles, L. H. Donald, and B. Marlin, *Polymer Engineering & Science*, **40,** 179 (2000).

23. Manish S., S. G. Hatzikiriakos, and M. C. Thomas, *Polymer Engineering & Science*, **42,** 743 (2002).

24. Kazatchkov I. B., F. Yip, and S. G. Hatzikiriakos, *Rheologica Acta*, **39,** 583 (2000).

25. Palza H., B. Reznik, M. Kappes, F. Hennrich, I. F. C. Naue, and M. Wilhelm, *Polymer*, **51,** 3753 (2010).

26. Kharchenko S. B., J. F. Douglas, J. Obrzut, E. A. Grulke, and K. B. Migler, *Nat Mater*, **3,** 564 (2004).

27. Hatzikiriakos S. G., R. Nimish, and B. M. Edward, *Polymer Engineering & Science*, **45,** 1098 (2005).

28. Manish S. and S. G. Hatzikiriakos, *Journal of Vinyl and Additive Technology*, **7,** 90 (2001).

29. Kim Y. C. and K. S. Yang, *Polymer Journal*, **31,** 579 (1999).

30. Muliawan E. B., N. Rathod, S. G. Hatzikiriakos, and M. Sentmanat, *Polymer Engineering & Science*, **45,** 669 (2005).

31. Lee S. M. and J. W. Lee, in *Proceeding ANTEC, Technical Paper* New York, USA, (2001).

32. Seth M., F. Yip, and S. G. Hatzikiriakos, in *Proceeding ANTEC, Technical Paper* pp. 2649, Dallas, TX, (2000).

33. Yip F., R. Diraddo, and S. G. Hatzikiriakos, *Journal of Vinyl and Additive Technology*, **6,** 196 (2000).

34. Kim Y. C., S. J. Lee, J. C. Kim, and H. Cho, *Polymer Journal*, **37,** 206 (2005).

35. Hotta S. and D. R. Paul, *Polymer*, **45,** 7639 (2004).

36. Százdi L., Á. Ábrányi, B. Pukánszky, and J. G. Vancso, *Macromolecular Materials and Engineering*, **291,** 858 (2006).

37. Macosko C. W., *Rheology Principles, Measurements, and Applications*, Wiley-VCH, New York (1994).

38. Filipe S., I. Vittorias, and M. Wilhelm, *Macromolecular Materials and Engineering*, **293,** 57 (2008).

39. Sentmanat M. and S. G. Hatzikiriakos, *Rheologica Acta*, **43,** 624 (2004).

40. Larson R. G., *Rheologica Acta*, **31,** 213 (1992).

41. Kissi N. E., L. Léger, J. M. Piau, and A. Mezghani, *Journal of Non-Newtonian Fluid Mechanics*, **52,** 249 (1994).

CHAPTER THREE

Rheology and organoclay assisted slip in the extrusion of HDPE using Particle Image Velocimetry

Ayuba A. Adesina[†], Pedro N. Marques[‡], Paulo Teixeira[‡], Loic Hilliou[‡], Jose A. Covas[‡], Ibnelwaleed A. Hussein[*,†]

[†]Department of Chemical Engineering, King Fahd University of Petroleum and Minerals, 31261, Dhahran, Saudi Arabia

[‡] Department of Polymer Engineering/Inst. Polymers & Composites/I3N University of Minho, Campus Azurem, 4800-058, Guimaraes, Portugal

Abstract

Wall slip is seen to be a source of flow enhancement and at times plays significant role during certain melt instabilities in polymer processing. In the present investigation, the effect of organoclay on the wall slip of high density polyethylene (HDPE) was investigated with the aid of particle image velocimetry (PIV). The study showed that organoclay did not cause significant wall slip during low shear testing in a parallel plate rheometer. However, during continuous extrusion of HDPE PIV measurements showed that organoclay induced more wall slip. In the presence of high shear flow, organoclay was suggested to align in the flow direction and migrate towards the die wall. The alignment and migration affect the bulk rheological properties (increase in shear thinning) and surface properties (increase in wall slip) of HDPE. Such effects contributed to the reduction in the extrusion pressure of HDPE and possibly elimination/postponement of melt instabilities in HDPE during continuous extrusion.

3.1 Introduction

Wall slip in polymer science has been an interesting topic for many decades [1, 2]. Its relevance to polymer processing and rheometry is mirrored in the large amount of review papers on the subject [3-6]. Wall slip is not currently seen as merely a rheometric complication; it can be a source of flow enhancement [7-11] and plays major role during certain melt instabilities [5, 12, 13]. Wall Slip was reported to occur in two major flow types: pressure driven flow [9, 10, 12, 14-16] and drag flow [17-19]. Many flow phenomena in pressure driven and drag flows were attributed to the effect of wall slip. Examples of such phenomena are: reduction in the polymer viscosities as the dimensions of the flow channel are reduced [1, 17, 20], sudden increase in volumetric flow rate of polymer above a critical stress , aperiodic oscillations of shear stress [21], non-sinusoidal (which may eventually be asymmetric) and decay of shear stress during large amplitude oscillation shear (LAOS) [17, 18, 22, 23] and start up of steady shear flows [24], and birefringence [3, 25] . The experimental techniques often used in quantifying the wall slip are generally subdivided into two major groups: indirect and direct methods. The indirect method is basically gap-dependent measurements. Such measurement was used in a planar couette [17, 18, 23], torsional [19, 26, 27] and pressure driven [12, 28, 29] shear flows. Direct methods were being employed more recently due to their higher sensitivity to wall slip than the other methods [21] and they provide 'direct' quantitative measurement of the relative motion of polymer melt and solid at the interface. These methods include fringe pattern fluorescence recovery after photobleaching [30], hot film [31, 32], and local velocimetry [33-40] methods. Velocimetry is the most common technique out of the direct methods. However, due to difficulty to manage velocimetry techniques with polymer melts at

high temperatures and pressure, there are no many publications in this area as compared to indirect method [34-36, 38, 40, 41]. There are several variations in velocimetry techniques. The most common were Laser Doppler Velocimetry (LDV) and Particle Image Velocimetry (PIV). LDV is very accurate and convenient since seeding is not required. However, it is time consuming due to its point by point measurement. So, for transient flows as in extrusion and injection molding, PIV gives more global picture of the flow pattern hence it is used in the study of flow instabilities and wall slip [38]. Moreover, LDV was found not to be good in the detection of partial slip [41].

Most of the work done so far on wall slip with the aid of the above experimental techniques was on polymer solutions and melts. However, slip is seen as an intrinsic feature of the response of disperse systems [42]. For example, wood flour could cause wall slip in polymers particularly high density polyethylene [43]. The wall slip was reported to increase with shear rate and wood content in the polymer [43, 44]. The host polymer is often highly filled with wood flour above 40 wt%. On the other hand, processing aids like fluoropolymer processing additives (FPPA) were reported to cause strong slip by its migration to the interface between the polymer and the wall [45]. Such slip often resulted in the elimination of sharkskin and reduction in the extrusion pressure [34, 46, 47]. FPPA would result in strong slip at concentrations less than 0.1 wt% in polyolefin. Rodríguez-González et al. recently used PIV to study the slip effect of FPPA [34]. The slip effect of solid-based processing additives like boron nitride and organoclay is not yet very clear. Rosenbaum et al. [48] observed that boron nitride did not result in a reduction of extrusion pressure of polyolefins. Based on this observation they suggested that boron nitride may not likely induce strong slip in polyolefins (i.e. 0.1 wt %). However, apparent slip may

be possible [48]. Addition of organoclay to polyolefin generally resulted in a decrease in extrusion pressure (low viscosity or high throughput) during capillary [49] and recently in slit die extrusion [50] and stress decay in high density polyethylene during the large amplitude oscillatory shear (LAOS) [51]. The mechanism underlying these observed effects is still under discussion. It was reported that organoclay has effect on the elastic properties of HDPE but experimental evidence of wall slip induced by the addition of organoclay is yet to be reported. This is the main focus of this study. We will use PIV to study the effect of organoclay on the flow kinematics of extruded HDPE in a slit die.

3.2 Experimental

3.2.1 Materials

Commercial grade HDPE (relative density= 0.952, peak melting point = 132^{o}C and melt flow index=0.05g/10min) was used in this study. The polymer was supplied by Saudi Basic Industries Corporation (Riyadh, Saudi Arabia). It has an average-weight molecular weight (M_w) of 285 kg/mol with molecular weight distribution of 26.5. Cloisite$^{(R)}$ 15A (C15A) organoclay was obtained from Southern Clay, USA. According to the supplier of the clay, the d_{001} spacing of C15A was 31.5 Å. An antioxidant, 50/50 weight blend of Irganox 1010 and Irgafos 168, supplied by Ciba Specialty Chemicals, Switzerland was added at 1000 ppm to prevent thermo mechanical degradation [52]. Oleamide was used as a slip agent to ascertain the extent of slip detection with the aid of PIV. Oleamide has a relative density of 0.93 and a melting point of 73^{o}C. It is used in this study since it migrates very fast to the layer between the wall and the polymer.

3.2.2 Melt Blending and Morphology Characterization

A Brabender 50 EHT mixer supplied with a Plastograph (Brabender® GmbH & Co. Germany) was used in the preparation of the organoclay HDPE nanocomposites. The organoclays were first heated in a vacuum oven at 108°C for more than 24 hours to remove physico adsorbed water. HDPE was ground and physically pre-mixed with organoclay and antioxidant. A desired final concentration of a particular blend was obtained by mixing additional virgin HDPE to the master batch using the same mixer. The structures of the organoclay- HDPE nanocomposites was characterized by FE-SEM Nova™ Nanosem 230 (FEI, USA) and XRD-6000 Shimadzu diffractometer (Shimadzu, Japan), as described in length elsewhere [50]. The previous results showed that the mixing-dilution method resulted in a good dispersion of organoclay in HDPE. The blending was done at a temperature of 200°C and a screw speed of 50 rpm for 10 minutes. The final concentrations of C15A in HDPE were 0.1 wt% (HDPE-1000) and 0.05 wt % (HDPE-500). Such concentrations were shown to ease the processing of HDPE [49, 50]. Oleamide of 0.5 wt % was added to HDPE (HDPE-Oleamide). HDPE-Oleamide was prepared with the aid of Brabender mixer at a screw speed of 50 rpm and temperature 200°C for 10 minutes and 1000 ppm of antioxidant were added as well.

For rheological measurements, discs of 25 mm diameter and 2 mm thickness were prepared in a Carver press from melt blended samples at a temperature of 200°C.

3.2.3 Rheological Measurement

An ARES rheometer (TA Instruments USA) equipped with 25mm diameter parallel plates was used for all the rheological measurements. Linear and non-linear viscoelastic experiments were performed. The plates were heated for at least 20 minutes

to equilibrate the temperature. Samples were allowed to relax on the plates for 100s before any rheological experiment. Frequency sweep experiments were performed in the frequency range between 0.01 rad/s and 100 rad/s. The applied strain was 10%. The strain was within the linear regime as determined by a separate strain sweep test.

Table 3.1: Crossover frequency, parameters (a and m) and correlation factors of the power law model (between wall slip velocity and wall shear stress) for all the samples during drag flow rheometry experiment in parallel plates

Sample	Cross Over Frequency (rad/s)	a ($m\ s^{-1}\ MPa^{-m}$)	m	Correlation Factor
HDPE	1.65	0.061	2.64	0.995
HDPE-Oleamide	3.93	0.034	2.18	0.996
HDPE-1000	2.37	0.032	2.16	0.997
HDPE-500	4.29	0.059	2.57	0.966

Fourier transform rheology (FT-rheology) was conducted at an excitation frequency of 0.1 Hz (0.63 rad/s) within a strain range of 10-400%. The excitation frequency was below the cross over frequency for all the samples as shown in Table 3.1. Raw torque data from ARES rheometer was digitized using 16-bit analog- to- digital converter card (ADC) from National Instruments. In this study, sampling rate of 200 data points per cycle was used whereas the ADC worked at a velocity of 25 ksamples. Thus FT analysis of oversampled data were used as detailed elsewhere [53]. It was shown that the shear stress response involves harmonics. The intensities and phases of such harmonics were used in the characterization of non-linearity in the polymer rheology. Most importantly the relative intensity of the second and third harmonics ($I_{2/1}$ and $I_{3/1}$ respectively) and relative phase angle of the third harmonic (Φ_3) were found to be very sensitive parameters in FT-rheology [53, 54]. The Experimental errors in the harmonics were found to be less than 5% and less than 5^o for Φ_3. $I_{3/1}$ and Φ_3 are sensitive to

polymer architecture and structural changes in complex soft materials [55]. $I_{2/1}$ is sensitive to flow behaviors like wall slip [56], shear banding or yield [57]. In this work, these parameters were used to analyze the impact of organoclay on FT- rheology of polyethylenes.

Steady shear rate sweep tests were conducted between 0.001 and 1 s^{-1}. The delay time before steady state was reached at each shear rate was kept at 30 s while measurement time for each steady shear rate was 30 s. Wall slip analysis in parallel plate was performed based on the assumption that wall slip is a function of shear stress only [19]. Hence, the relationship between true shear rates and apparent shear rates based on the wall slip at different gaps between the plates is:

$$\dot{\gamma}_{AR_i}(\tau_R) = \dot{\gamma}_{R_i}(\tau_R) + u_s \frac{2}{H_i} \quad (1)$$

$\dot{\gamma}_{AR_i}(\tau_R)$ is the apparent shear rate at a particular gap (H_i) between the parallel plates. $\dot{\gamma}_{R_i}(\tau_R)$ is the true shear rate at H_i. Both $\dot{\gamma}_{AR_i}(\tau_R)$ and $\dot{\gamma}_{R_i}(\tau_R)$ are function of wall shear stress, τ_R. The wall slip is represented as $u_s$in the equation. In this study, three different gaps (i.e. $i = 1,2\ and\ 3$) were used to increase the accuracy of the estimated parameters. Linear regression analysis was used to calculate both $\dot{\gamma}_{R_i}(\tau_R)$ and u_s as functions of shear stress.

3.2.3 Set-up for Rheo-PIV

Materials were processed using a single screw mini extruder (L/D=26) which is the scale down of an industrial machine and allows outputs as small as tens of grams per hour. A slit die specially designed for both rheometry and PIV measurements was attached to the mini extruder. The slit die has a rectangular section (0.001 m x 0.01 m)

with a length of 0.068 m and is equipped with two Dynisco pressure transducers located at 0.009m and 0.051m downstream from the die entrance. The pressure transducers were connected to a Dynisco's 1390 strain gage indicator. The raw data was externally digitized using 16-bit analog-to-digital converter (ADC) card (NI USB- 9215 with BNC, National Instruments, Austin, TX). The output pressure was recorded using home-written Lab VIEW programs ((LabVIEW 5.1, National Instruments).

The top surface of the slit has a sapphire transparent window (0.01m x 0.01m) at an axial position 0.037 m downstream for the PIV measurements to allow flow visualization. A gear pump (Xaloy Europe GmbH, Germany) was attached between the extruder and the die with a special adaptation device in order to stabilize the flow rate at the entrance of the slit die. This accessory was critical to exclude any extrusion instability from the present study. However, the pressure range in the gear pump was limited and the maximum attainable pressure in the slit was 35 MPa. As a result, the largest accessible shear rate in the slit die was 51 s^{-1} for the materials considered in this study.

3.2.3.1 PIV measurements

The PIV set-up was shown in Figure 3.1. The material flowing in the slit die was illuminated using a double-pulsed 532 nm Nd-YAG laser (Solo PIV III-15Hz, New Wave Research) connected to the coaxial illumination port of an optical tube (Zoom 70XL Upper Iris and 1.0X TV Tube with internal 10 mm focus, Optem, Optical Lens System) by an optical fiber. A CCD camera (FlowSense 2M CCD, Dantec Dynamics) with 1600x1186 pixels, working at a maximum repetition rate of 15 Hz and 8/10-bit intensity resolution, is connected to the optical tube, with a 590 nm epi-fluorescent filter

placed in front. The flowing melts were seeded with 0.075 wt% fluorescent polymer particles, FPP (Micro Particles GmbH, Germany). The FPP has high melting point and mean diameter of 300 ^{o}C and 9.84 μm, respectively. The maximum excitation and emission wavelengths of the FPP were 550nm and 590nm, respectively. The images taken by this optical set-up had a field of view (FOV) of 0.0105m x 0.0078m located at 36 mm from the entrance of the slit die. However, the rectangular FOV became spherical because the Teflon used as a support for the optical window formed a thin ring along its edge. The depth of field used in this work was 0.905 mm. Series of 30 image pairs (time delay between pairs of images range from 1.5 to 5 ms depending on the flow rate) were acquired for each flow condition. All images were analyzed using FlowManager v4.71 software (Dantec Dynamics). Images were divided in interrogation areas (IA) with 32x64 pixels (210 μm x 421.5 μm). Masking was used to remove areas of no interest in the images and spurious back scattered light was removed with the aid of min-max pixel values algorithm. An adaptive correlation algorithm with a central difference approximation was used to calculate the velocity vectors and produce the two dimensional velocity vectors maps, using a 50% IA overlap in both axes.

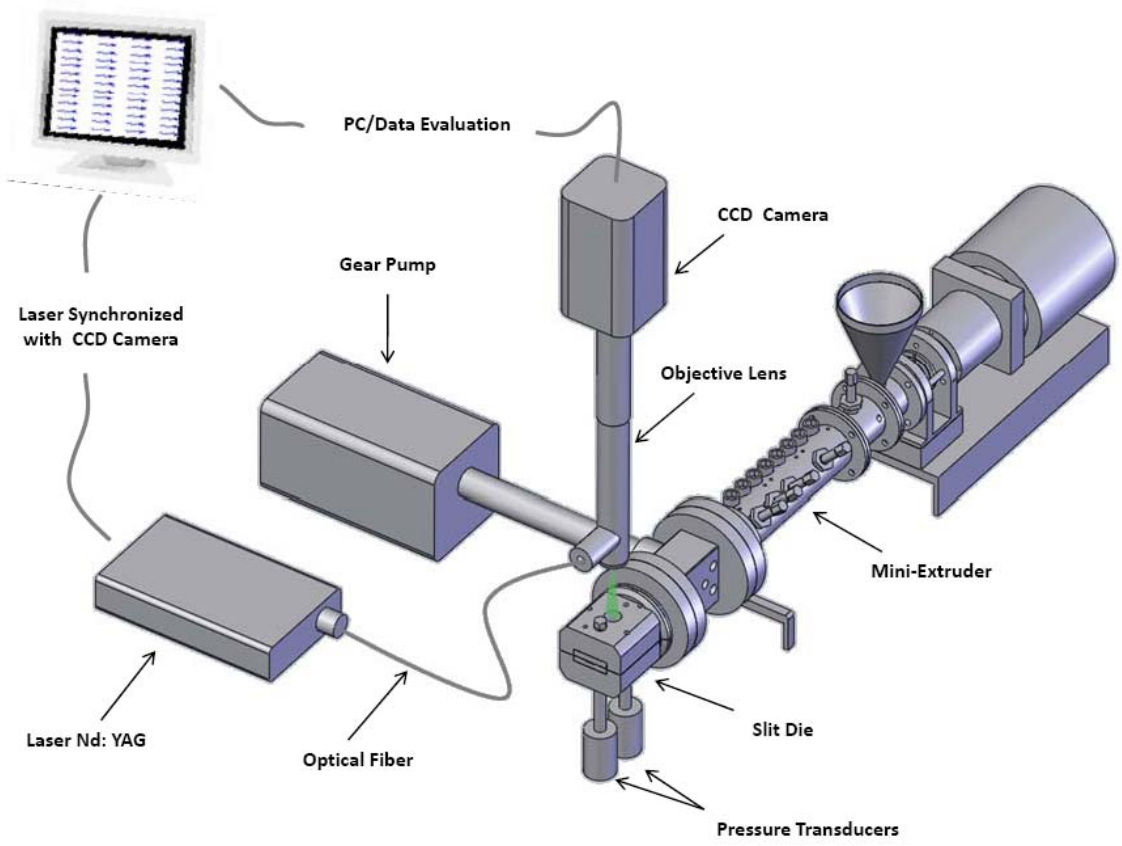

Figure 3.1: Schematic representation of the experimental set-up

3.3 Results and Discussion

3.3.1 Morphological Characterization

The wide-angle x-ray diffraction (WAXD) spectra for C15A, HDPE-1000 and HDPE-500 were displayed in Figure 3.2a. The WAXD showed that C15A has two peaks. These peaks occurred at 2.99^{o} (d_{001}=2.953nm) and 7.13^{o} (d_{002}=1.239nm), respectively. The reported experimental d_{001} differed by ≈ 6 % when compared to the manufacturer's d_{001} value. The peaks were not seen in HDPE-1000 and HDPE-500.The disappearance might be as a result of exfoliation of organoclay in HDPE or the dilution

effect during sample preparation as previously discussed in our work [50]. The SEM image of HDPE-500 shown in Figure 3.2b was obtained after etching. The figure shows that C15A was present and dispersed. Similar SEM result was obtained for HDPE-1000 as discussed in a previous publication by Adesina and Hussein [50].

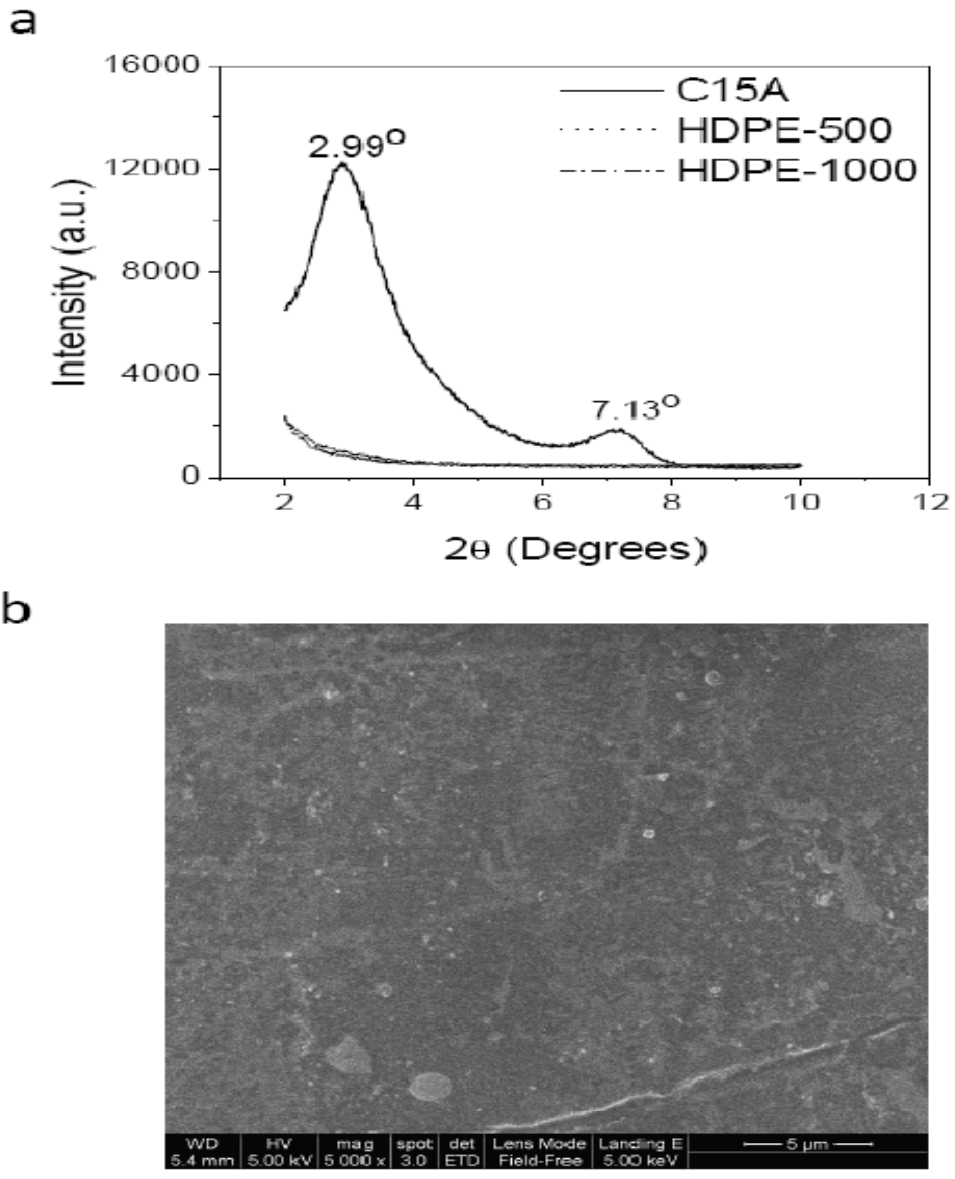

Figure 3.2: (a) WAXD for organoclay (C15A), HDPE-500 and HDPE-1000 (b) SEM for HDPE-500.

3.3.2 Rheological Results

The frequency sweep test was used to assess the influence of organoclay and Oleamide on the morphology of HDPE. Van Gurp Palmen plot in Figure 3.3 shows that organoclay had effect on the morphology of HDPE at frequency lower than the cross over frequency.

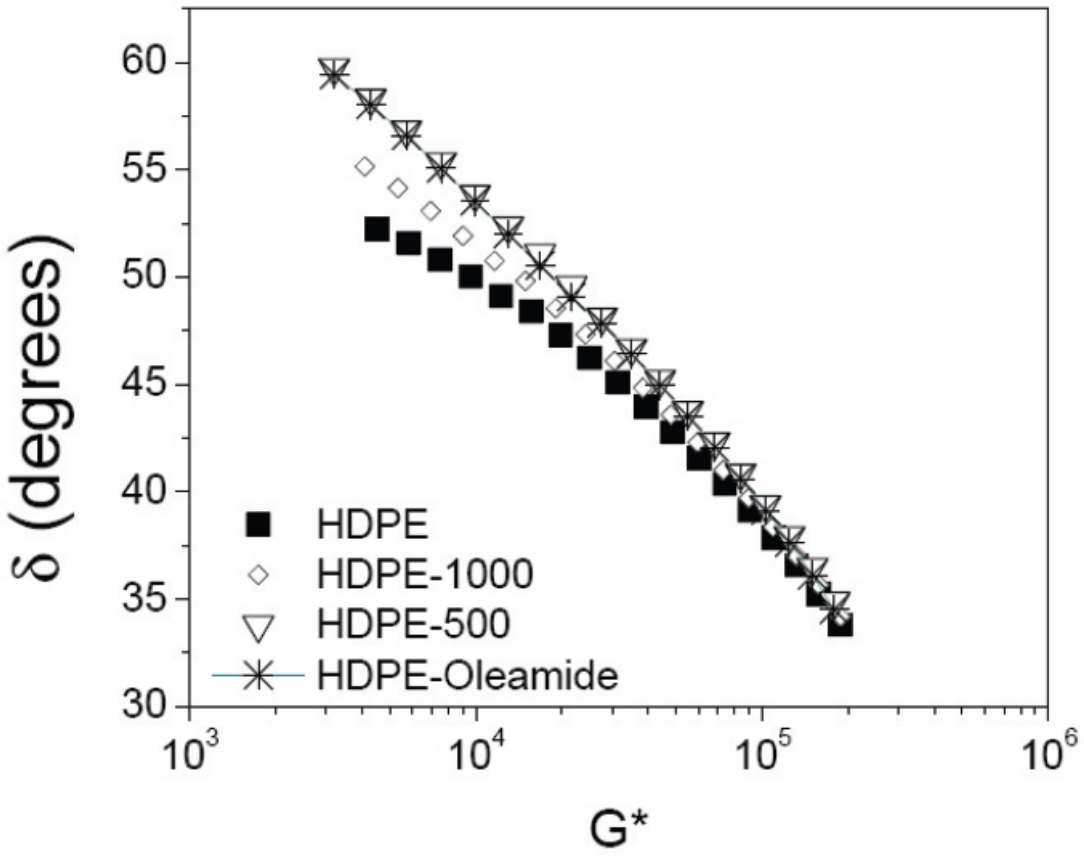

Figure 3.3: $\delta \left[= tan^{-1} \frac{G''}{G'}\right]$ versus strain amplitudes for HDPE, HDPE-500, HDPE-1000 and HDPE-Oleamide.

The plot showed that δ shifted upward. This implied that the material became more viscous (or less elastic) with the addition of organoclay. As the clay loading decreased from 0.1 to 0.05 wt%, HDPE nanocomposites showed increase in δ.

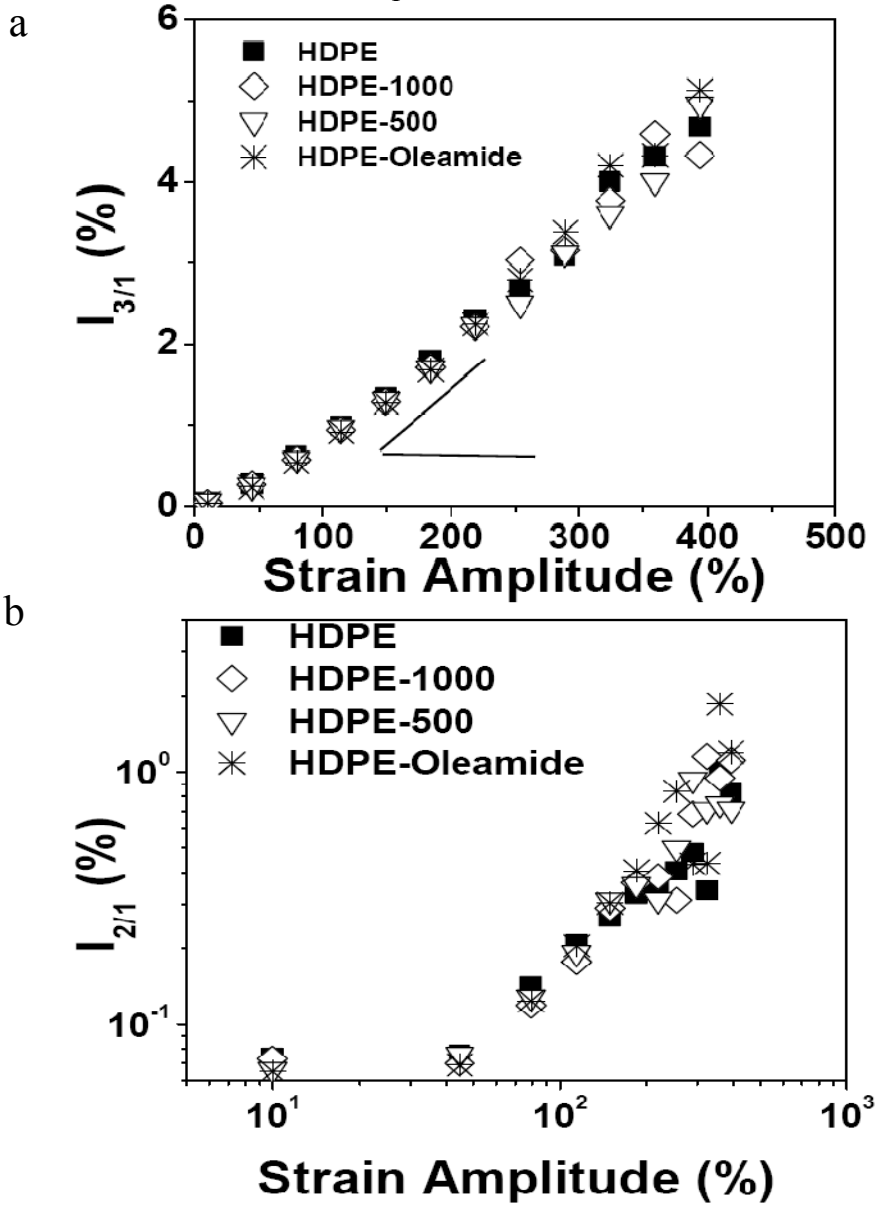

Figure 3.4 : Relative intensity of the (a) third harmonic and (b) second harmonic as functions of strain amplitude at 200^{o}C for HDPE, HDPE-500, HDPE-1000 and HDPE-Oleamide.

In an effort to further characterize the extent of non-linearity in HDPE due to the presence of organoclay, FT-rheology was implemented as described in the experimental set-up. The relative amplitude (I_3) and phase angle (Φ_3) of the third harmonic were as given in Figure 3.4 and 3.5 respectively.

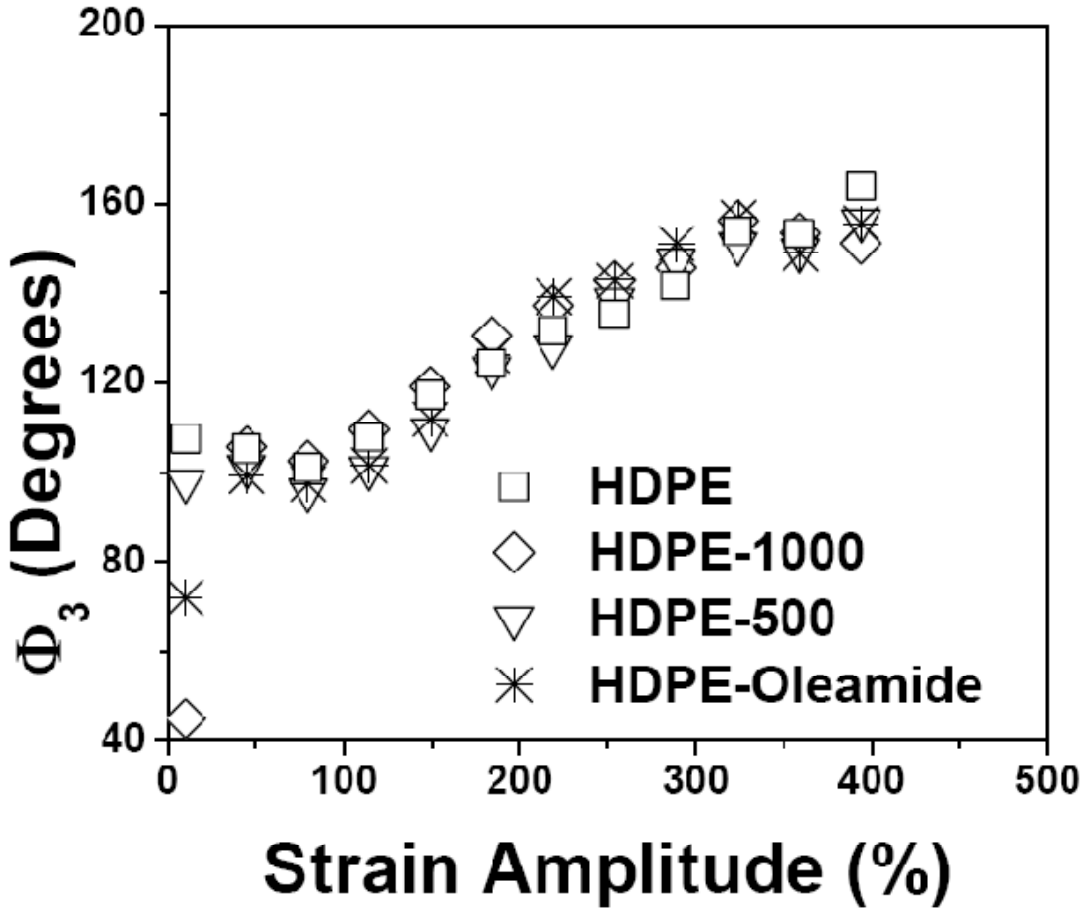

Figure 3.5: Relative phase angle of the third harmonic as a function of strain amplitude at 200^{o}C for HDPE, HDPE-500, HDPE-1000 and HDPE-Oleamide.

Figure 3.4a shows that the log-log plot of $I_{3/1}$ versus strain amplitude is the same for all the samples under the large amplitude oscillatory shear (LAOS, strain amplitude=10%-400%). Its average slope is approximately 1.3 with standard deviation of 0.03. This implies that $I_{3/1}$ does not vary quadratically with strain amplitude. Such behavior is common to HDPE that shows strain hardening behavior [58]. Extensional

rheology of the HDPE used in this work was reported earlier and the results showed that it exhibited strain hardening behavior (see Figure 9 in Adesina and Hussein [50]). However, the reported slope in the work of Hyun et al. was 1.56 [58]. The difference might be due to the difference in the polydispersity index. Figure 3.5 shows that for all samples, Φ_3 increases with the strain to attain a plateau at about 160^o. Such behavior is related to the shear thinning behavior of the samples. The slight decrease in Φ_3 due to the effect of 0.05 wt% organoclay can be neglected because it is less than 10^o (within the limits of experimental error). However, there was stress decay (figure not shown) in all the samples immediately at strain amplitude of 155 %. To analyze the cause of the stress decay, Figure 3.4b shows the plot of $I_{2/1}$ as a function of strain amplitude. The appearance of $I_{2/1}$ is an indication of non- mechanical behaviors like wall slip, shear banding, yielding or edge melt fracture [55]. Below strain amplitude of 155 %, $I_{2/1}$ for all the samples were the same. The difference in $I_{2/1}$ above the strain 155 % was obvious. Such difference might be due to the edge melt fracture effect (as observed at the end of the experiment) or a combination of wall slip and edge melt fracture. To quantify the extent of wall slip in HDPE and its nanocomposites, gap-dependent rheology as described by Yoshimura and Prud'homme [19] was utilized as discussed below.

The effect of organoclay and Oleamide on the viscosity of HDPE as a function of shear rate was shown in Figure 3.6.

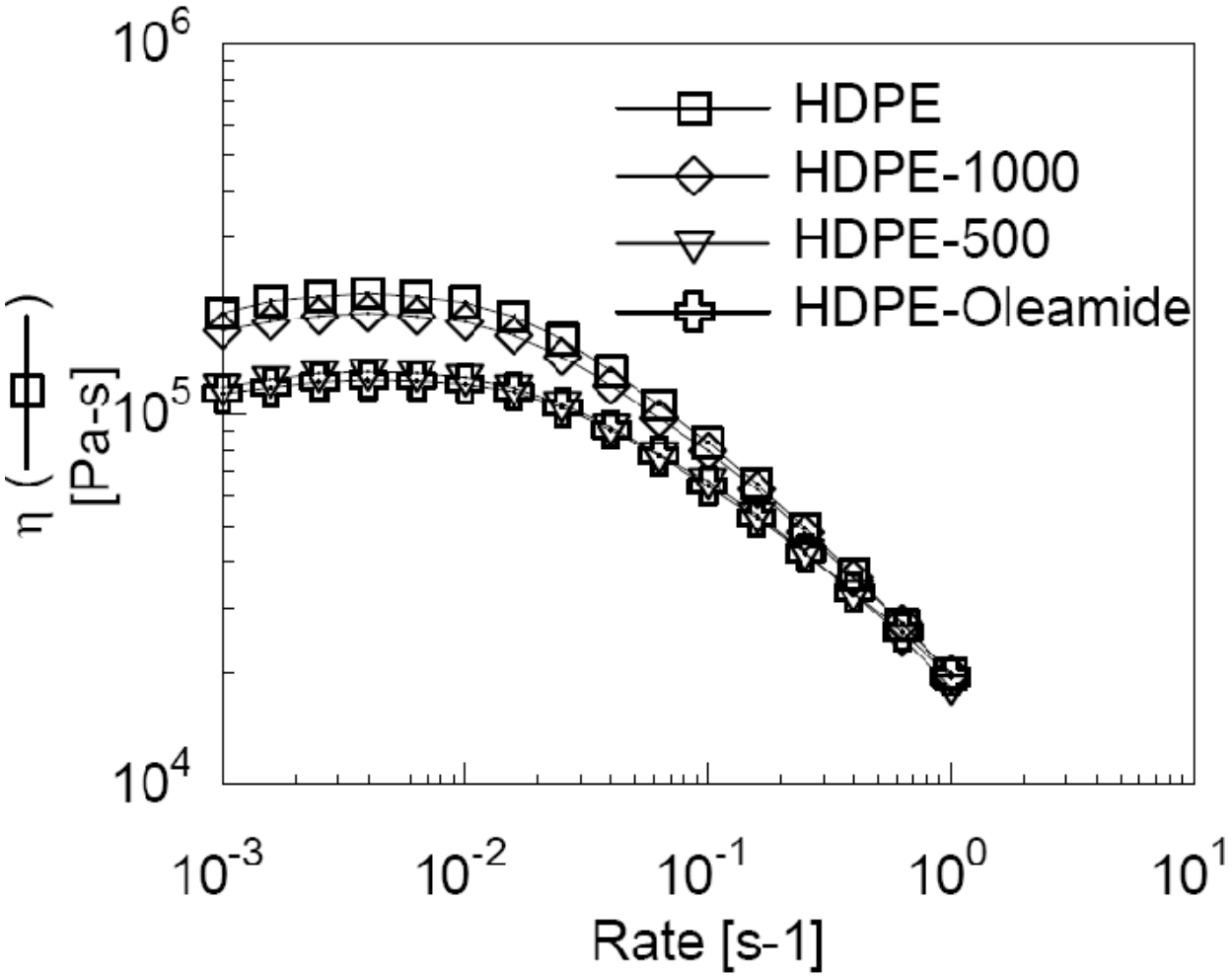

Figure 3.6 : Effect of organoclay at different clay loadings (0.1 wt % and 0.05 wt %) and slip agent on the viscosity (η) of HDPE during steady shear rate sweep test in parallel plates.

When the gap between the parallel plates was reduced from 1.5 mm to 1.2 mm, it was only HDPE that showed a small decrease in viscosity as shown in Figure 3.7. The wall slip (u_s) was obtained as defined in equation 1. It increases as the shear stress (τ_w) increases (Figure 3.8). The power law relation [$u_s = k\tau_w{}^n$] fits the plot with correlation factor of 0.987.

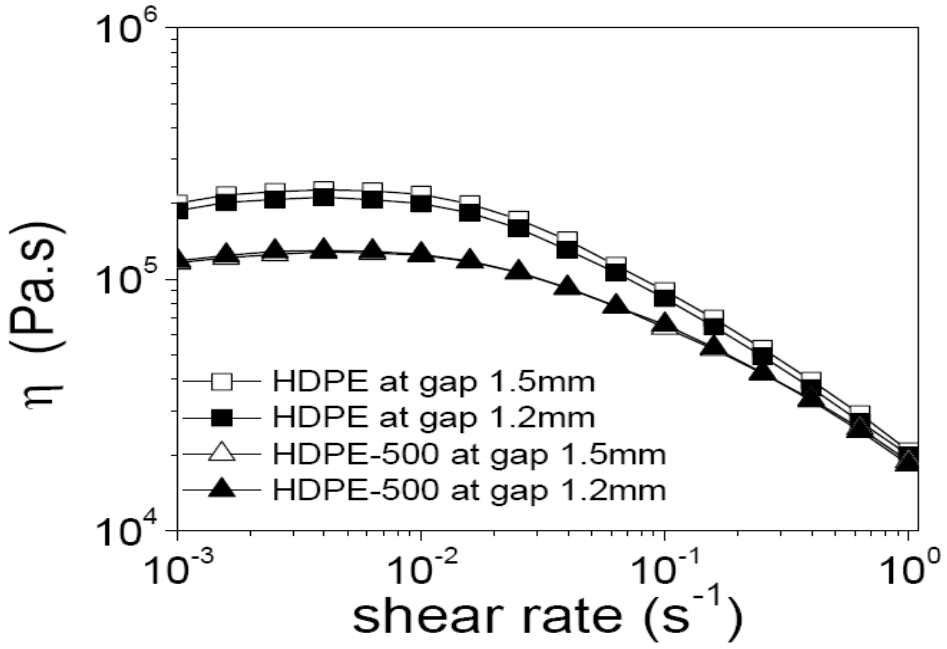

Figure 3.7 : The effect of gap between parallel plates on the viscosity of HDPE and HDPE-500 during steady shear rate sweep test.

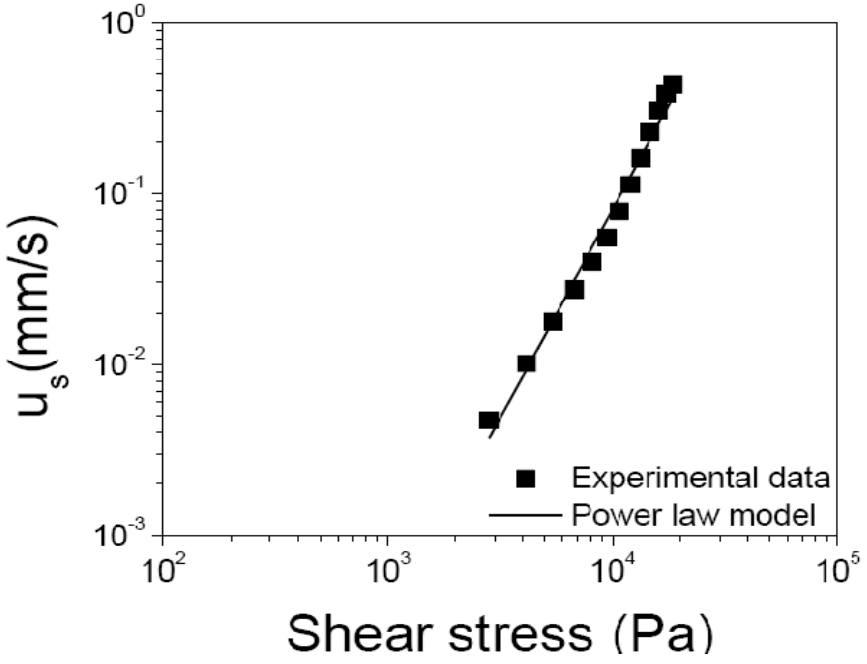

Figure 3.8 : Wall slip velocity (u_s) as a function of steady shear stress in parallel plates for HDPE.

The power law constants k and n were 6.19 $m/s^{-1}\,MPa^{-n}$ and 2.44, respectively. These values were of the same order as those reported by Hatzikiriakos and Dealy (see Table II [17]). However, the small difference in exponent n might be due to the difference in the polydispersity index of the HDPE.

3.3.3 Rheo-PIV Results

The experimental velocity profiles obtained in the channel with the PIV set up were analyzed with two different models as described by Munstedt et al [35] :

$$v_z = v_o\left[1 - \left|\frac{2x}{H}\right|^{n+1/n}\right] \tag{2}$$

and

$$v_z = v_s + v_o\left[1 - \left|\frac{2x}{H}\right|^{n+1/n}\right] \tag{3}$$

where z, x and y are the direction of flow, directions along the width of the channel and along the depth of the channel respectively. The dimensions of x and y in mm are $5 \leq x \geq -5$ and $0.5 \leq y \geq -0.5$ respectively. Also, v_o, H, n and v_s are the maximum velocity, height of the slit die, flow index from viscosity-based power law model and slip velocity at the wall, respectively. The above mentioned models were used to verify the occurrence or absence of wall slip. All the PIV measurements were taken at a depth (y) very close to the middle of the die.

3.3.3.1 PIV Measurements for HDPE

The typical velocity map in the slit die for HDPE was shown in Figure 3.9. No significant change was observed in the velocity map in this low shear rate region. The flow was expectedly unidirectional in this region as already observed by Munstedt et al. [35]. So, the flow is simply $v_z = v_z(x)$ which may either be expressed as in equation 2 or 3.

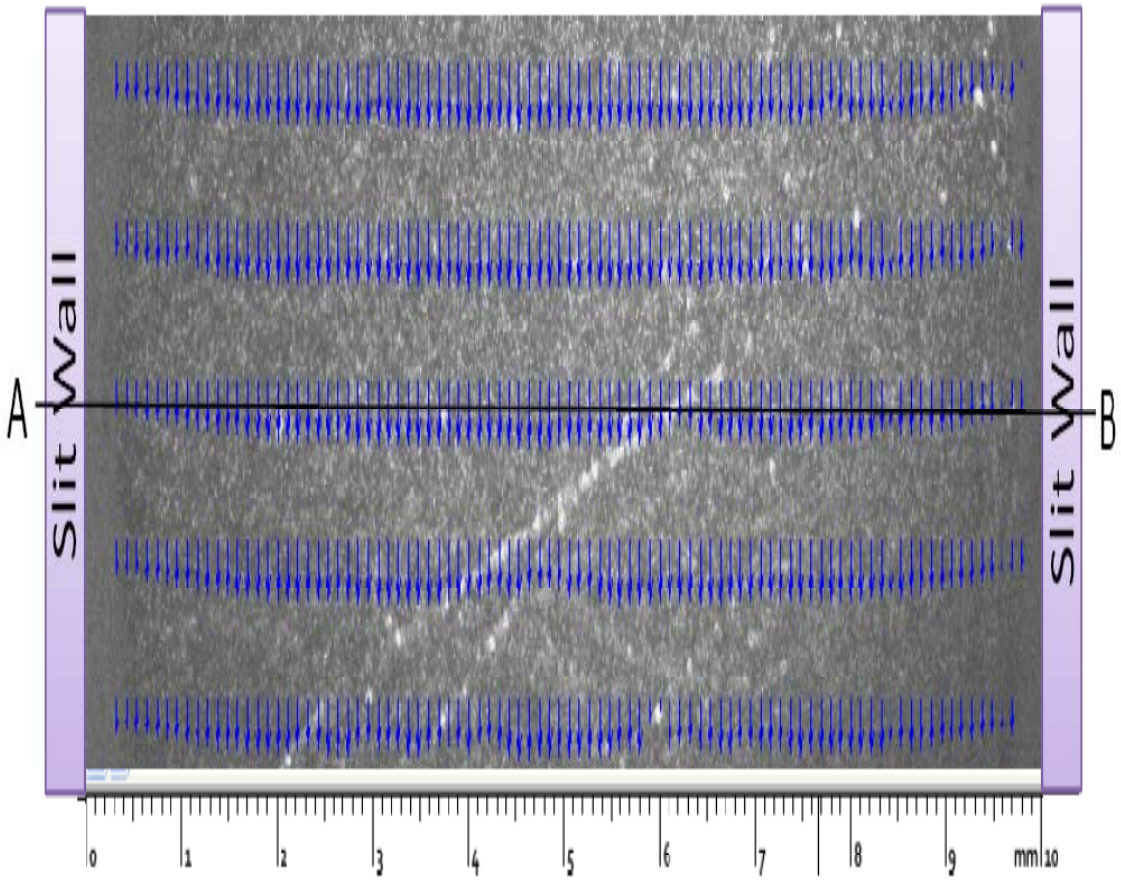

Figure 3.9 : Velocity map for the apparent shear rate 15 s^{-1} in the low shear rate region of HDPE.

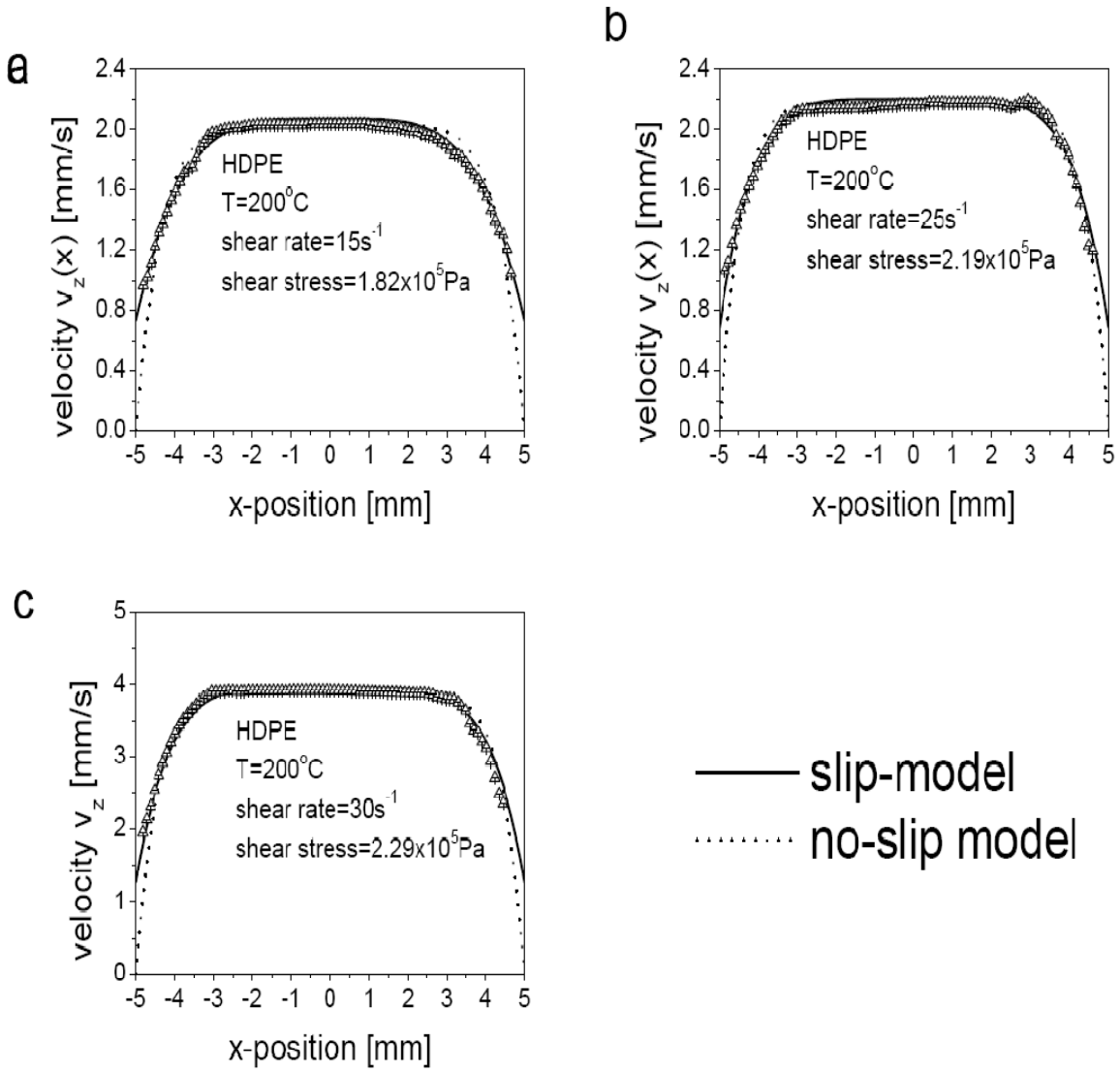

Figure 3.10 : Velocity profiles for the different apparent shear rates in the low shear rate region of HDPE.

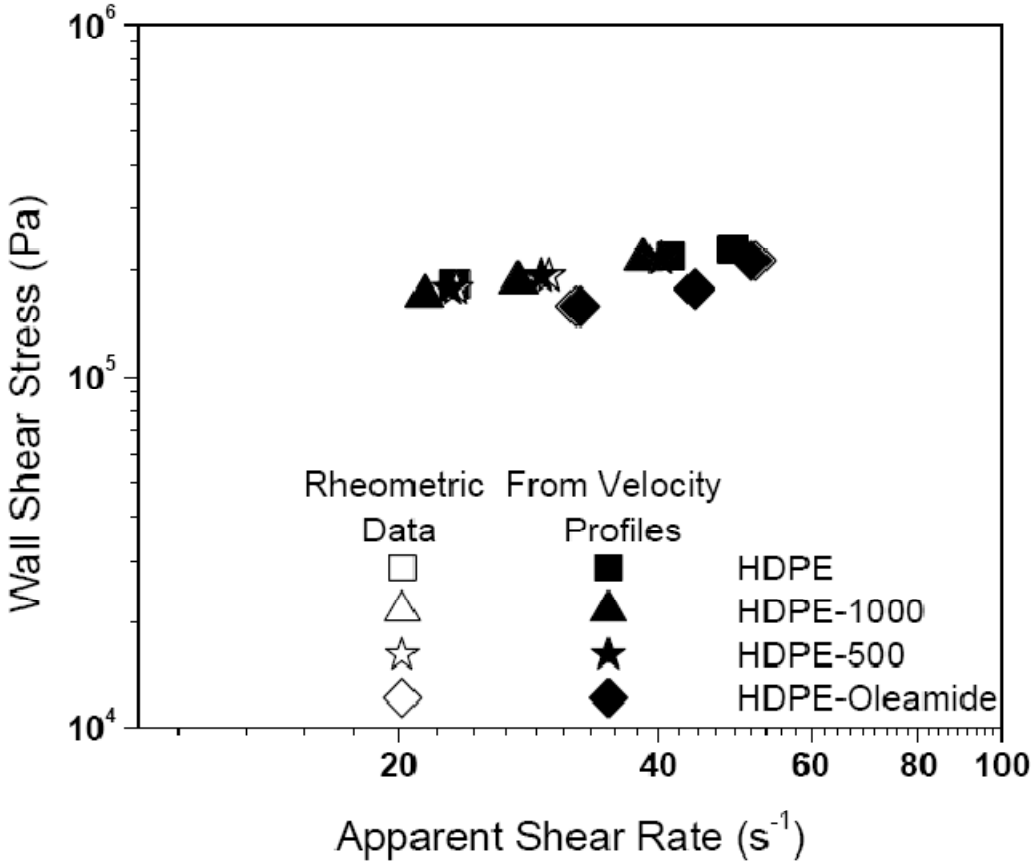

Figure 3.11 : Flow curve for HDPE, HDPE-1000, HDPE-500 and HDPE-Oleamide obtained at 200^{o}C. The filled legend corresponds to the apparent shear from rheometrical measurement while the open legend was calculated from the velocimetry measurement.

Figure 3.10 presents velocity profiles along the width of the die for different screw speed and thus corresponding shear rate. Profiles were computed at the cross section AB indicated by a dashed line in Figure 3.9. As the shear rate increases, the maximum velocity increases. The velocity profiles were well described by power law model and there was a good agreement between the rheometrical and PIV results as shown in Figures 3.11 for HDPE and its organoclay nanocomposites. The shear rates for PIV results in Figure 3.11 were obtained by differentiating equation 3 with respect to x, and

as such is a local shear rate. Also, the shear rate from rheometrical data was corrected using Rabinowitsch method. The difference between both methods at all the shear rates was less than 1%. Both equations 2 and 3 were used to fit the experimental velocity profiles. Equation 3 which included the slip velocity was the most appropriate fit for the profiles as shown by the correlation factors given in Table 3.2. Hence, wall slip occurs in HDPE at the shear rates studied in this work. These results were in agreement with similar studies by Mustedt et al. [35] and Robert et al. [36]. Such slip is typical for linear polyethylene with high molecular weight since the higher the molecular weight, the larger the slip velocity [41].

Table 3.2: The obtained correlation factors when the 'slip model' and 'no-slip model' were used to fit the experimental velocity profiles

	Correlation factor							
	HDPE		HDPE-1000		HDPE-500		HDPE-Oleamide	
Shear Rate (s^{-1})	Slip Model	No-Slip Model	Slip Model	No-Slip Model	Slip Model	No-Slip Model	Slip Model	No-Slip Model
15	0.986	0.910	0.988	0.951	0.988	0.914	0.995	0.932
19	-	-	0.967	0.760	0.992	0.912	0.987	0.880
25	0.974	0.897	0.965	0.826	0.971	0.919	0.990	0.962
30	0.974	0.902	-	-	-	-	-	-

3.3.3.2 PIV Measurement for High Density Polyethylene and 0.5 wt% Oleamide (HDPE-Oleamide)

A typical velocity map for HDPE mixed with 0.5 wt% Oleamide was shown in Figure 3.12. The velocity map was similar to that of HDPE. Also, the velocity maps at other shear rates were similar. The velocity profiles for HDPE-Oleamide at different shear rates were as shown in Figure 3.13. The slip velocity model described in equation 3 was more suitable for this analysis. The accuracy of the velocity profile data was reflected in the agreement between the rheometrical and PIV results for HDPE-Oleamide as shown in Figure 3.11.

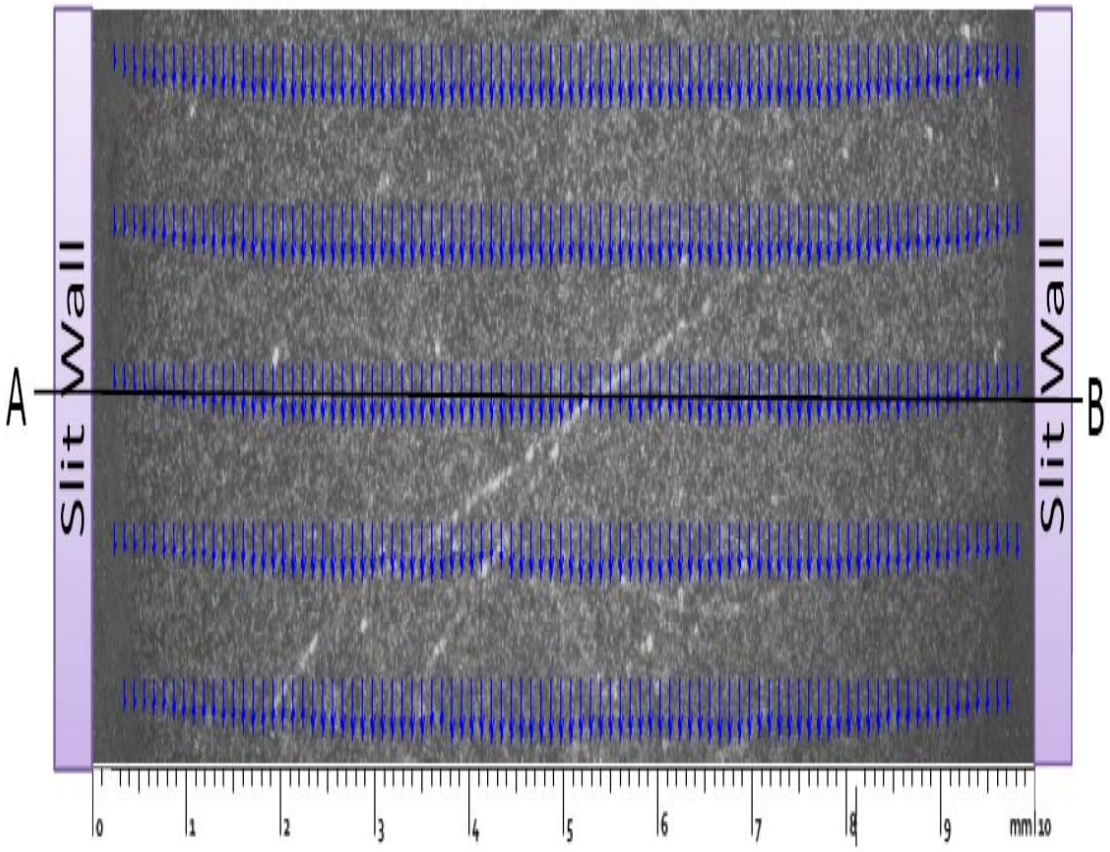

Figure 3.12 : Velocity map for HDPE-Oleamide at apparent shear rate 15 s^{-1} in the stable flow regime.

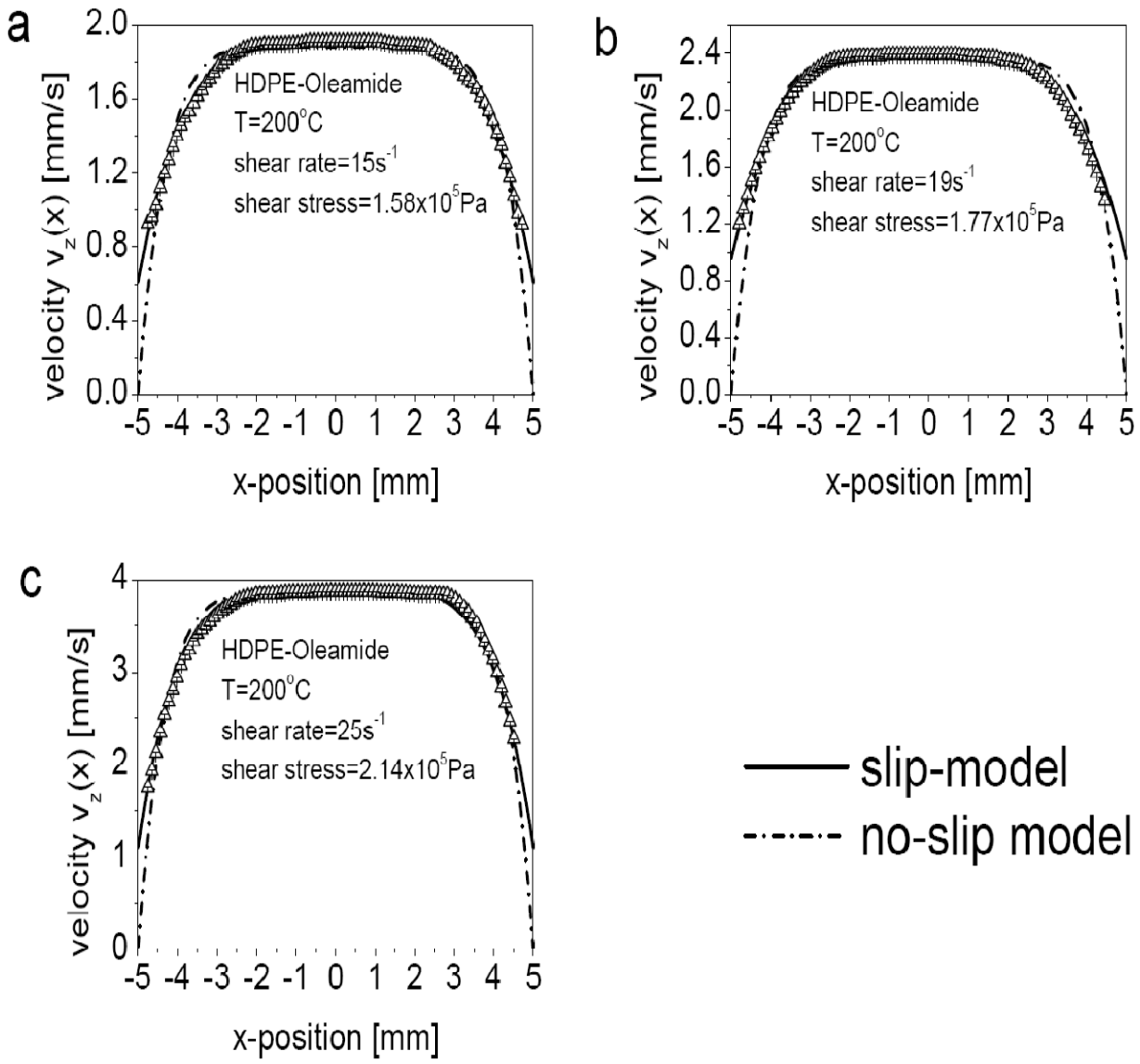

Figure 3.13 : Velocity profiles for the different apparent shear rates in the low shear rate regime of HDPE-Oleamide.

3.3.3.3 PIV Measurement for HDPE and Organoclay at low loadings (HDPE-1000 and HDPE-500)

The velocity maps (figures not shown) for both 0.1 wt% (HDPE-1000) and 0.05 wt % (HDPE-500) organoclay in HDPE were similar to the velocity map of HDPE and HDPE-Oleamide. Figures 3.14 and 3.15 showed the velocity profiles for HDPE-1000 and HDPE-500, respectively. Again, the slip velocity model was used to fit the experimental data and then a comparison was made with the results of no-slip model as expressed in equation 2. The results showed that slip occurred in pure HDPE melt containing a slip agent (Oleamide) and HDPE containing organoclay at low clay loading. There is a need to compare the extent of induced slip in these samples.

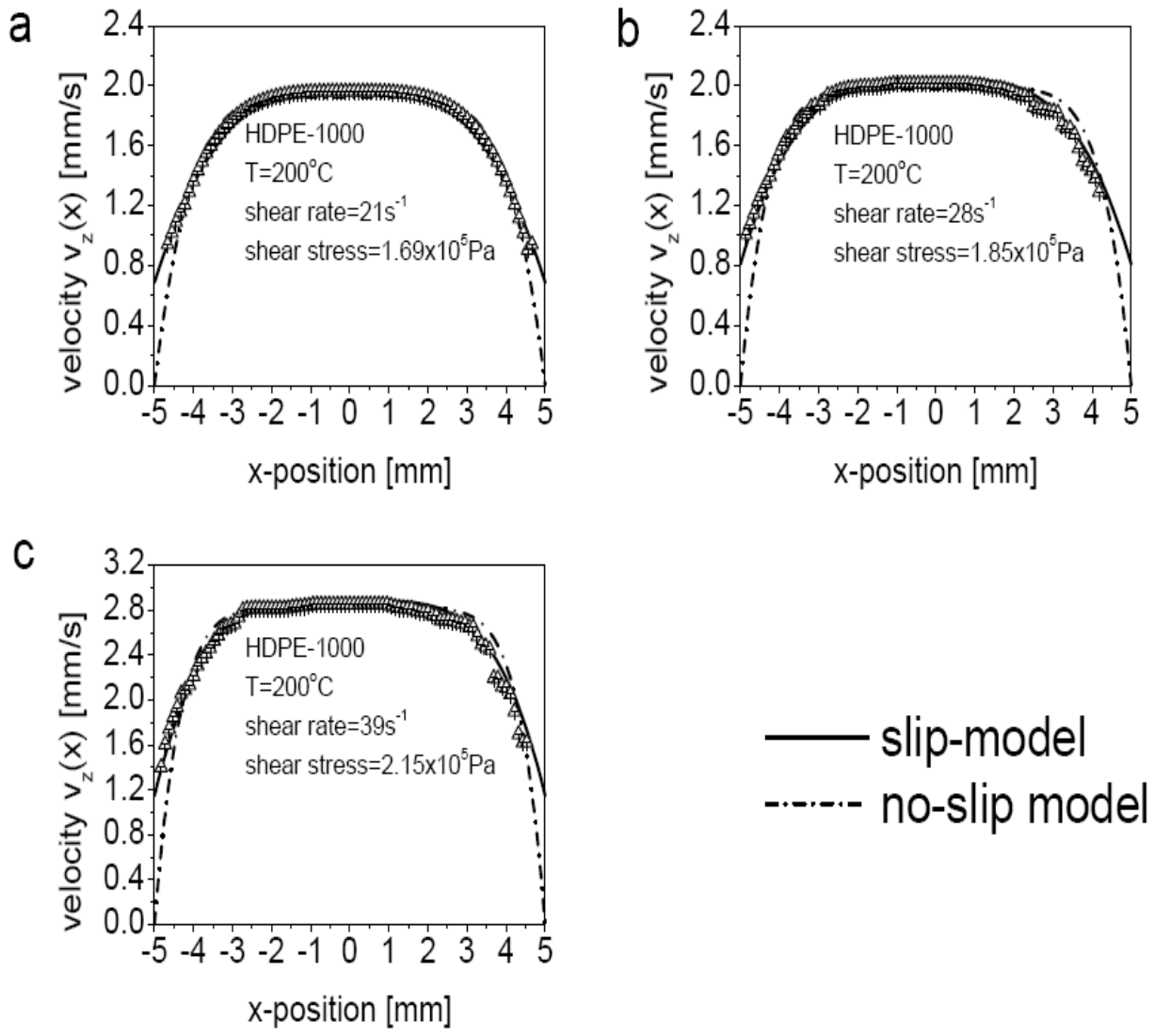

Figure 3.14 : Velocity profiles for HDPE-1000 at different apparent shear rates in the stable flow region.

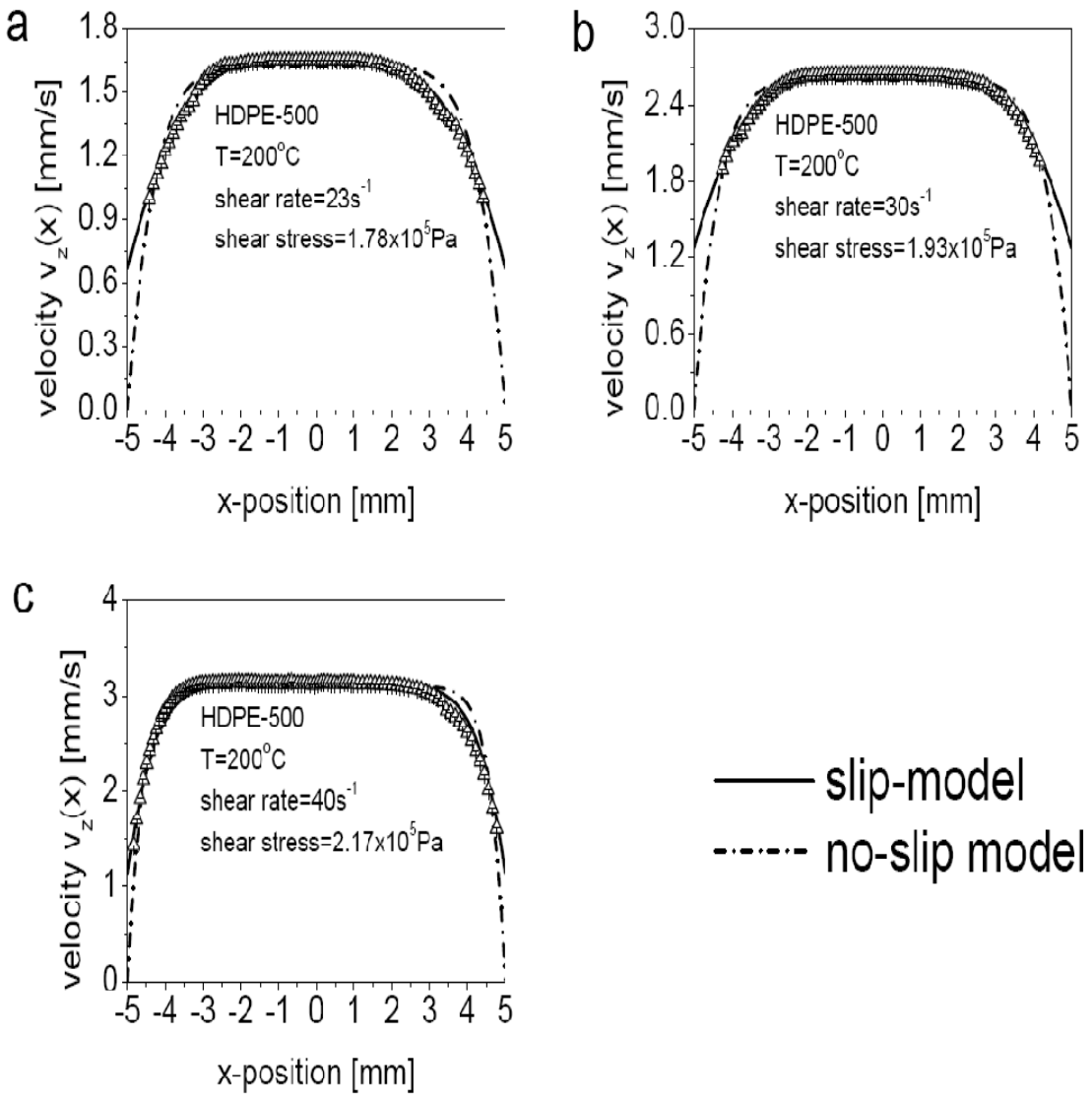

Figure 3.15 : Velocity profiles for the different apparent shear rates in the low shear rate regime of HDPE-500.

3.3.3.4 The stress dependency of slip velocity

The slip velocity (v_s) within the stable flow regime during the extrusion can approximately be described by [17, 35] :

$$v_s = a\tau_w^m \tag{4}$$

where v_s is in m/s and τ_w is in Pa.

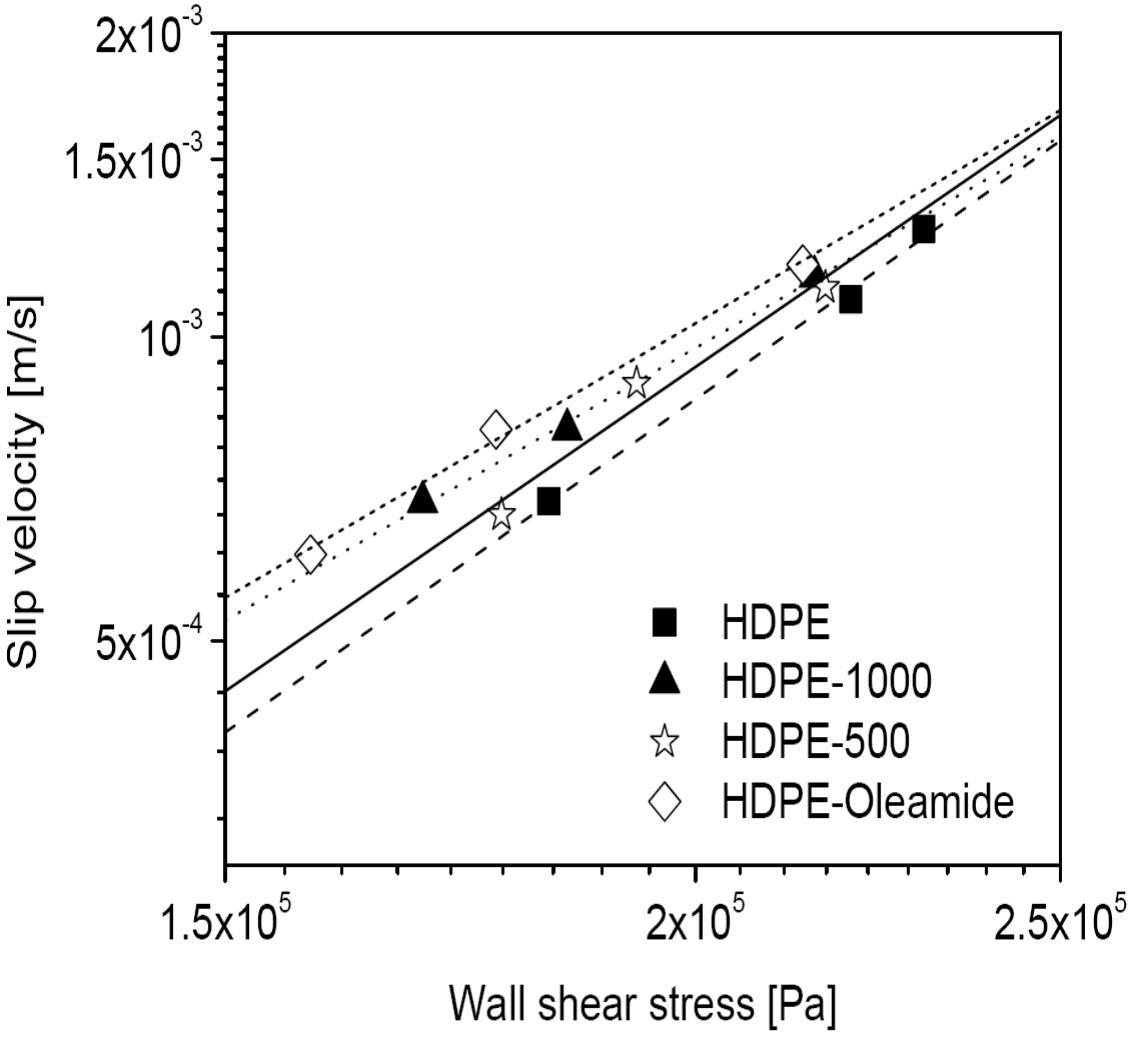

Figure 3.16 : Wall slip velocity (u_s) as a function of wall shear stress for HDPE, HDPE-500, HDPE-1000 and HDPE-Oleamide in the stable flow regime.

For all the samples considered in this study, the wall slip depends on wall shear stress and increases as the wall stress increases. Figure 3.16 shows the variation of wall slip with different wall shear stress. Table 3.1 shows the calculated values of a , m and corresponding correlation factors for each sample obtained by fitting equation 4 to the data displayed in Figure 3.16. The results from this work were compared to previous literature as shown in Table 3.3. The table showed that a and m depend on the composition of the wall material and polydispersity index (PDI) and molecular weight (Mw) of the material. However, the m from this work is very close to the obtained result by Mustedt et al. [35] since the PDI and Mw of HDPE were similar in both works. The results in Figure 3.16 showed that the highest wall slip occurred in HDPE-Oleamide. The wall slip in HDPE increased with the addition of organoclay. However, there was no clear cut in the trend of the variation of wall slip with wall shear stress for both HDPE-1000 and HDPE-500. At relatively low shear stress in the plot, the wall slip in HDPE-1000 was higher but the slope of HDPE-500 became steeper at higher wall shear stress.

Table 3.3: Comparison between power law model (between wall slip velocity and wall shear stress) parameters from this work and literature for HDPE

Temperature and HDPE properties	Rheometer Fixture	Wall material	a ($m\,s^{-1}\,MPa^{-m}$)	m
200°C;Mw/Mn=9.4; Mw=178kg/mol [a]	Sliding Plate	type 420 stainless steel	15.7	3.3
180°C;Mw/Mn=9.4; Mw=178kg/mol [a]	Sliding Plate	type 420 stainless steel	11.05	3.29
190°C;Mw/Mn=15; Mw=250kg/mol [b]	slit die	Steel 40 CrMnMo7	0.743	2.31
200°C;Mw/Mn=26.5; Mw=285kg/mol (This work)	Parallel Plate	type 316 stainless steel	6.19	2.44
200°C;Mw/Mn=26.5; Mw=285kg/mol (This work)	Slit die	Steel (0.42 % C and 13 % Cr)	0.061	2.64

a: Ref. 17; b: Ref. 35.

3.4 Further Discussion

The rheological results suggested that the organoclay did not induce additional wall slip in the parallel plate. However, the steady shear rate sweep test in ARES rheometer indicated that as the clay loading decreased from 0.1 wt% to 0.05 wt%, the shear rate dependent viscosity decreases. The decrease in viscosity was probably due to non Einstein like effects induced by the inclusion of low amount of organoclay in HDPE [59, 60]. Alternatively, we may conclude that, in the range of shear rates probed by rotational rheometry, the plasticizing effect of organoclay was mainly in the bulk rather than at the surface, since no slip could be detected using the indirect method.

Further investigation with PIV at higher shear rates in a slit die as compared to the rates in parallel plates showed that wall slip in HDPE-500 and HDPE-1000 were higher than that of HDPE. This is an indication that the phenomenon occurring at high shear rates may be different than that taking place at low shear rates such as in parallel plates. However, there is a need for further analysis at higher shear rates to determine the effect of different clay loading on the wall slip. It is likely that at the attained shear rate in slit die, the flow is strong enough to push the organoclay towards the wall. At the wall, the organoclay form a layer in the direction of flow which possibly led to the slip of the melt as observed in the case of wood flour in HDPE [43, 44]. Nevertheless, the bulk effect due to shear thinning may not be precluded. It was reported in our previous work [51] that the critical shear rate for the onset of shear thinning decreased with the addition of organoclay. This is an indication that organoclay caused more shear thinning along with more wall slip during the extrusion of HDPE. This finding is important since it may

offer explanation for the mechanism through which organoclay postpone melt instabilities in HDPE and at the same time reduced the extrusion pressure.

3.5 Conclusions

In this study, we investigated the effect of organoclay at low clay loading on the slip of HDPE at the wall during extrusion. The results showed that the reduction in the shear rate dependent viscosity of HDPE in parallel plates was due to the enhanced shear thinning. The enhancement occurred due to the presence of low amount of organoclay. Wall slip did not play any role in the reduction of viscosity at low shear rates. The results further showed that the shear thinning affected the bulk properties (i.e. decrease in elastic modulus) of HDPE. PIV was used in this study to quantify the magnitude of wall slip of HDPE with and without organoclay during continuous extrusion. PIV was found to be sensitive to the measurement of wall slip at low shear rates attainable in our set-up. The good agreement between the flow curves obtained via rheometry and PIV methods confirmed the accuracy of the PIV techniques. From the results of PIV measurements, organoclay induced more wall slip in HDPE at all shear rates. Hence, it is apparent that the mechanism that explains the effect of organoclay on HDPE during continuous extrusion should involve both bulk effect like shear thinning and surface effect like wall slip. Furthermore, the experimental findings confirmed our previous analysis that the organoclay, in the presence of high shear flow, align in the direction of flow and migrate to the surface. Such alignment and migration resulted in dual effect on bulk and surface properties of HDPE. However, there is still a need to conduct PIV measurements at higher shear rates where melt instabilities like gross melt fracture

occurred. Such experiment will confirm the role of wall slip in elimination/postponement of melt fracture in HDPE by organoclay.

3.6 References

1. Mooney, M. *Journal of Rheology* **1931,** 2, (2), 210-222.

2. Reiner, M. *Journal of Rheology* **1931,** 2, (4), 337-350.

3. Denn, M. M. *Annual Review of Fluid Mechanics* **2001,** 33, (1), 265-287.

4. Schowalter, W. R. *Journal of Non-Newtonian Fluid Mechanics* **1988,** 29, 25-36.

5. Granick, S.; Binder, K.; de Gennes, P. G.; Giannelis, E.; Grest, G.; Hervet, H.; Krishnamoorti, R.; Léger, L.; Manias, E.; Raphaël, E.; Wang, S. Q.; Wang, S.-Q., Molecular Transitions and Dynamics at Polymer / Wall Interfaces: Origins of Flow Instabilities and Wall Slip. In *Polymers in Confined Environments*, Springer Berlin / Heidelberg: 1999; Vol. 138, pp 227-275.

6. Joshi, Y. M.; Lele, A. K.; Mashelkar, R. A. *Journal of Non-Newtonian Fluid Mechanics* **2000,** 89, (3), 303-335.

7. Done, D. S.; Baird, D. G.; Everage, A. E. *Chemical Engineering Communications* **1983,** 21, (4), 293 - 309.

8. Ghanta, V. G.; Riise, B. L.; Denn, M. M. *Journal of Rheology* **1999,** 43, (2), 435-442.

9. PÃ©rez-GonzÃ¡lez, J.; Denn, M. M. *Industrial & Engineering Chemistry Research* **2001,** 40, (20), 4309-4316.

10. Piau, J. M.; El Kissi, N.; Tremblay, B. *Journal of Non-Newtonian Fluid Mechanics* **1988,** 30, (2-3), 197-232.

11. Piau, J. M.; Nigen, S.; El Kissi, N. *Journal of Non-Newtonian Fluid Mechanics* **2000,** 91, (1), 37-57.

12. Kalika, D. S.; Denn, M. M. *Journal of Rheology* **1987,** 31, (8), 815-834.

13. Ramamurthy, A. V. *Journal of Rheology* **1986,** 30, (2), 337-357.

14. Perez-Gonzalez, J. *Journal of Rheology* **2001,** 45, (4), 845-853.

15. Piau, J. M.; El Kissi, N. *Journal of Non-Newtonian Fluid Mechanics* **1994,** 54, 121-142.

16. Piau, J. M.; Kissi, N.; Mezghani, A. *Journal of Non-Newtonian Fluid Mechanics* **1995,** 59, (1), 11-30.

17. Hatzikiriakos, S. G.; Dealy, J. M. *Journal of Rheology* **1991,** 35, (4), 497-523.

18. Reimers, M. J.; Dealy, J. M. *Journal of Rheology* **1996,** 40, (1), 167-186.

19. Yoshimura, A.; Prud'homme, R. K. *Journal of Rheology* **1988,** 32, (1), 53-67.

20. Henson, D. J.; Mackay, M. E. *Journal of Rheology* **1995,** 39, (2), 359-373.

21. Archer, L. A., Wall Slip: Measurement and Modeling Issues. In *Polymer Processing Instabilities: Control and Understanding*

Hatzikiriakos, S. G.; Migler, K. B., Eds. Marcel Dekker: U.S.A, 2005; pp 73-120.

22. Black, W. B.; Graham, M. D. *Physical Review Letters* **1996,** 77, (5), 956.

23. Dhori, P. K.; Giacomin, A. J.; Slattery, J. C. *Journal of Non-Newtonian Fluid Mechanics* **1997,** 71, (3), 215-229.

24. Dao, T. T.; Archer, L. A. *Langmuir* **2002,** 18, (7), 2616-2624.

25. Barone, J. R.; Wang, S. Q. *Journal of Rheology* **2001,** 45, (1), 49-60.

26. Hay, G.; Mackay, M. E.; McGlashan, S. A.; Park, Y. *Journal of Non-Newtonian Fluid Mechanics* **2000,** 92, (2-3), 187-201.

27. Mackay, M. E.; Henson, D. J. *Journal of Rheology* **1998,** 42, (6), 1505-1517.

28. Hay, G.; Mackay, M. E.; Awati, K. M.; Park, Y. *Journal of Rheology* **1999,** 43, (5), 1099-1116.

29. Yang, X.; Ishida, H.; Wang, S.-Q. *Journal of Rheology* **1998,** 42, (1), 63-80.

30. Migler, K. B.; Hervet, H.; Leger, L. *Physical Review Letters* **1993,** 70, (3), 287.

31. Kraynik, A. M.; Schowalter, W. R. *Journal of Rheology* **1981,** 25, (1), 95-114.

32. Lim, F. J.; Schowalter, W. R. *Journal of Rheology* **1989,** 33, (8), 1359-1382.

33. Mhetar, V.; Archer, L. A. *Macromolecules* **1998,** 31, (19), 6639-6649.

34. Rodríguez-González, F.; Pérez-González, J.; de Vargas, L.; Marín-Santibáñez, B. *Rheologica Acta* **2010,** 49, (2), 145-154.

35. Munstedt, H.; Schmidt, M.; Wassner, E. *Journal of Rheology* **2000,** 44, (2), 413-427.

36. Robert, L.; Demay, Y.; Vergnes, B. *Rheologica Acta* **2004,** 43, (1), 89-98.

37. Mitsoulis, E.; Schwetz, M.; Münstedt, H. *Journal of Non-Newtonian Fluid Mechanics* **2003,** 111, (1), 41-61.

38. Fournier, J. E.; Lacrampe M. F. ; Krawczak, P. *eXPRESS Polymer Letters* **2009,** 3, 569-578.

39. Mackley, M. R.; Moore, I. P. T. *Journal of Non-Newtonian Fluid Mechanics* **1986,** 21, (3), 337-358.

40. Nigen, S.; El Kissi, N.; Piau, J. M.; Sadun, S. *Journal of Non-Newtonian Fluid Mechanics* **2003,** 112, (2-3), 177-202.

41. Rodríguez-González, F.; Pérez-González, J.; Marín-Santibáñez, B. M.; de Vargas, L. *Chemical Engineering Science* **2009,** 64, (22), 4675-4683.

42. Buscall, R. *Journal of Rheology* **2010,** 54, (6), 1177-1183.

43. Hristov, V.; Takács, E.; Vlachopoulos, J. *Polymer Engineering & Science* **2006,** 46, (9), 1204-1214.

44. Li, T. Q.; Wolcott, M. P. *Polymer Engineering & Science* **2005,** 45, (4), 549-559.

45. Hatzikiriakos, S. G.; Dealy, J. M. *International Polymer Processing* **1993,** 1, 36-43.

46. Kharchenko, S. B.; McGuiggan, P. M.; Migler, K. B. *Journal of Rheology* **2003,** 47, (6), 1523-1545.

47. Migler, K. B.; Lavallee, C.; Dillon, M. P.; Woods, S. S.; Gettinger, C. L. *Journal of Rheology* **2001,** 45, (2), 565-581.

48. Rosenbaum, E. E.; Randa, S. K.; Hatzikiriakos, S. G.; Stewart, C. W.; Henry, D. L.; Buckmaster, M. D., A New Processing Additive Eliminating Surface and Gross Melt Fracture in the Extrusion of Polyolefins and Fluoropolymers. In *ANTEC'98*, Atlanta, 1998; Vol. 44.

49. Hatzikiriakos, S. G.; Rathod, N.; Muliawan, E. B. *Polymer Engineering & Science* **2005,** 45, (8), 1098-1107.

50. Adesina, A. A.; Hussein, I. A. *Journal of Applied Polymer Science* **in press**.

51. Adesina, A. A.; Hussein, I. A. **submitted**.

52. Hussein, I. A.; Ho, K.; Goyal, S. K.; Karbashewski, E.; Williams, M. C. *Polymer Degradation and Stability* **2000,** 68, (3), 381-392.

53. Vittorias, I.; Parkinson, M.; Klimke, K.; Debbaut, B.; Wilhelm, M. *Rheologica Acta* **2007,** 46, (3), 321-340.

54. Neidhofer, T.; Wilhelm, M.; Debbaut, B. *Journal of Rheology* **2003,** 47, (6), 1351-1371.

55. Hilliou, L.; Wilhelm, M.; Yamanoi, M.; Gonçalves, M. P. *Food Hydrocolloids* **2009,** 23, (8), 2322-2330.

56. Michael, D. G. *Journal of Rheology* **1995,** 39, (4), 697-712.

57. Klein, C. O.; Spiess, H. W.; Calin, A.; Balan, C.; Wilhelm, M. *Macromolecules* **2007,** 40, (12), 4250-4259.

58. Hyun, K.; Baik, E. S.; Ahn, K. H.; Lee, S. J.; Sugimoto, M.; Koyama, K. *Journal of Rheology* **2007,** 51, (6), 1319-1342.

59. Mackay, M. E.; Dao, T. T.; Tuteja, A.; Ho, D. L.; Van Horn, B.; Kim, H.-C.; Hawker, C. J. *Nat Mater* **2003,** 2, (11), 762-766.

60. Tuteja, A.; Mackay, M. E.; Hawker, C. J.; Van Horn, B. *Macromolecules* **2005,** 38, (19), 8000-8011.

CHAPTER FOUR

Rheology and Enhancement of Extrusion of linear and branched Polyethylenes using low amount of Organoclay

Ayuba A. Adesina[1], Abdulhadi A. Al-Juhani[1], Nouar Tabet[2], Anwar Ul-Hamid[3], Ibnelwaleed A. Hussein[1]*

[1]*Department of Chemical Engineering, King Fahd University of Petroleum and Minerals, 31261, Dhahran, Saudi Arabia*

[2]*Department of Physics, King Fahd University of Petroleum and Minerals, 31261, Dhahran, Saudi Arabia*

[3]*Research Institute, King Fahd University of Petroleum and Minerals, 31261, Dhahran, Saudi Arabia*

Abstract

Interaction between 0.05 wt% organoclay and polyethylenes of different branch content (BC) is the focus of this work. The organoclay is considered as a processing aid in polyethylene provided the clay loading is low. Linear rheology (van Gurp-Palmen plot) is used to study the effect of organoclay on the molecular structure of the polyethylene. Organoclay has effect only on the van Gurp-Palmen plot of linear polyethylene without branching. FT-rheology, extrusion at high shear rates in a slit rheometer, transient stress growth analysis and extensional rheology were conducted to understand the behavioral pattern of organoclay as a processing aid. Organoclay reduced the transient stress overshoot, normal stress difference, zero-shear viscosity, onset of shear thinning and extrusion pressure of polyethylene. The reduction is more pronounced in linear polyethylene without branching. Such effects gradually decrease as the branch content

increases. The trend is independent of the type of flow (shear and extensional). It is striking to note that FT-rheology is not effective in explaining the impact of organoclay on polyethylene. The work concludes with the proposition that organoclay (as low as 0.05 wt %) is a good processing aid for linear polyethylene and polyethylenes with low BC.

Keywords: Organoclay, Polyethylene, Long Chain Branching, Linear and Non-linear rheology

*Corresponding Author: Email: ihussein@kfupm.edu.sa; Tel/Fax: +96638602235/4234

4.1 Introduction

Polymer- organoclay nanocomposites had attracted the attention of industrialists and researchers because of their different properties enhancement as compared to virgin polymers. The credit goes to the inclusion of organoclay in the polymers. Enhanced mechanical and rheological properties, decreased gas permeability, increased heat resistance and reduced permeability are some of the unique features of these nanocomposites [1-6]. These improvements were achieved at relatively clay loading of 1-10 wt % [7]. Further, Hatzikiriakos et al. [8] and recently Adesina and Hussein [9] showed that addition of low loading (0.05-1wt%) of organoclay can shift polyolefin melt instabilities, especially gross melt fracture, to higher shear rate. Also, Lee et al. [10] obtained novel blown-film polyethylene-clay nanocomposite foams with a clay loading of less than 1wt % in the presence of supercritical carbon dioxide.

Rheology serves as indicator of polymer melt behavior in processes such as extrusion [8] and injection molding [11]. Indeed, it is a well established practice that rheology is related to processability in many aspects and it plays a key role in optimizing polymer processing operations [12, 13]. Many publications investigated the effect of dispersion and clay loading on the rheology of polyolefin- organoclay based nanocomposites. Above percolation threshold [13-16], organoclay was reported to have strong effects on linear and non linear rheology of the polymer matrix [11]. Generally, organoclay contributes to the increase in viscosity and elasticity of the host matrix [11]. For small angle oscillatory shear experiment, the storage modulus in the terminal regime is a solid-like plateau. There is a shear thinning at low shear rate where the host polymer matrix would ordinarily have zero shear viscosity [7, 11, 17]. Critical strain, at

which rheological response become nonlinear, is said to be dependent on clay loading and extent of exfoliation and shifts to lower values with increasing solid volume fraction of organoclay [17-19]. The clay loading considered in all the above mentioned cases is above 1 wt%. Treece et al. [16] showed that low clay loadings and poor exfoliation did not show shear thinning at low shear rates but modest increase in the zero shear viscosity due to the inclusion of the solid particles. Hatzikiriakos et al. [8] reported that the presence of organoclay causes a small decrease in the linear viscoelastic properties of the polymer for low concentration of 0.1wt% and in many cases this difference may not be noticed. They concluded, based on the frequency sweep test, that organoclay had no effect on the shear rheology of the host polymer [8]. Further, low clay loading (< 0.5 wt %) reduces the extensional stresses in polymers at high Hencky strain rates [8]. Organoclay, at less than 0.5 wt %, was suggested as a good processing aid due to its ability to reduce the high shear [9] and extensional stresses [8, 9]. It is apparent that many issues are yet to be resolved regarding the impact of low organoclay loading on the rheology of polyolefins. For instance, the authors [9] showed that there is a reduction in steady shear viscosity at low shear rates with the addition of organoclay. Can this effect be bulk- related or interfacial slip of the nanocomposite melt at the wall? This issue becomes more important when it was observed that there was a shift in the flow curve of some polymers towards lower shear stress during capillary extrusion [8].

Moreover, it is generally believed that extrusion of polyolefins involves several types of melt instabilities at high shear rates. These instabilities are functions of many factors including the topology, molecular weight, polydispersity index (PDI), and

branch content of the polymers among others. For instance, according to Filipe et al. [20], materials with high molecular weights and PDI are more prone to stick-slip instabilities while low molecular weight and PDI polymers are often presented with sharkskin. Several authors have also shown that branch content (BC) had significant influence on the structure and morphology of polyethylenes [21-23]. As far as we know, the effect of low clay loading on the melt rheology and extrusion of polyethylene has not been carried out systematically. So, this paper will try to consider the interaction between organoclay and the topology of polyethylene especially the branch content and distribution. Fourier transform rheology had been successfully used to characterize different linear and branched commercial polyethylenes especially in non-linear flow regimes [20, 24-26]. It was found to be sensitive to structural changes especially at the onset of non-linearity [27]. So, in this work, we will as well employ Fourier transform rheological tools to analyze the effect of low clay loading on the different commercial polyethylenes in an effort to relate this to their extrusion in the presence of low amount of organoclay. The clay loading used in this study is 0.05 wt% because this ratio gave the most promising result as discussed in our recent publication [9].

4.2 Experimental

4.2.1 Materials

HDPE and five linear low density polyethylene (LLDPE) samples of different BC, type of catalyst and co-monomer were used in this study. All samples were commercial resins produced by Exxon-Mobil. Two commercial metallocene ethylene-butene (EB) LLDPEs of different BC (13 and 19 CH_3/1000 C) and two commercial ethylene-octene (EO) LLDPEs of different BC (16 and 33 CH_3/1000 C) were tested to

examine the influence of BC and co-monomer type. The LLDPEs were selected such that they have similar melt index (MI), density and average weight molecular weight. On the other hand, one Ziegler Natta (ZN) LLDPE was selected for a comparison with m-LLDPE to examine the influence of composition distribution. Here, the overall objective is to investigate the interaction of organoclay with polyethylene based on the composition distribution and BC while other molecular parameters were kept very similar. Table 4.1 provides characterization data for all the six samples. The properties such as average weight molecular weight (Mw) and PDI were determined by Gel Permeation Chromatography (GPC) and BC was determined by 13C NMR. Details of GPC and NMR characterization were given elsewhere [28]. Density, peak melting temperatures and melt index (MI) data were provided by the manufacturer. The sample name reflects its catalyst type (metallocene or Ziegler-Natta), co-monomer type (EB or EO) and contains a number that indicates its BC (CH_3 /1000 C). For example, m-EB19 is a metallocene ethylene-butene copolymer with a BC of 19 CH_3/1000C.

Table 4.1: Investigated polyethylene samples: density, peak melting temperature (T_m), Melt Index (MI), weight-average molecular weight (Mw), and polydispersity Index (PDI) and branch content (BC) as the total number of all branches (SCB and LCB) determined by NMR

Polymer Sample	Density (g/cm^3)	Peak Melting Temperature (^oC)	MI (g/10min)	M_w (kg/mol)	PDI	BC (CH_3/1000C)
HDPE_L	0.961	140	0.7	102	6.71	0
ZN-EB13	0.918	120	1	118	3.07	13.2
m-EB15	0.91	104	1.2	108	1.95	14.5
m-EB19	0.9	92	1.2	110	1.78	18.5
m-EO16	0.902	97	1.1	90	2.04	16.32
m-EO33	0.882	70	1.1	95	1.99	32.67

The organoclay used in this work is Cloisite(R) 15A (C15A) from Southern Clay, USA. The surfactant in the organoclay is di-methyl, dehydrogenated tallow, quaternary ammonium. It has a d_{001} spacing of 31.5Angstrom. 0.05 wt% of C15A was used in the preparation of the polyethylene- organoclay nanocomposites. So, m-EB15-C15A means metallocene ethylene butene copolymer with BC of 15 CH_3/1000 C containing 0.05 wt% C15A as organoclay processing additive.

4.2.2 Melt Blending and Morphology Characterization

The Brabender 50 EHT mixer supplied with the Plastograph (Brabender® GmbH & Co. Germany) was used in the preparation of the nanocomposite. The organoclay was first heated in a vacuum oven at 108^{o}C for more than 24 hours to remove physico adsorbed water. The grounded polymer sample was pre mixed with organoclay before

introduced into the mixer using manual feeder. The blending was done for 10 minutes at 50 rpm. The blending temperature for each sample was 50^{o}C above its peak melting temperature. Addition of 0.1 wt% of antioxidant (AO) to the nanocomposite during melt blending is necessary to prevent thermal degradation. The AO is a 50/50 blend of Irganox 1010 and Irgafos 168 from Ciba- Geigy Specialty, Switzerland.

The structure of the PE/organoclay nanocomposites was characterized by Nova^{TM} NanoSEM 230 (FEI, USA). Nova^{TM} NanoSEM 230 is a field emission scanning electron microscope. It was configured to get information down to nanometer level on non-conductive materials.The SEM samples were made into thin film and etched for 4 hours. The etching solution was made from a solution of $H_2SO_4/H_3PO_4/H_2O$ (10/4/1) and 0.01 g/ml $KMnO_4$ as detailed in [9]. Figure 4.1 shows a typical SEM micrograph for HDPE-L-C15A. The results showed that there was a good dispersion of organoclay in polyethylene with master batch-dilution technique. Similar results were shown in our previous publication [9]. The samples for tests in ARES rheometer (TA Instruments USA) were prepared from melt blended samples at a temperature of 50^{o}C above the melting temperature (T_m) of the polymers. The pressure of up to 30 Pa was applied in a Carver press. The disc samples with dimensions of 25 mm diameter and 2 mm thickness were prepared for shear rheology.

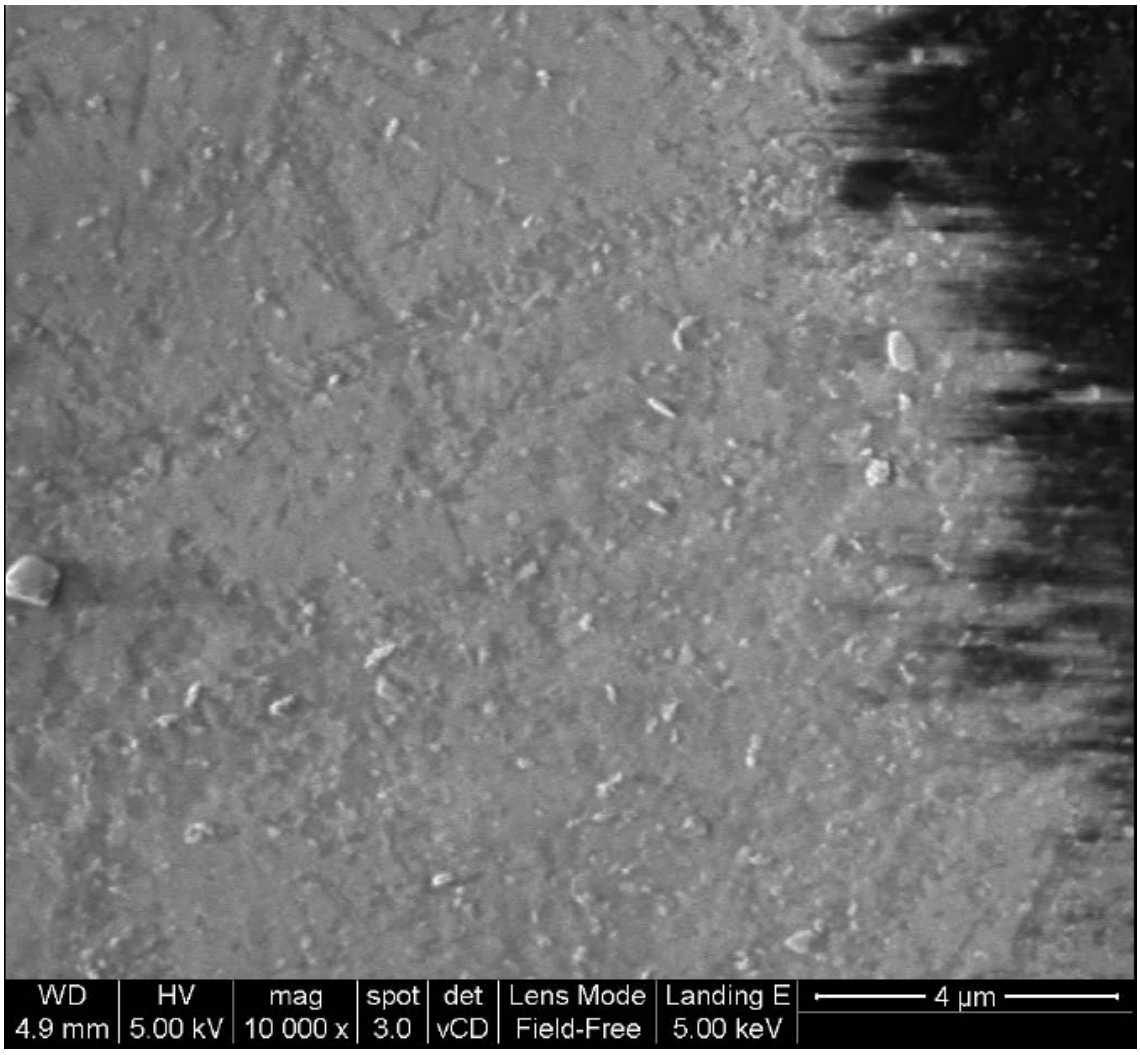

Figure 4.1 : Scanning Electron Micrograph for HDPE-L-C15A

4.2.3 Rheological Measurement

ARES controlled strain rheometer (TA Instruments USA) was used for all rheological measurements. It was equipped with heavy transducer (range 0.02-20 N for normal force; 2 x 10^{-5}-2 x 10^{-1} Nm for torque). The linear and non-linear viscoelastic experiments were performed using 25 mm parallel plates. The plates were heated for at least 20 minutes to equilibrate the temperature. For reproducibility of results, a pre-steady shear rate of 0.1 s^{-1} was applied for 20 s for all the tests in the parallel plates and

time delay of 100 s before the actual tests. Different rheological tests were conducted to study the material properties under different rheological conditions. The tests were performed at a temperature of T_m + 50^oC for different samples. The variation in the testing temperature was to prevent differences in the melt state properties of the samples as previously explained by Palza et al. [29]. The differences could arise from dissimilarity in branch content and molecular weight.

Frequency sweep experiments from 0.1 to 100 rad/s with a strain of 10% (in the linear regime) were conducted. Most of the experiments were repeated three times. The maximum deviation was less than 5 % from the mean. Then, van Gurp-Palmen plot [δ (arctan G"/G') versus complex modulus, G*] was used to investigate the effect of organoclay on the structure of polyethylene.

Fourier transform rheology (FT-rheology) was conducted at a frequency of 0.1 Hz for a strain range 10-400%. Raw torque data from ARES rheometer was digitized using 16-bit analog- to- digital converter card from National Instruments. In this work, sampling rate of 200 data points per cycle was used. Details of the experimental work can be seen elsewhere [30]. It had been shown that the shear stress response involves harmonics. The intensities and phases of such harmonics are used in the characterization of non-linearity in polymer. Most importantly the relative intensity of the second harmonic ($I_{2/1}$), relative intensity of the third harmonic ($I_{3/1}$) and relative phase angle of the third harmonic (Φ_3) were found very useful in such analysis [30, 31]. They are defined as:

$$I_{3/1} = \frac{I(3w_1)}{I(w_1)} \tag{1}$$

$$I_{2/1} = \frac{I(2w_1)}{I(w_1)} \tag{2}$$

and

$$\Phi_3 = \varphi_3 - \varphi_1 \tag{3}$$

where $I(2w_1)$, $I(3w_1)$ and φ_3 are the shear stress intensity of the second and third harmonics and phase angle of the third harmonic, respectively. $I(w_1)$ and φ_1 are the shear stress intensity and phase angle of the first harmonic, respectively. Most of the experiments were repeated three times. The maximum deviation in $I_{3/1}$ and $I_{2/1}$ were found to be less than 5% of the mean and less than $\pm 5^o$ around the mean for Φ_3.

Another important shear test conducted was stress growth experiment. This was done to examine the effect of organoclay on the polyethylene during a transient shear process. A step shear rate of $1s^{-1}$ was applied on the samples placed between the parallel plates (1mm apart). The applied shear rate was kept constant for 200 s. The results were reproducible with maximum deviation of 10% around the mean.

Furthermore, Extrusion pressure at relatively high shear rates was studied in a continuous MiniLab^{TM} II Rheomex CTW5 (Thermo Scientific Germany) shown in Figure 4.2.

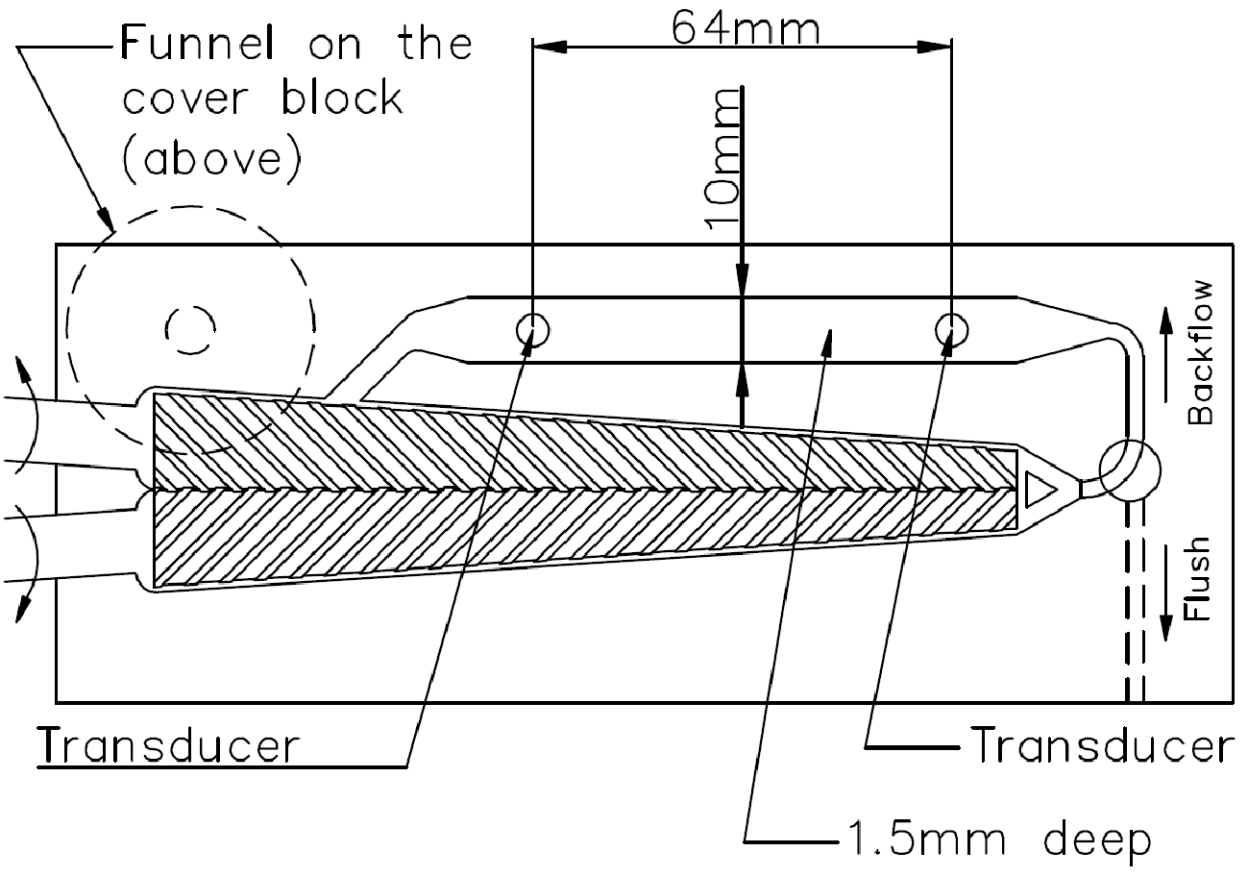

Figure 4.2 : Longitudinal section of MiniLab^{TM} - A mini twin screw extruder with slit die along its backflow channel

The MiniLab^{TM} consists of conical counter rotating twin screw with backflow channel. The backflow channel was designed as a slit capillary (64 mm x 10 mm x 1.5 mm) with two pressure transducers at the capillary entrance and exit. The maximum allowable pressure at the entrance and exit of the backflow channel are 200 and 100 bar, respectively. The maximum obtainable screw speed is 360 rpm. To study the effect of organoclay on the extrusion pressure, the speed of the screw was varied from 20 to 300 rpm at a temperature approximately 50^{o}C above the melting point of each sample. The

samples were introduced into the MiniLab^{TM} in 3 steps with 2-3 ml fed-in during each step. It should be noted that the MiniLab^{TM} is only good for comparative studies between samples. This is due to the inaccessibility to the actual extruded sample volume during the rheometry study. The developed melt flow instabilities during the rheometry were as well not observable due to the MiniLab^{TM} mode of operation. Despite the instabilities, there exists good reproducibility of results. As found in this work, the results were reproducible with maximum deviation of ±4% around the mean for all the allowable shear rates. Cross model (equation 4) serves as a good regression model for the obtained flow curve.

$$\tau = \dot{\gamma}\left[\frac{\eta_o}{(1 + (\dot{\gamma}/\dot{\gamma}_b)^n)}\right] \tag{4}$$

τ (Pa) is the shear stress while $\dot{\gamma}$ (s^{-1}) is the apparent shear rate . η_o (Pa.s) is the zero-shear viscosity. n is the Cross rate constant (dimensionless) and $\dot{\gamma}_b$ (s^{-1}) is the critical shear rate at the onset of shear thinning.

The Extensional Viscosity Fixture (EVF) in ARES rheometer was used in the study of extensional rheology. The sample was pre stretched with a strain rate of $0.04\ s^{-1}$ to remove sagging. Then, it was left in the fixture for 3 minutes to relax any accumulated stress before the start of the experiment. The used Hencky strain rate was $20\ s^{-1}$. Also, the extensional experiments were performed at a temperature of 15^{o}C above the melting temperatures of the samples. The results were reproducible with maximum deviation of 10% around the mean.

4.3 Results

4.3.1 Linear Polyethylene (HDPE-L)

The results of dynamic shear tests were analyzed using TA Orchestrator (ARES software from TA Instruments) to obtain cross over modulus, G_c, and longest relaxation time, λ_c. The results are shown in Table 4.2.

Table 4.2: Investigated samples: testing temperature, cross over modulus (G_c), longest relaxation time $\boldsymbol{\lambda_c}$ and power law parameters for FT-rheology

Sample	Testing Temperature (°C)*	G_c (MPa)	λ_c (s)**
HDPE-L	190	5.62×10^{-2}	0.107
HDPE-L-C15A	190	6.37×10^{-2}	0.083
ZN-EB13	150	1.64×10^{-1}	0.083
ZN-EB13-C15A	150	1.61×10^{-1}	0.081
m-EB15	160	2.46×10^{-1}	0.059
m-EB15-C15A	160	2.5×10^{-1}	0.059
m-EB19	150	2.33×10^{-1}	0.08
m-EB19-C15A	150	2.29×10^{-1}	0.08
m-EO16	150	1.34×10^{-1}	0.078
m-EO16-C15A	150	1.35×10^{-1}	0.077
m-EO33	120	1.13×10^{-1}	0.22
m-EO33-C15A	120	1.11×10^{-1}	0.216

G_c of HDPE-L increased by 13% while its λ_c decreased by 22% with the addition of organoclay. However, plateau modulus was not attained at the temperature used in this work. Figure 4.3 shows the van Gurp-Palmen plot of HDPE-L and HDPE-L-C15A.

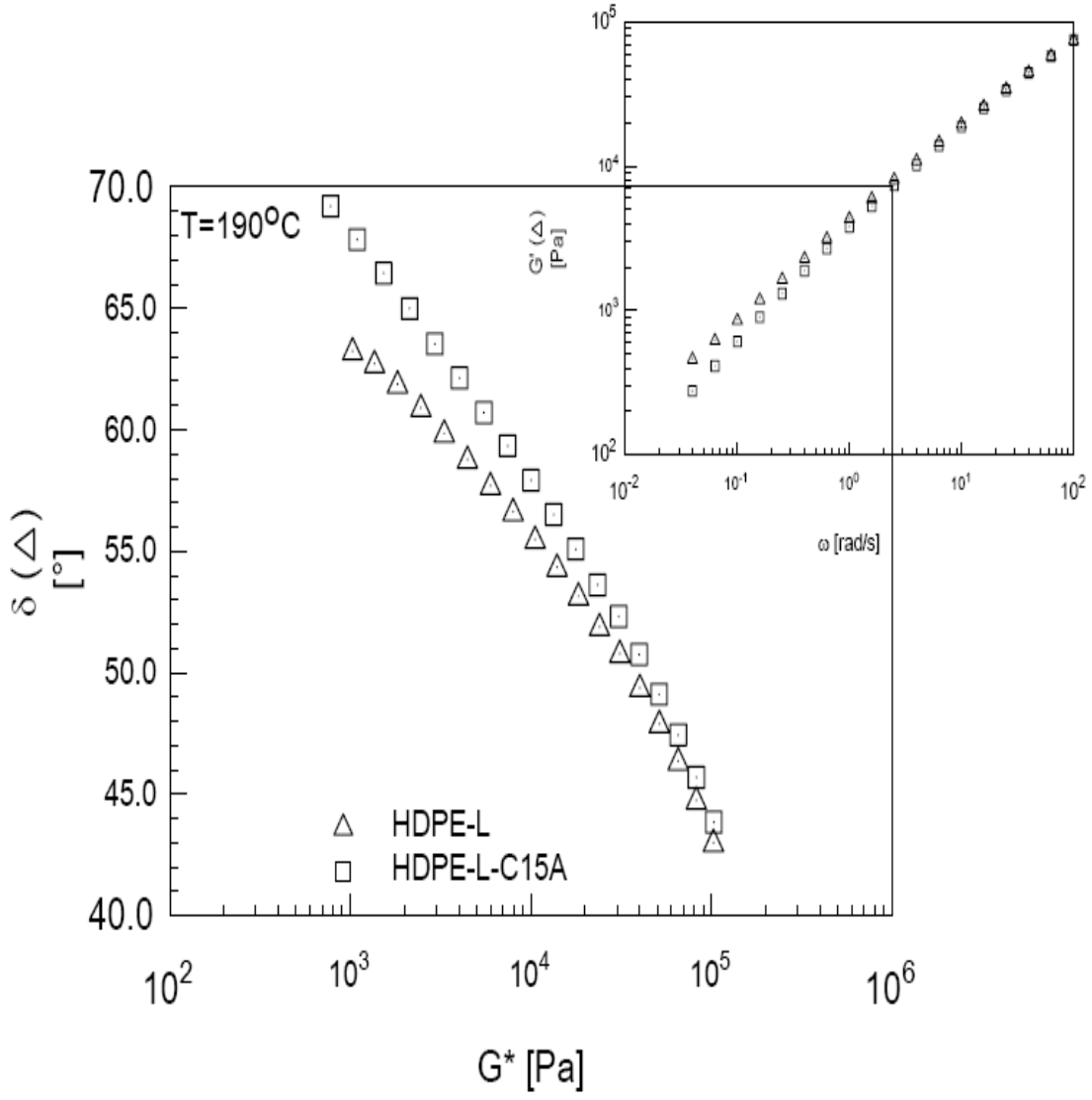

Figure 4.3: van Gurp-Palmen plot for HDPE-L and HDPE-L-C15A. The testing temperature was T_m+50°C (190°C)

The shape of linear HDPE (HDPE-L) showed in the figure is similar to the linear polyethylene presented in the work of Vittorias and Wilhelm [24]. However, the curve is less steep as compared to the one reported by them [24]. The variation in the steepness is likely due to differences in the PDI of the linear polymers and testing

temperatures in both works. Organoclay influences the van Gurp-Palmen plot of HDPE-L. The effect is more pronounced below the cross over frequency. The plot of HDPE-L shifted upward. This is an indication that organoclay reduces the elasticity of the HDPE-L and hence more viscous as shown in the inset plot of Figure 4.3. The increase in G_c, the decrease in λ_c and the upward shift in van-Gurp Palmen plot of HDPE-L showed that organoclay has effect on the linear viscoelastic properties of linear polyethylene.

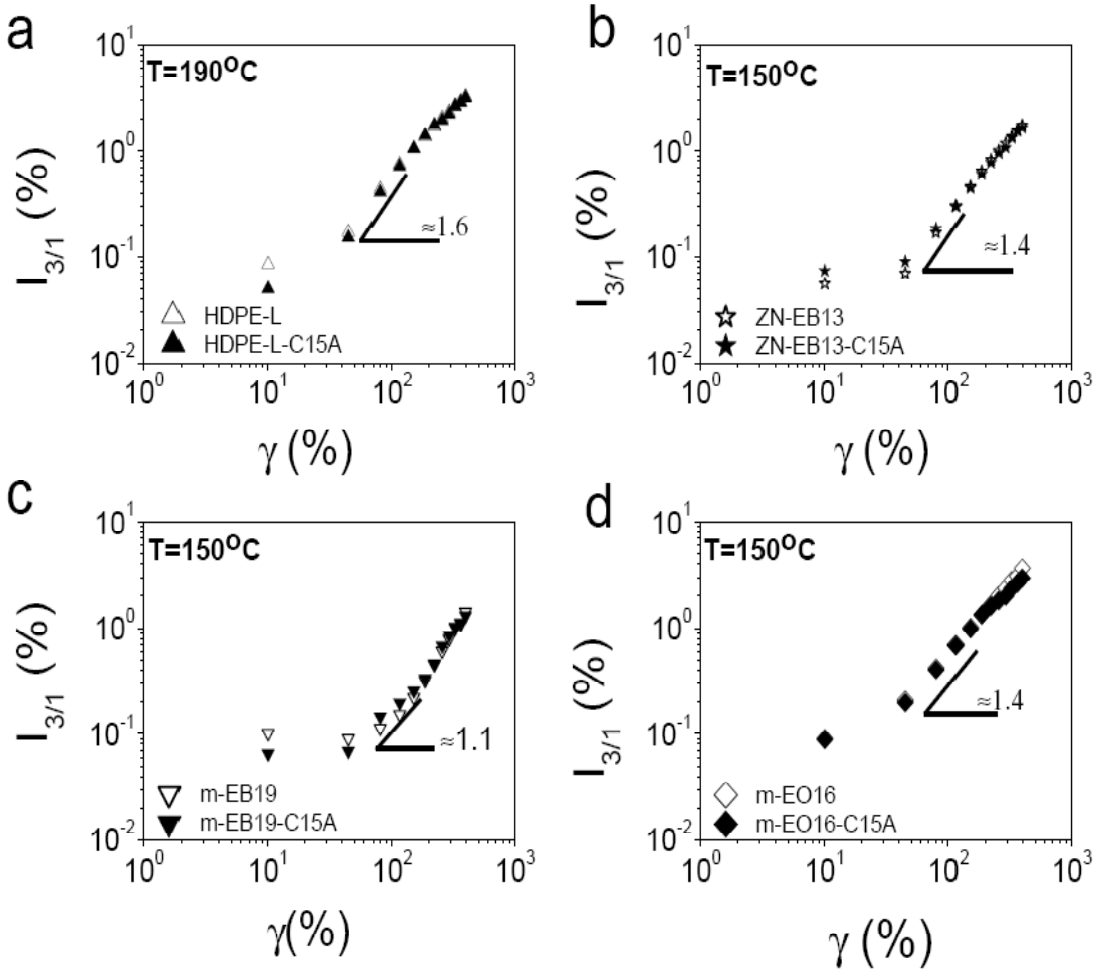

Figure 4.4: Relative intensity of the third harmonic as a function of strain amplitude at T_m +50°C for (a) HDPE-L and HDPE-L-C15A (b) ZN-EB13 and ZN-EB13-C15A (c) m-EB19 and m-EB19-C15A (d) m-EO16 and m-EO16-C15A

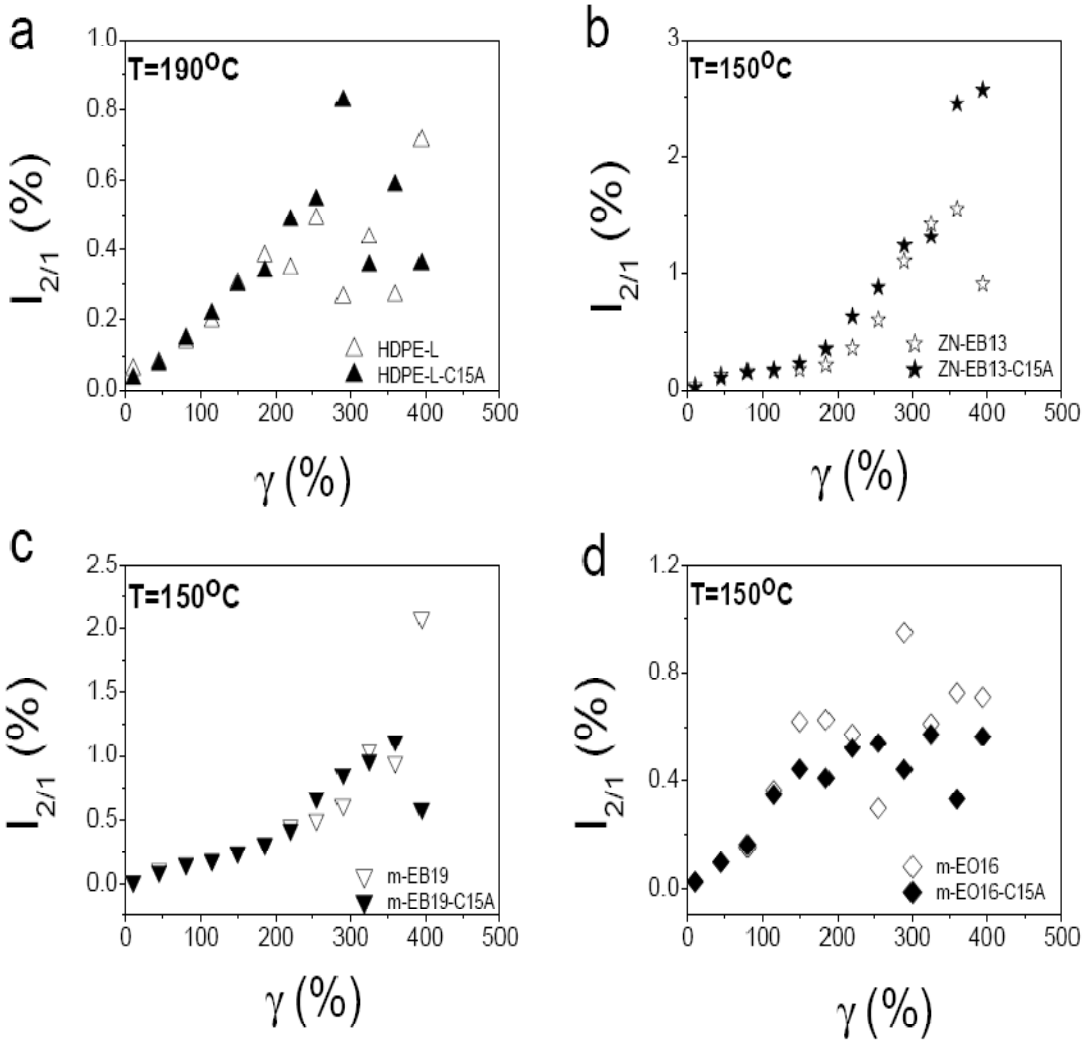

Figure 4.5: Relative intensity of the second harmonic as a function of strain amplitude at T_m +50°C for (a) HDPE-L and HDPE-L-C15A (b) ZN-EB13 and ZN-EB13-C15A (c) m-EB19 and m-EB19-C15A (d) m-EO16 and m-EO16-C15A

The effect of organoclay on the $I_{3/1}$ of all the polyethylenes is given in Figure 4.4. Generally, slope of the log-log plot of $I_{3/1}$ versus γ is less than 2. Figure 4.4a shows that relative amplitude of the third harmonic for both HDPE-L and HDPE-L-C15A is the same. Similarly, organoclay has no effect on the relative phase angle of the third harmonic (figure not shown) up to strain amplitude of 155 %. Stress decay occurred above strain amplitude 155 %. Such decay is an attribute of slip during large amplitude oscillatory shear [20, 35, 36]. $I_{2/1}$ has been reported to be sensitive to flow behaviors like wall slip [43]. Figure 4.5(a) shows that organoclay has no effect on the $I_{2/1}$ of HDPE-L up to strain amplitude of 155 %. Above this amplitude, there is a difference in the trend between HDPE-L and HDPE-L-C15A. However, no comment can be made on the trends because edge melt fracture was observed at the end of the experiment in all the cases.

Another important consideration during processing is the flow behavior of polymers during transient condition. One way to correlate rheology to processing is to perform transient stress growth experiment. The stress growth results for HDPE-L and HDPE-L-C15A are shown in Figure 4.6. The overshoots in the stress growth and normal stress difference reduce with the inclusion of organoclay. At about 3.4 s after the start up of the stress growth test, the overshoot in stress growth reduced by 15% while the overshoot in normal stress difference of HDPE-L, at about 47.9 s, reduced by 28%. Such reduction in normal stress difference is an indication that organoclay reduces the elasticity of the melt which plays a major role in melt fracture of linear polyethylene. This subject was discussed in details in our previous work [9].

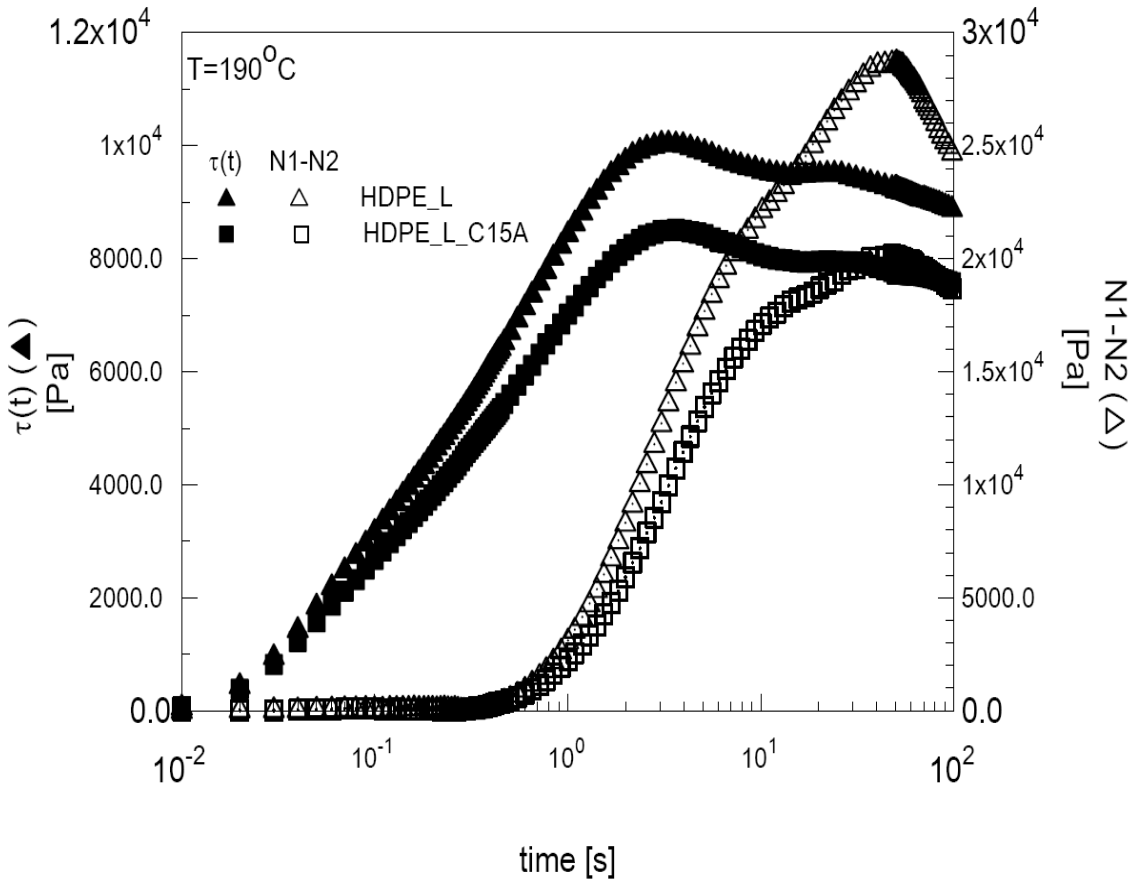

Figure 4.6: Transient shear stress and normal stress difference during stress growth test for HDPE-L and HDPE-L-C15A at 190°C

Flow curves from MiniLab™ for HDPE-L and HDPE-L-C15A are displayed in Figure 4.7. Addition of 0.05 wt% of organoclay to HDPE-L resulted in a decrease in the shear stress throughout the allowable range in MiniLab™. This implies a decrease in the extrusion pressure (more throughputs).

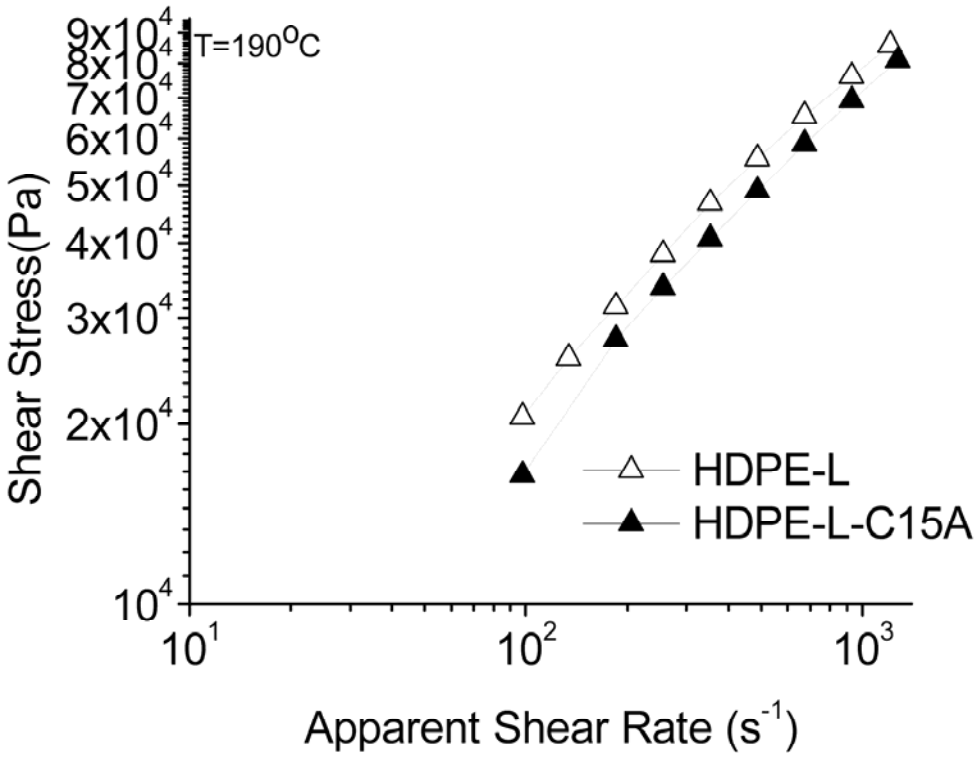

Figure 4.7: Transient shear stress and normal stress difference during stress growth test for HDPE-L and HDPE-L-C15A at 190°C

Cross model in the form given in equation (4) is used to quantify the extent of effect of organoclay on the flow curve of polyethylene at low clay loading. The results of the regression analysis are given in Table 4.3. The reduction in η_o of HDPE-L was 23% in the presence of 0.05 wt% organoclay. However, the onset of shear thinning cannot be compared since the samples have different zero-shear viscosity (η_o). To resolve this problem, the degree of freedom in the Cross model equation was reduced to 2-based parameters by fixing the η_o as a constant. The results are as shown in Table 4.3. The onset of shear thinning occurred at lower shear rate with the addition of 0.05

wt% of organoclay to HDPE-L. This is an indication that addition of low loading of organoclay to HDPE-L enhances its processability.

Table 4.3: Cross model parameters for all the tested samples

	3-based Parameters			2-based Parameters		
Sample	η_o (Pa.s)	$\dot{\gamma}_b$ (s^{-1})	n	η_o (Pa.s)	$\dot{\gamma}_b$ (s^{-1})	n
HDPE-L	345.4	178.4	0.71	345.4	178.4	0.71
HDPE-L-C15A	265.7	243.2	0.704	345.4	115.6	0.621
ZN-EB13	454.1	458.8	0.899	454.1	458.8	0.899
ZN-EB13-C15A	399.8	550.4	0.999	454.1	411.2	0.887
m-EB15	592.2	527.1	1.009	592.2	527.1	1.009
m-EB15-C15A	549.4	552	1.097	592.2	480.9	0.951
m-EB19	766.3	413.8	1.063	766.3	300	1.063
m-EB19-C15A	630.6	403	0.906	766.3	243.7	0.72
m-EO16	788.4	162.9	0.758	788.4	162.9	0.758
m-EO16-C15A	615.7	216.3	0.805	788.4	116.5	0.716
m-EO33	1415	87.54	0.765	1415	87.54	0.765
m-EO33-C15A	1392	94.03	0.787	1415	90.44	0.781

It has been previously confirmed that extensional behavior of polymer during melt extrusion is very important towards understanding the occurrence of melt instabilities [8, 37]. Extensional flow plays an important role at the die exit. Reduction in extensional stress and strain at break may lead to the postponement of melt instabilities. The interaction of organoclay with HDPE-L is sensitive to extensional rheology as shown in Figure 4.8. The results show that after 2.19 s, 0.05 wt% of organoclay reduced the maximum extensional stress in HDPE-L by 37%. The Hencky strain at break decreased from 3.9 to 3.49 with the addition of organoclay. So, for linear

HDPE, we observed a decrease in both the extensional and normal stresses as a result of the addition of 0.05 wt% of organoclay. In addition, organoclay cause a decrease in the extrusion pressure of HDPE-L.

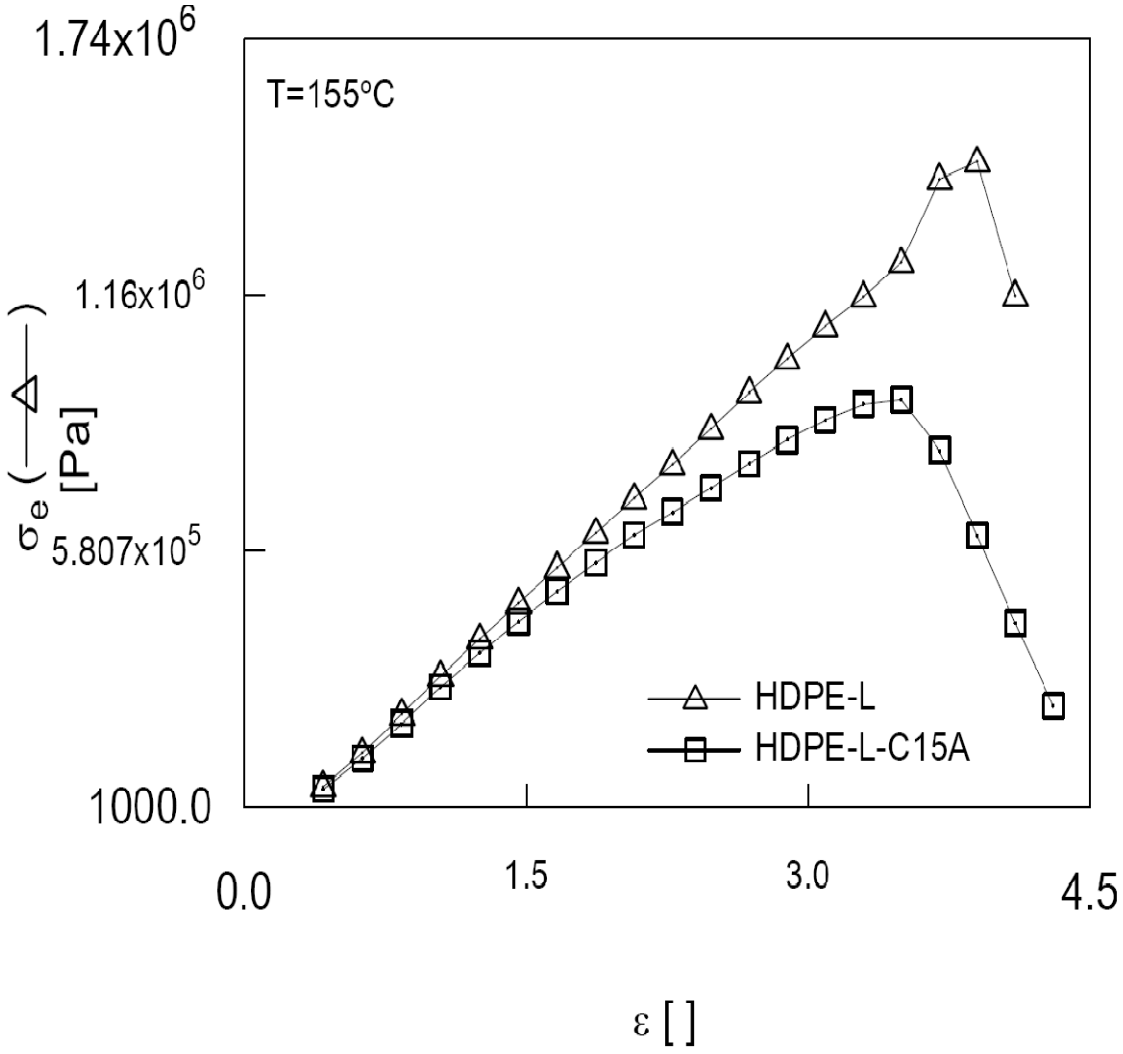

Figure 4.8: Extensional stress growth against extensional strain at Hencky strain rate of $20s^{-1}$ and temperature of $190^{o}C$ for HDPE-L and HDPE-L-C15A

4.3.2 Ziegler-Natta-based Polyethylene (ZN-EB13)

Table 4.2 shows that the addition of 0.05 wt% organoclay had no effect on the cross over frequency and longest relaxation time of ZN-EB13. In general, 0.05 wt% organoclay has no effect on the linear viscoelastic properties of ZN-EB13.

The relative amplitude (Figure 4.4b) and phase angle (Figure not shown) of the third harmonics of ZN-EB13 remained unchanged with the addition of organoclay. Up to the strain amplitude of 155 %, the relative amplitude of the second harmonic is the same for ZN-EB13 and ZN-EB13-C15A (Figure 4.5b). As observed in the case HDPE-L, the differences in $I_{2/1}$ above 155 % cannot be discussed due to onset of edge melt fracture.

The effect of organoclay on transient stress growth of ZN-EB13 is shown in Figure 4.9. At about 3 s after the start up of the stress growth experiment, the overshoot in stress growth of ZN-EB13 reduces by 3% (not significant) while the overshoot in its normal stress difference at $\approx$ 9.4 s, reduces by 11%. It should be noted that the decrease in the normal stress difference in ZN-EB13 due to organoclay inclusion is less than the decrease in HDPE-L.

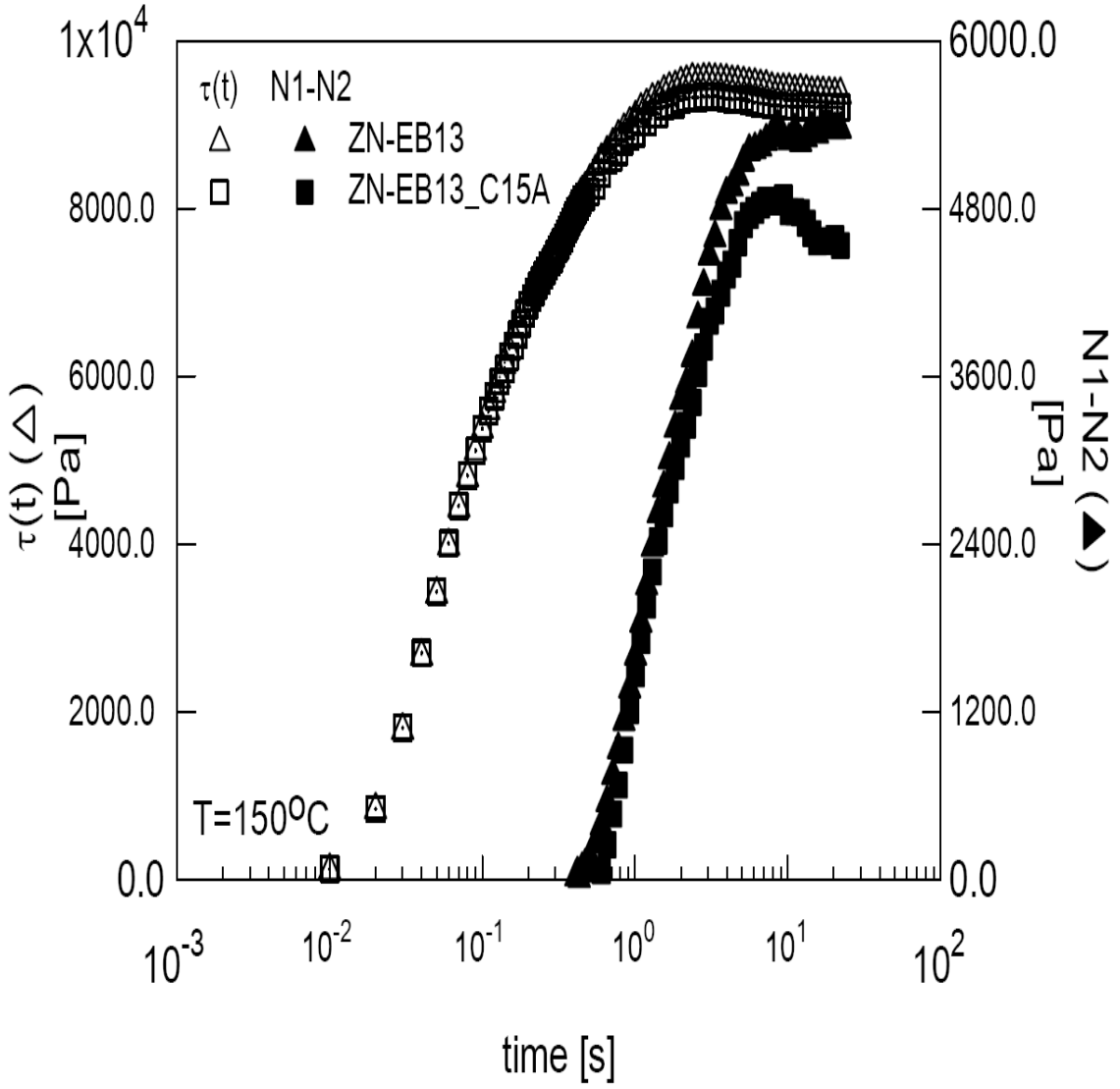

Figure 4.9: Transient shear stress and normal stress difference during stress growth test for ZN-EB13 and ZN-EB13-C15A at 150^{o}C

Organoclay's addition to ZN-EB13 resulted in the decrease in zero-shear viscosity of the polymer by 12%. The onset of shear thinning for ZN-EB13-C15A occurred at lower shear rate compared to ZN-EB13 (Table 4.3). This is similar to what occurred between HDPE-L and HDPE-L-C15A. Furthermore, the extensional stress in ZN-EB13 reduces by 16% while the Hencky strain at break decreases from 4.7 to 3.9 in

the presence of 0.05 wt% organoclay (Figure not shown). Similar trend was observed in the interaction between HDPE-L and organoclay. However, the influence of organoclay on HDPE-L seems higher as compare to its impact on ZN-EB13.

4.3.3 Metallocene-based LLDPE

The results given in Table 4.2 suggest that the organoclay has no effect on the cross over modulus and longest relaxation time of metallocene- based polyethylenes. It also has no influence on their van-Gurp-Palmen plots (Figures not shown). Hence, organoclay's effect on the linear viscoelastic properties of metallocene-based polyethylene is negligible.

The influence of organoclay on the $I_{3/1}$ of metallocene- based polyethylenes is insignificant (Figures 4.4c and d). Below strain amplitude 155 %, the slip behavior of metallocene-based polyethylenes and their corresponding organoclay nanocomposites is similar (Figures 4.5c and d). The trends above strain amplitude 155 %, as observed in the cases of HDPE-L and ZN-EB13, cannot be relied upon.

Similar to our previous observations on ZN-EB13, the reduction in the stress growth and normal stress difference of metallocene- based polyethylene due to inclusion of organoclay are insignificant. For example, Figure 4.10 shows the transient stress growth and normal stress difference of m-EO33 and m-EO33-C15A. At about 3 s after the start up of the stress growth test, the overshoot in stress growth in m-EO33 reduces by 7% while the overshoot in its normal stress difference at about 31.2 s, reduces by 9%. Due to data reproducibility as mentioned under experimental set-up, such reductions are negligible.

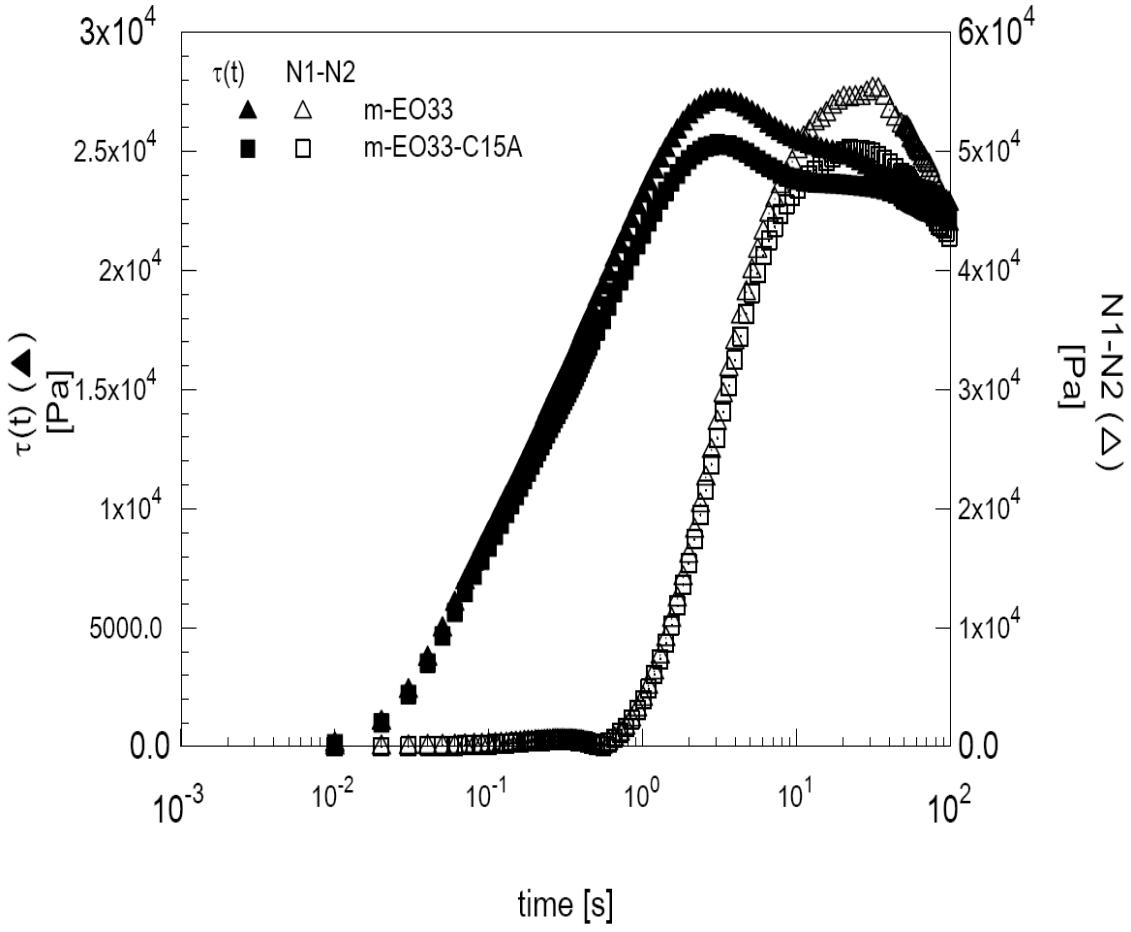

Figure 4.10: Transient shear stress and normal stress difference during stress growth test for m-EO33 and m-EO33-C15A

The MiniLab^{TM} results show that addition of organoclay to metallocene-based polyethylenes has effect on their zero-shear viscosity and onset of shear thinning up to certain BC. For example, organoclay reduces zero-shear viscosity of m-EB19 by 18% while the shear rate at which the onset of shear thinning occurs is reduced by 19% (Table 4.3). However, the reduction of zero-shear viscosity in m-EO33 is ~2% while the shear rate at which shear thinning set- in remains unaffected by the addition of organoclay.

Figure 4.11 shows the extensional results of m-EO33 and m-EO33-C15A. Similar results were obtained for all metallocene- based polyethylene. The reduction in extensional stress for metallocene- based polyethylenes in the presence of 0.05 wt% organoclay is less than 10 %. The trend is independent of the type of co-monomer. Such decrease is unreliable because of the issue of data reproducibility. The Hencky strain rate used in the experiment was 20 s^{-1}. Efforts to attain higher Hencky rate were futile because of the equipment limitation. It is possible that the effect of organoclay on the metallocene-based polyethylene may be more noticeable at higher Hencky strain rates.

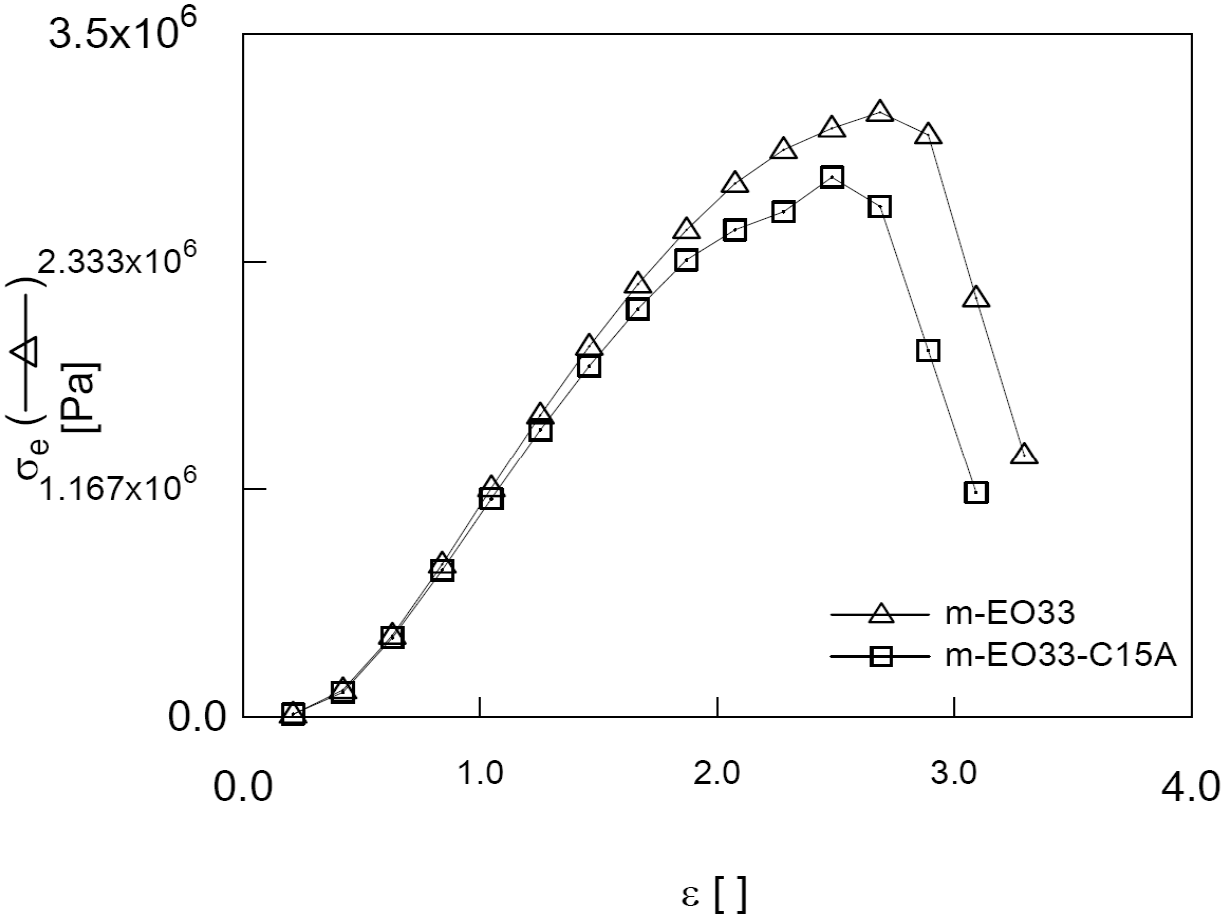

Figure 4.11: Extensional stress growth against extensional strain at Hencky strain rate of $20s^{-1}$ and temperature of $120^{o}C$ for m-EO33 and m-EO33-C15A

4.3.4 Further Discussion

The results presented so far indicate that there is an interaction between organoclay and topology of polyethylenes especially BC. The impact of organoclay on HDPE-L is very obvious. Organoclay affect both linear and non-linear viscoelastic properties of linear polyethylene without branching because the entanglement is minimal. The organoclay could easily streamline the flow and align in the flow direction. Similar observation was reported with respect to the inclusion of wood flour in high density polyethylene. However, the wood flour, according to the authors, further migrate to the wall surface to initiate slip [38-40]. As the BC increases, such streamlining and alignment in the flow direction become difficult. The effect is the same regardless of the type of catalyst, co-monomer and composition distribution. The trend in the interaction between organoclay and BC is the same in both shear and extensional flows.

4.4 Conclusion

The effect of organoclay on the rheology and processing of polyethylene of different BC was studied. The results showed that organoclay has effect only on linear viscoelastic properties of linear polyethylene without branching. FT-rheology may be very good as 'finger printing' for BC effect in polyethylene [20, 24, 30, 41, 42], its usefulness in studying the effect of organoclay on polyethylene at low clay loading was not successful. Organoclay does not induce more slip in the polyolefins as characterized using $I_{2/1}$. However, there is a need for further studies in this area to examine if organoclay induces slip at high shear flow. This becomes more necessary since at high shear rates during extrusion, extrusion pressure of HDPE-L reduced in the

presence of organoclay. Such reduction might be due to slip. This will be the focus of our future research. The transient stress overshoot and normal stress difference were reduced when 0.05 wt % organoclay was added to the linear polyethylene without branching. Also, extensional stresses became dissipated in the presence of organoclay. The work concluded with the assertion that such effect became reduced as the BC increases. In addition, the trend is independent of the type of flow. The results indicated that organoclay may be a good processing aid in polyethylenes especially the linear polyethylene and polyethylenes with small short chain branch.

4.5 References

[**1]** **Emmanuel PG:** Polymer Layered Silicate Nanocomposites. *Adv. Mat.*, 1996, **8**(1), 29-35.

[2] **Krishnamoorti R, Vaia RA, Giannelis EP:** Structure and Dynamics of Polymer-Layered Silicate Nanocomposites. *Chem. Mater.* , 1996, **8**(8), 1728-1734.

[3] **Wang KH, Chung IJ, Jang MC, Keum JK, Song HH:** Deformation Behavior of Polyethylene/Silicate Nanocomposites As Studied by Real-Time Wide-Angle X-ray Scattering. *Macromolecules*, 2002, **35**(14), 5529-5535.

[4] **Wang KH, Xu M, Choi YS, Chung IJ:** Effect of aspect ratio of clay on melt extensional process of maleated polyethylene/clay nanocomposites. *Polym. Bull.*, 2001, **46**(6), 499-505.

[5] **Susteric Z, Kos T:** Rheological Idiosyncrasies of Elastomer/Clay Nanocomposites. *Appl. Rheol.*, 2008, **18 ,**54894.

[6] **Katsikis N, Koniger T, Munstedt H,:** Elongational viscosities of polymethylmethacrylate / nano-clay composites. *Appl. Rheol.*, 2007, **17**, 52751.

[7] Solomon MJ, Almusallam AS, Seefeldt KF, Somwangthanaroj A, Varadan P: Rheology of Polypropylene/Clay Hybrid Materials. *Macromolecules*, 2001, **34**(6), 1864-1872.

[8] Hatzikiriakos SG, Rathod N, Muliawan EB: The effect of nanoclays on the processibility of polyolefins. *Polym. Eng. Sci.*, 2005, **45**(8), 1098-1107.

[9] Adesina AA, Hussein IA: Impact of Organoclay and Maleated Polyethylene on the Rheology and Instabilities in the Extrusion of High Density Polyethylene. *J. Appl. Polym. Sci.*, in press.

[10] Lee YH, Wang KH, Park CB, Sain M: Effects of clay dispersion on the foam morphology of LDPE/clay nanocomposites. *J. Appl. Polym. Sci.*, 2007, **103**(4), 2129-2134.

[11] Krishnamoorti R, Ren J, Silva AS: Shear response of layered silicate nanocomposites. *J. Chem. Phys.*, 2001, **114**(11), 4968-4973.

[12] Rosenbaum EE, Randa SK, Hatzikiriakos SG, Stewart CW, Henry DL, Buckmaster M: Boron nitride as a processing aid for the extrusion of polyolefins and fluoropolymers. *Polym. Eng. Sci.*, 2000, **40**(1), 179-190.

[13] Wissbrun KF, Dealy JM: *Melt Rheology and Its Role in Plastics Processing - Theory and Applications* (Springer, 1999).

[**14] Gu, SY, Ren J, Wang QF:** Rheology of poly(propylene)/clay nanocomposites *J. Appl. Polym. Sci.*, 2004(91), 2427-2434.

[15] Jin Z, Alexander BM, Joseph DH: Rheological characterization of polystyrene–clay nanocomposites to compare the degree of exfoliation and dispersion *Polymer*, 2005, **46**, 8641- 8660.

[16] Treece MA, Oberhauser JP: Processing of polypropylene-clay nanocomposites: Single-screw extrusion with in-line supercritical carbon dioxide feed versus twin-screw extrusion. *J. Appl. Polym. Sci.*, 2007, **103**(2), 884-892.

[17] Ren J, Krishnamoorti R: Nonlinear Viscoelastic Properties of Layered-Silicate-Based Intercalated Nanocomposites. *Macromolecules*, 2003, **36**(12), 4443-4451.

[18] Jian L, Cixing Z, Gang W, Zhao D: Study on rheological behavior of polypropylene/clay nanocomposites *J. Appl. Polym. Sci.*, 2003, **89**(13), 3609-3617.

[19] Thierry A, Tolotrahasina R, Médéric P: Rheological investigation of the melt state elastic and yield properties of a polyamide-12 layered silicate nanocomposite *J. Rheol.*, 2005, **49**(2), 425- 440.

[20] Filipe S, Vittorias I, Wilhelm M: Experimental Correlation between Mechanical Non-Linearity in LAOS Flow and Capillary Flow Instabilities for Linear and Branched Commercial Polyethylenes. *Macromol. Mater. Eng.*, 2008, **293**(1), 57-65.

[21] Hussein IA: Melt miscibility and mechanical properties of metallocene linear low-density polyethylene blends with high-density polyethylene: influence of comonomer type. *Polym. Int.*, 2005, **54**(9), 1330-1336.

[22] Hussein IA, Hameed T, Sharkh BFA, Mezghani K: Miscibility of hexene-LLDPE and LDPE blends: influence of branch content and composition distribution. *Polymer*, 2003, **44**(16), 4665-4672.

[23] Usami T, Gotoh Y, Takayama S: Generation mechanism of short-chain branching distribution in linear low-density polyethylenes. *Macromolecules*, 1986, **19**(11), 2722-2726.

[24] Vittorias I, Wilhelm M: Application of FT Rheology to Industrial Linear and Branched Polyethylene Blends. *Macromol. Mater. Eng.*, 2007, **292**(8), 935-948.

[25] Filipe S, Becker A, Barroso V, Wilhelm, M: Evaluation of melt flow instabilities of high-density polyethylenes via an optimised method for detection and analysis of the pressure fluctuations in capillary rheometry. *Appl. Rheol.*, 2009, **19**, 23345.

[26] Klein C, Venema P, Sagis L, van Dusschoten D, Wilhelm M, Spiess H, van der Linden E, Rogers S, Donald A: Rheo-optical Measurements using Fast Fourier Transform and Oversampling. *Appl. Rheol.*, 2007, **17**, 45210.

[27] Wilhelm M, Reinheimer P, Ortseifer M, Neidhöfer T, Spiess HW: The crossover between linear and non-linear mechanical behaviour in polymer solutions as detected by Fourier-transform rheology. *Rheol. Acta*, 2000, **39**(3), 241-246.

[28] Hameed T, Hussein IA: Rheological study of the influence of Mw and comonomer type on the miscibility of m-LLDPE and LDPE blends. *Polymer*, 2002, **43**(25), 6911-6929.

[29] Palza H, Filipe S, Naue IFC, Wilhelm M: Correlation between polyethylene topology and melt flow instabilities by determining in-situ pressure fluctuations and applying advanced data analysis. *Polymer*, 2010, **51**(2), 522-534.

[30] Vittorias I, Parkinson M, Klimke K, Debbaut B, Wilhelm M: Detection and quantification of industrial polyethylene branching topologies via Fourier-transform rheology, NMR and simulation using the Pom-pom model. *Rheol. Acta*, 2007, **46**(3), 321-340.

[31] Neidhofer T, Wilhelm M, Debbaut B: Fourier-transform rheology experiments and finite-element simulations on linear polystyrene solutions. *J. Rheol.*, 2003, **47**(6), 1351-1371.

[32] Wilhelm M: Fourier-Transform Rheology. *Macromol. Mater. Eng.*, 2002, **287**(2), 83-105.

[33] Bourgeois JR, Peter WB: HDPE**.** In Epel JN, Margolis JM , Newman S eds. *Engineeered Materials Handbook***,** pp. 163 (Metal Park, Ohio USA, 1988).

[34] Lohse DJ, Milner ST, Fetters LJ, Xenidou M, Hadjichristidis N, Mendelson RA, GarcÃ-a-Franco CA, Lyon MK: Well-Defined, Model Long Chain Branched Polyethylene. 2. Melt Rheological Behavior. *Macromolecules*, 2002, **35**(8), 3066-3075.

[35] Chen YL, Larson RG, Patel SS: Shear fracture of polystyrene melts and solutions. *Rheol. Acta*, 1994, **33**(4), 243-256.

[36] Hatzikiriakos SG, Dealy JM: Role of slip and fracture in the oscillating flow of HDPE in a capillary. *J. Rheol.*, 1992, **36**(5), 845-884.

[37] Hatzikiriakos SG, Migler KB: *Polymer Processing Instabilities Control and Understanding*. (Marcel Dekker, New York, 2005).

[38] Hristov V, Takács E, Vlachopoulos J: Surface tearing and wall slip phenomena in extrusion of highly filled HDPE/wood flour composites. *Polym. Eng. Sci.*, 2006, **46**(9), 1204-1214.

[39] Becraft ML, Metzner AB: The rheology, fiber orientation, and processing behavior of fiber-filled fluids. *J. Rheol.*, 1992, **36**(1), 143-174.

[40] Knutsson BA, White JL, Abbas KB: Rheological and extrusion characteristics of glass fiber- reinforced polycarbonate. *J. Appl. Polym. Sci.*, 1981, **26**(7), 2347-2362.

[41] Schlatter G, Fleury G, Muller R: Fourier Transform Rheology of Branched Polyethylene: Experiments and Models for Assessing the Macromolecular Architecture. *Macromolecules*, 2005, **38**(15), 6492-6503.

[42] Vega JF, Santamar ÃA, MuÃoz EA, Lafuente P: Small-Amplitude Oscillatory Shear Flow Measurements as a Tool To Detect Very Low Amounts of Long Chain Branching in Polyethylenes. *Macromolecules*, 1998, **31**(11), 3639-3647.

[43] **Michael, DG:** J Rheol 1995**,** 39, 4, 697-712.

CHAPTER FIVE

Comparative Analysis of the Effect of Organoclay, Boron Nitride, Fluoropolymer on the Rheology and Extrusion of High Density Polyethylene

Adesina A. A., Hussein I. A.*

Abstract

This paper focuses on the effect of different processing additives on the instabilities of the extrusion of high density polyethylene (HDPE). The concentration of each processing additive in HDPE was fixed at 0.05 wt%. The rheological tests on the HDPE containing organoclay, boron nitride and fluoropolymer showed that the phase angle of HDPE during frequency sweep reduced below the crossover frequency. Organoclay, boron nitride and fluoropolymer reduced the overshoot in transient shear viscosity of HDPE. Also, combined organoclay and fluoropolymer led to the same result. However, the decrease caused by the combined organoclay and fluoropolymer was less than that caused by the individual additive. The trend in extensional rheology was similar to that of transient shear stress growth. The flow regimes in HDPE during extrusion were: smooth, stick slip and gross melt fracture regimes. The extrudate was weak sharkskin -like towards the end of the smooth regime. All the processing aids eliminated the weak sharkskin-like instability. However, the fluoropolymer did not succeed in eliminating the stick-slip fracture. The gross melt fracture in HDPE was not eliminated by boron nitride and organoclay at apparent shear rate of 114 s^{-1}. However, both moment and distortion factor analyzed were able to quantify the visual trends in

the extrudates. The quantifying tools indicated that the combined organoclay and fluoropolymer had a better performance over the individual additives in terms of the reduction in the pressure fluctuations.

Keywords melt fracture, extrusion, high density polyethylene, distortion factor, processing additives

*Department of Chemical Engineering, King Fahd University of Petroleum and Minerals, 31261, Dhahran, Saudi Arabia

Corresponding author: Hussein I. A.

Tel/Fax:+966-3-8602235/4234; Email: *ihussein@kfupm.edu.sa*

5.1 Introduction

The major challenge during extrusion is the onset of melt instabilities that hinder high productivity (Larson 1992). Processing aids are often added to polyolefins during their extrusion to make the processes economically viable. With the addition of these additives, the processing window is expanded. The most common processing additive for polyolefin is fluoropolymer (Achilleos et al. 2002; Anastasiadis and Hatzikiriakos 1998; Guadarrama-Medina et al. 2005; Hatzikiriakos et al. 1995; Kazatchkov et al. 1995; Kharchenko et al. 2003; Migler et al. 2001; Rodríguez-González et al.; Xing and Schreiber 1996). Stearates(Hatzikiriakos et al. 1997), silicon- based additives, hyper-branched polymers (Hong et al. 1999; Hong et al. 2000) and blends of polymers (Shih 1976; Fujiyama and Kawasaki 1991) are other forms of conventional processing aids. Another processing aid found useful in the elimination of gross melt fracture is boron nitride (Achilleos et al. 2002; Rosenbaum et al. 2000). Recently, it was shown that organoclay is also a good candidate as a processing additive (Hatzikiriakos et al. 2005). There is a good review on the processing additives in (Hatzikiriakos and Migler 2005).

Fluoropolymer is added to polyolefins either as an additive or as a coat on the die (Kazatchkov et al. 1995) to increase the through-put of polyolefins. As an additive, fluoropolymer is added in small quantity less than 0.1 wt%. Due to its high incompatibility with polyolefins, a two-phase blend is formed during extrusion. As a result, master batch-dilution mode of preparation is often adopted in the preparation of the blend. Fluoropolymer thus promotes wall slip due to its strong interaction with the die wall (Migler et al. 2001; Migler et al. 2002; Kazatchkov et al. 1995; Rodríguez-González et al.; Guadarrama-Medina et al. 2005). The interaction was reported to occur

due to cohesive failure (Migler et al. 2001) or adhesive failure (Anastasiadis and Hatzikiriakos 1998; Hill et al. 1990; Stewart 1993) . The flow curve of high density polyethylene shifted to higher shear rates in the presence of fluoroelastomer (Achilleos et al. 2002) in an extrusion through a capillary rheometer. Fluoropolymer was suggested to have eliminated both sharkskin and stick-slip instability in several polyolefins (Achilleos et al. 2002; Hatzikiriakos et al. 1995; Xing and Schreiber 1996; Barone et al. 1998). Furthermore., fluoropolymer reduced the extrusion pressure (shear stress) by coating the die entrance of the die and then migrated as streaks to the die exit where the sharkskin is eliminated (Kharchenko et al. 2003). The coating time reduces with increasing fluoropolymer concentration. However, excessive amount of fluoropolymer could lead to excessive lubrication of the extruder barrel, hence undesired effects (Hatzikiriakos and Migler 2005). In addition, fluoropolymer enhances other properties in polyolefins. For example, the fluoropolymer-induced slip could lead to a decrease in the shear stress in the bulk and hence produces increase in draw ratio and melt strength during stretching (Guadarrama-Medina et al. 2005). An addition of fluoropolymer could as well lead to gel reduction, reduced die build up and elimination of draw resonance in film casting (Hatzikiriakos and Migler 2005). However, fluoropolymer could not eliminate gross melt fracture.

As a processing aid, a very small amount of boron nitride (typically less than 0.5 wt %) is added to polyolefin. It was reported that such small amount of boron nitride has no effect on the linear and nonlinear viscoelastic properties of polyethylenes (Yip et al. 2000b; Rosenbaum et al. 2000; Yip et al. 2000a). However, boron nitride slowed down the relaxation of metallocene polyethylenes during “relaxation after cessation of

steady shear" (at shear rate of 1 s^{-1}) but disappeared at higher shear rates (Hatzikiriakos and Migler 2005; Rosenbaum et al. 2000). Also, boron nitride can eliminate surface melt fracture and postpone gross melt fracture at high shear rates in metallocene polyethylenes (Rosenbaum et al. 2000) and high density polyethylene (Yip et al. 2000a). Similar to fluoropolymer, it was proposed that boron nitride migrates to the surface of the die especially at the die exit hence stick-slip is eliminated (Yip et al. 2000a). Boron nitride eliminates the gross melt fracture in polypropylene by making the discontinuous streamlines in the polymer bulk flow smoother at the die entry (Kazatchkov et al. 2000). It has no effect on the flow curve of polyethylene in capillary flow (Rosenbaum et al. 2000) but a small decrease in extrusion pressure may occur(Yip et al. 2000a). The effectiveness of boron nitride is dependent on its concentration in polyethylenes. Generally, a concentration less than 0.1 wt% worked better in polyethylenes (Yip et al. 1999; Rosenbaum et al. 2000; Yip et al. 2000a). Extrusion temperature, induction time, particle size and dispersion of boron nitride in the polymer matrix and its surface energy were important factors in the elimination of gross melt fracture by boron nitride (Yip et al. 2000a; Seth et al. 2002). Boron nitride is also used as a processing aid in other polymer processing applications such as film blowing (Pruss et al. 2002) and melt spinning (Vogel et al. 2003).

In the case of organoclay, a very small amount was suggested for used (less than 0.5 wt %) in polyolefin processing (Hatzikiriakos et al. 2005; Adesina and Hussein Accepted). It was reported that the organoclay has effect on the linear and non-linear rheology of high density polyethylenes (Adesina and Hussein Accepted). However, its effect decreases as the branch content of the polyethylene increases (Adesina and

Hussein Submitted). Organoclay was recently reported to be effective in the elimination of surface melt fracture and postponement of gross melt fracture to higher shear rates (Adesina and Hussein Accepted; Hatzikiriakos et al. 2005). Furthermore, Particle Image Velocimetry (PIV) measurement was used to study the wall slip effect HDPE in the presence of organoclay (Adesina et al. Submitted). They reported that organoclay enhanced wall slip in HDPE. It was proposed that organoclay migrates to the interface between HDPE and wall while at the same time streamline the bulk flow. The mechanism is indeed similar to that of boron nitride. This is not surprising because both processing aids are platey in structure.

Fluoropolymer and boron nitride had been combined to enhance and expand the processing window of polyolefin. The onset of gross melt fracture and reduction of extrusion pressure can further be enhanced when the processing aids were used individually (Seth and Hatzikiriakos 2001; Yip et al. 2000a; Rosenbaum et al. 2000; Vogel et al. 2003). However, little work has been done to explore the interaction between organoclay and fluoropolymer (Hatzikiriakos et al. 2005).

In this work, boron nitride, organoclay, fluoropolymer and the combination of fluoropolymer and organoclay were used as processing aids in the extrusion of HDPE. A specially designed slit die containing highly sensitive pressure transducers was used for collection of pressure fluctuations in different melt flow regimes. The slit die is attached to a single screw extruder. The recorded fluctuations at these different regimes were compared to characterize the effectiveness of the individual and mixed additives. Such fluctuations were quantified using Moment and Fourier Transform analyses.

5.2 Experimental

5.2.1 Materials

Commercial grade HDPE (relative density = 0.952, melting point = 132^{o}C and melt flow index=0.05g/10mins at 190^{o}C and 2.16 kg load) was used in this work. Its average-weight molecular weight (M_w) and polydispersity index (PDI) are 285 kg/mol and 26.5 respectively. Organoclay, boron nitride and fluoropolymers were used with HDPE for comparison. The organoclay used in this work was Cloisite$^{(R)}$ 15A (C15A) from Southern Clay, USA. According to the supplier, the d_{001} spacing of C15A was 31.5 Angstrom. Boron nitride used in this work contained 0.2 % borates. It had mean diameter less than 1μm, surface area of 20 m^2/g and was supplied by Saint-Gobain Ceramics, USA. Dynamar, a free-flowing fluoropolymer from Dyneon, USA was used to represent a conventional processing additive. It is a copolymer of hexafluoropropylene (HFP), vinylidene fluoride (VF_2) and tetrafluoroethylene (TFE). It has bulk density of 0.7. Antioxidant (0.1 wt %) was added to all samples to avoid degradation during melt blending (Hussein et al. 2000). It is a 50/50 weight blend of Irganox 1010 and Irgafos 168 from Ciba- Geigy Speciality, Switzerland.

5.2.2 Melt Blending and Morphology Characterization

The Brabender 50 EHT mixer supplied with a Plastograph (Brabender® GmbH & Co. Germany) was used in the preparation of the nanocomposites. Details of pre treatment of C15A were given elsewhere (Adesina and Hussein Accepted). Boron nitride and Dynamar were used as received from the manufacturers. HDPE was grinded and physically pre-mixed with each processing additive. Antioxidant was added during the physical mixing. Then, master batches containing organoclay and boron nitride were

prepared in the Brabender mixer. A desired final concentration of a particular blend was obtained by mixing additional virgin HDPE with the master batch using the same mixer. The blending was done at a temperature of 200^{o}C and a screw speed of 50 rpm for 10 minutes.

The amount of each processing aid was fixed at 0.05 wt %. To study the synergistic effect between organoclay and conventional processing additive, a final batch containing 0.05 wt % of C15A and 0.05 wt % Dynamar was prepared. In this work, HDPE-C15A, HDPE-BN, HDPE-C15A-Fluoro indicate HDPE containing 0.05 wt % C15A, 0.05 wt % boron nitride and 0.05 wt % C15A + 0.05 wt% Dynamar were used, respectively.

The structures of the (nano) composites were characterized by field emission scanning electron microscopy (FE-SEM) and X-ray diffractometry (XRD). The XRD analysis was performed on XRD-6000 Shimadzu diffractometer (Shimadzu Japan) with CuKα radiation (λ=0.154nm) in a reflection mode, operating at 40 kV and 30 mA. Scanning speed of 1^{o}/min was used. The scan range was 2-20^{o} at room temperature. Scanning electron micrographs were obtained with FE-SEM Nova^{TM} Nanosem 230 (FEI, USA). It is possible to achieve ultra-high resolution on non-conductive nano-materials with Nova^{TM} Nanosem 230. The SEM samples were made into thin films and etched for 4 hours. The etching solution is a solution of $H_2SO_4/H_3PO_4/H_2O$ (10/4/1) and 0.01 g/ml $KMnO_4$. The etched samples were further covered with gold to make them conductive.

5.2.3 Rheological Measurement

An ARES rheometer (TA Instruments, USA) was used for all the rheological measurements. The plates were heated for at least 20 minutes to equilibrate the temperature. Strain sweep tests were conducted for all the samples to determine the linear viscoelastic region and for FT-rheology. A Strain range of 10-400% with shear amplitude of 1rad/s was used. The details on the FT-rheology were given in a previous publication (Adesina and Hussein Submitted). Frequency sweep experiments were performed in the frequency range between 0.01 rad/s and 100 rad/s. The applied strain was 10%. Van Gurp Palmen plots were drawn from the frequency sweep data. The responses of the samples during stress growth were conducted to study the effect of organoclay on the non-linear shear material function of HDPE. The imposed shear rate was $0.8\ s^{-1}$. Low shear rate was used due to the limitation of the parallel plate geometry. An Extensional Viscosity Fixture (EVF) from ARES was used for the study of extensional rheology. The samples were pre-stretched with a strain rate of $0.4\ s^{-1}$ to remove sagging. The sample was left in the fixture for 3 minutes to relax any accumulated stress before the start of the experiment. A Hencky strain rate of 10 s^{-1} at a temperature of 145^{o}C, was used during the extensional experiments. Such a high Hencky strain rate and low temperature were necessary to observe the effect of the processing additives on the extensional rheology of HDPE.

5.2.4 Set-up for Melt Flow Instabilities

Extrusion was carried out in a single screw extruder 19/25D (Brabender® GmbH & Co. Germany) equipped with a specially developed slit die. The slit die had a dimension of 0.8 mm height, 20 mm width and 160 mm length. The slit die has three

highly sensitive piezoelectric transducers located at 30 mm, 80 mm and 140 mm from the entrance of the die (Figure 5.1). The pressure and time resolutions of these transducers are of the order 10^{-1} mbar and 1ms respectively. Details about the set up were shown elsewhere (Adesina and Hussein Submitted). The temperature of the three heater bands along the extruder was 180°C while the temperature of the die was 170°C.

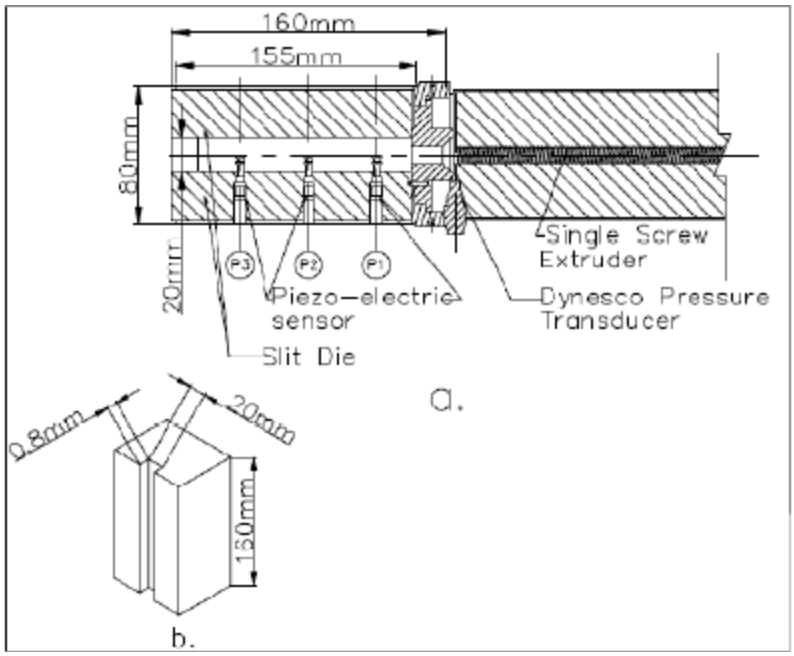

Figure 5.1: (a) Longitudinal section of the single screw extruder with slit die head having 3 highly sensitive piezoelectric pressure transducers along the die. This is the set-up for the study of melt instabilities during polymer extrusion. (b) The slit die with its dimensions

The pressure fluctuations from piezoelectric transducers were further analyzed using second order moment and Fourier transform analyses as defined in equations 1 and 2, respectively.

$$m_2 = \frac{1}{t_f - t_o} \int_{t_o}^{t_f} (p(t) - \bar{p})^2 dt \qquad (1)$$

where m_2 is the second moment of the pressure, $\bar{p}$ is the mean value which is the first moment around zero and $p(t)$ is the time dependent pressure fluctuation signal. The second moment is the variance and its square root is the standard deviation. In this work, the ratio of the standard deviation divided by the mean of the pressure fluctuation was used in the characterization of the melt instability.

$$p(t) = \bar{p} + \sum_{i\geq 1} l_i \cos(w_i t + \emptyset_i) \tag{2}$$

where $\bar{p}$ is the pressure mean value at $\frac{w}{2\pi} = 0$; $\frac{w_i}{2\pi}$, $\emptyset_i$ and l_i are the characteristic frequencies, phases, and amplitudes of the pressure fluctuation as quantified from the Fourier analysis of the processed signals, respectively. One of the most important parameters from the FT analysis in quantifying melt instabilities is the distortion factor (DF). This is a measure of the relative pressure fluctuation (RPF) as defined below:

$$DF = \frac{\sum_{i\geq 1} l_i}{l_o} \tag{3}$$

l_0 is the peak value at w=0 and it is related to the pressure mean value.

5.3 Results and Discussion

5.3.1 Morphological Characterization

The SEM of HDPE-C15A and HDPE-BN are as shown in Figures 5.2a and 5.2b. Figure 5.2a shows organoclay as dispersed in the HDPE matrix. However, the dispersion of boron nitride is accompanied with its agglomeration as shown in Figure 5.2b.The low distributive shearing effect of the mixer might have contributed to the agglomeration despite the residence time of 10 minutes.

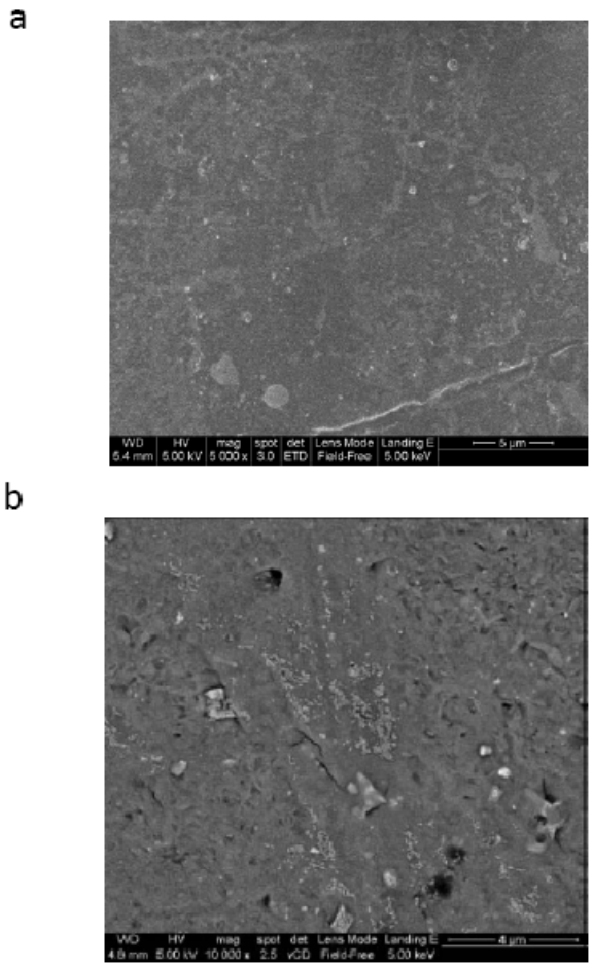

Figure 5.2: SEM of (a) HDPE-C15A and (b) HDPE-BN

5.3.2 Rheological Characterization

The frequency sweep data for each sample was presented in the form of van Gulp Palmen curve as shown in Figure 5.3. At the crossover region of the plot, no difference was observed in the phase angle. However, below the crossover frequency, the HDPE curve had the least slope. The observed increment in the phase angle for both HDPE-C15A and HDPE-BN was similar. The blend of fluoropolymer and HDPE also resulted in increase in phase angle of HDPE. The curve of HDPE-C15A-Fluoro was not

different from that of HDPE-Fluoro. So, the three processing additives gave higher phase angle below the longest crossover frequency. This implies that all the additives make HDPE more viscous.

The relative intensity and phase angle of the third harmonic of all the samples were as shown in Figures 5.4 and 5.5 respectively. The FT-rheology did not show the effect of processing additives on HDPE. Thus, the impact of processing additives on the higher harmonics, including the third harmonics, is negligible.

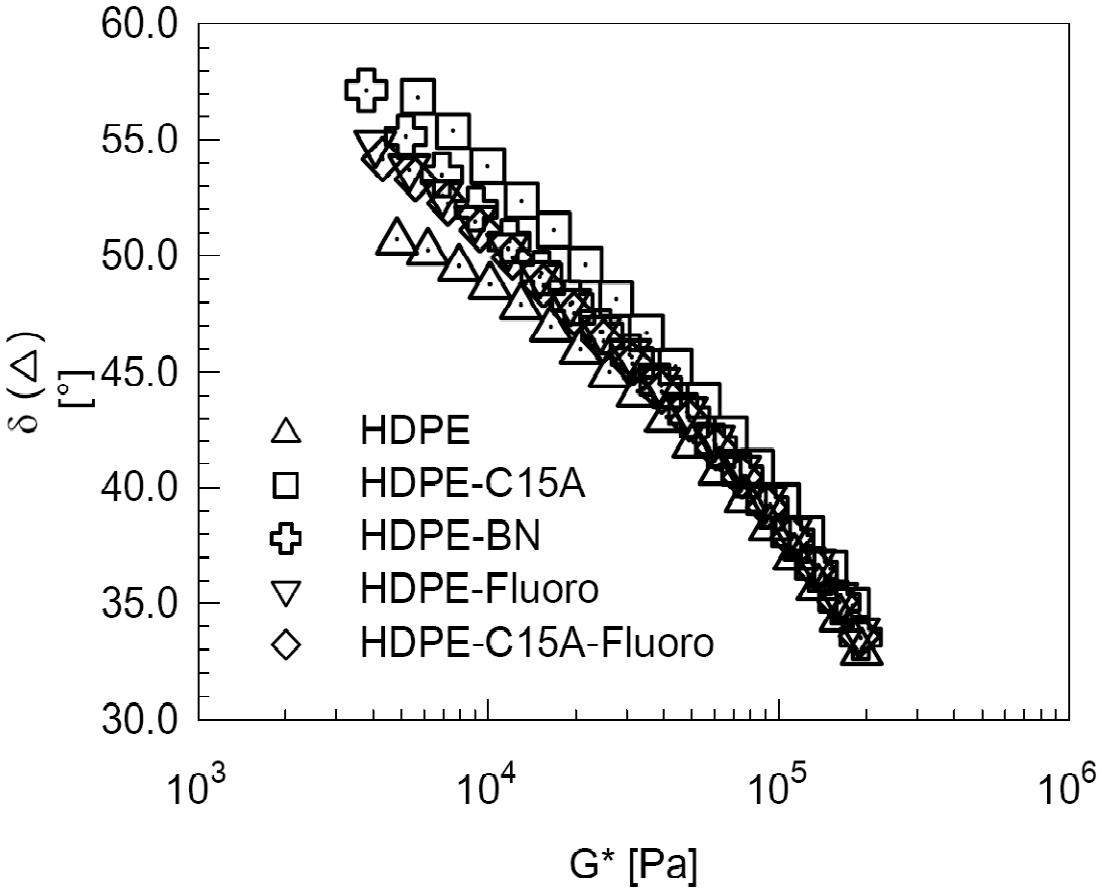

Figure 5.3: van Gurp Palmen plot for HDPE, HDPE-C15A, HDPE-BN, HDPE-Fluoro and HDPE-C15A-Fluoro

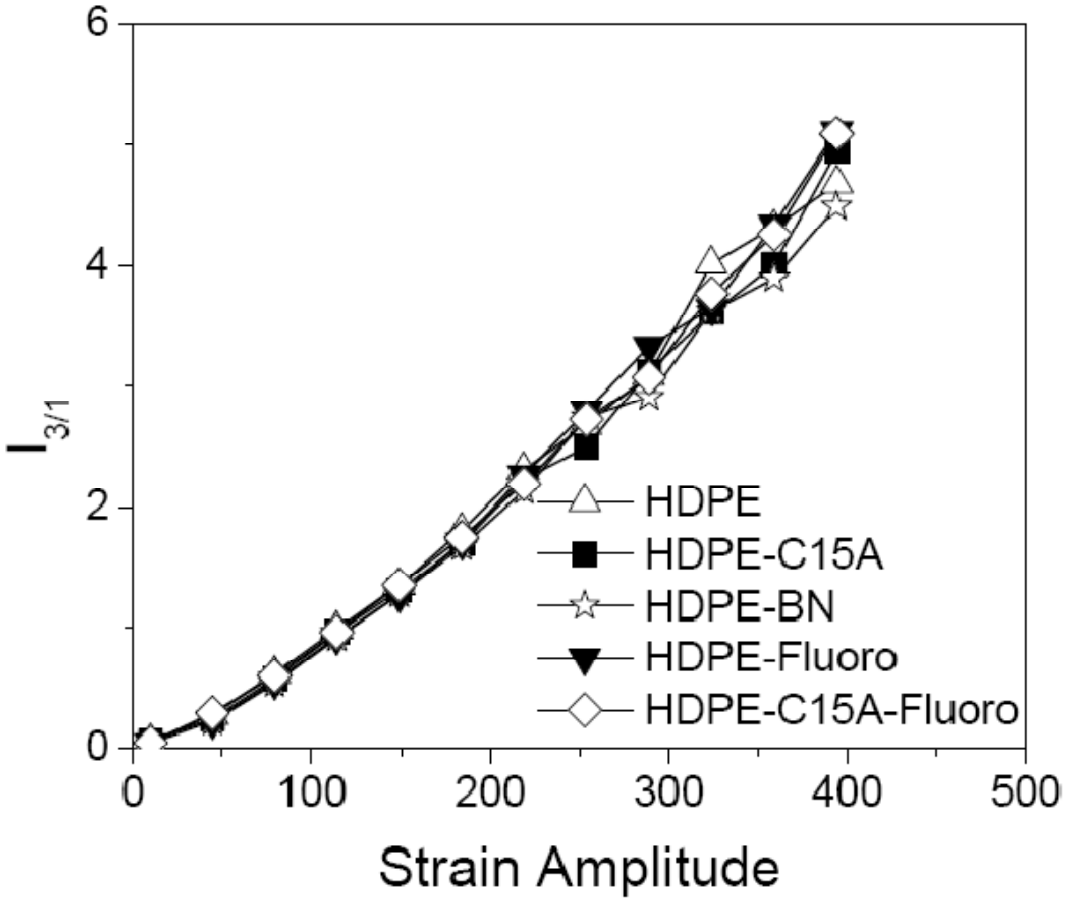

Figure 5.4: Relative intensity of the third harmonic as a function of strain amplitude at 200^{o}C for HDPE, HDPE-C15A, HDPE-BN, HDPE-Fluoro and HDPE-C15A-Fluoro

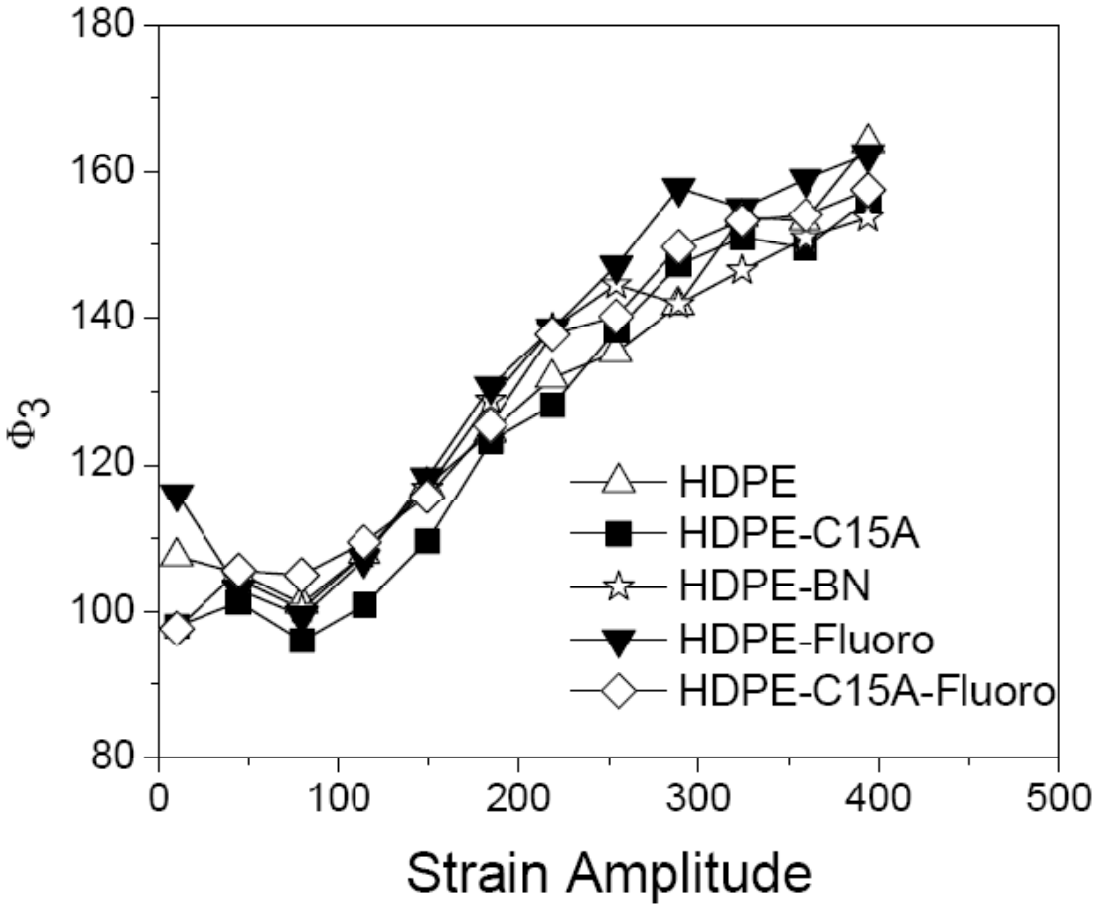

Figure 5.5: Relative phase angle of the third harmonic as a function of strain amplitude at 200^{o}C for HDPE, HDPE-C15A, HDPE-BN, HDPE-Fluoro and HDPE-C15A-Fluoro

The effect of different processing additives on HDPE during transient shear rheology was shown in Figure 5.6. All the additives resulted in the reduction of the transient shear viscosity of HDPE. The highest reduction in the transient viscosity of HDPE occurred with the addition of 0.05 wt % organoclay. The addition of both organoclay and fluoropolymer in HDPE resulted in a decrease in the transient viscosity of HDPE as well (figure not shown). The same trend was observed in the previous shear rheological results previously discussed (van Gurp Palmen plot), even though, not as obvious as observed during transient shear test experiment.

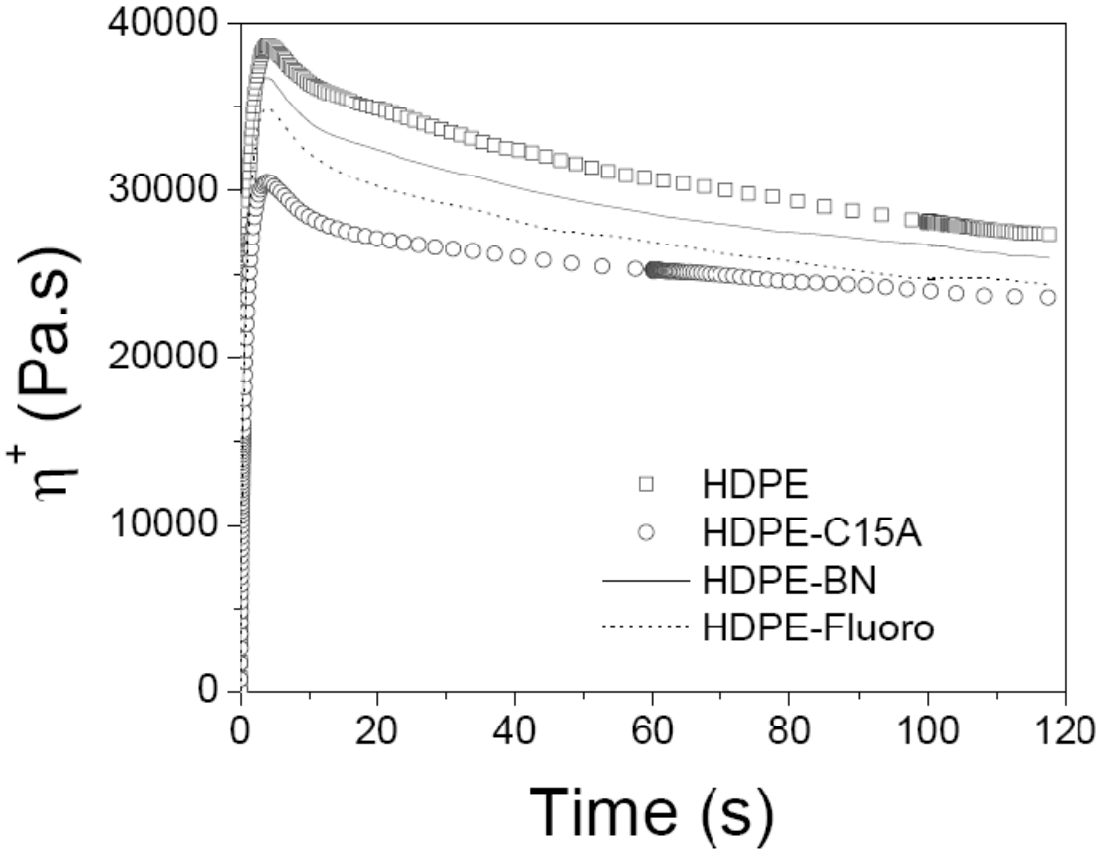

Figure 5.6: Transient shear growth test for HDPE, HDPE-C15A, HDPE-BN and HDPE-Fluoro

The extensional test results were shown in Figure 5.7. The trend was similar to the results discussed during the transient shear growth stress. All displayed processing additives reduced the extensional stress in HDPE. The highest reduction was observed with the addition of 0.05 wt% organoclay. The extensional strain in HDPE was reduced as well in the presence of all processing additives.

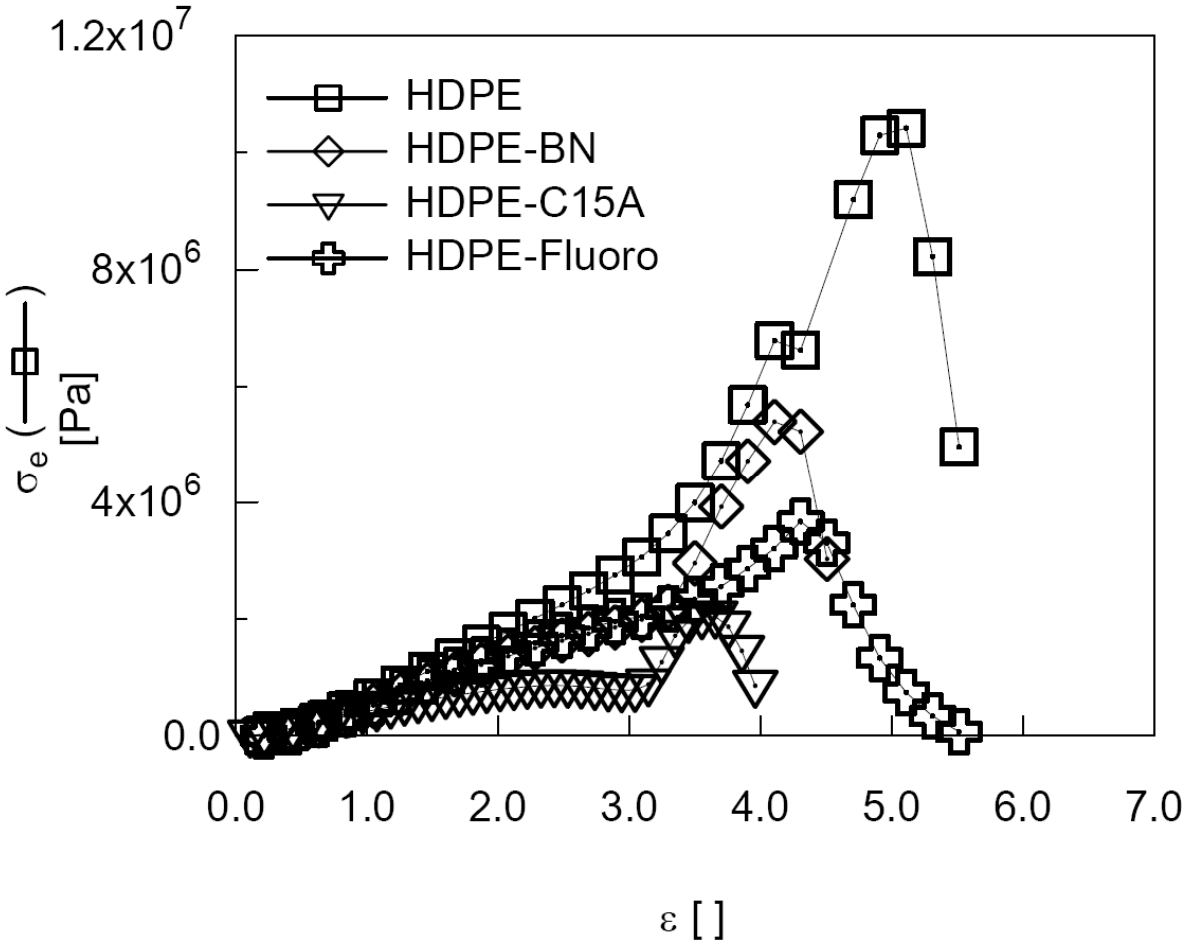

Figure 5.7: Extensional stress growth versus extensional strain for HDPE, HDPE-C15A, HDPE-BN and HDPE-Fluoro

5.3.3 Extrusion of HDPE with/without processing additives

The flow curve for the extrusion of HDPE at the set temperature (described above) was shown in Figure 5.8. Three different flow regimes were observed: smooth, stick-slip and gross melt fracture regimes. However, towards the end of the smooth regime the surface of the polymer melts slightly loses its glossiness as shown in Figure 5.9b. Figure 5.9a is a typical visualized extrudate before the onset of loss of glossiness at the smooth regime.

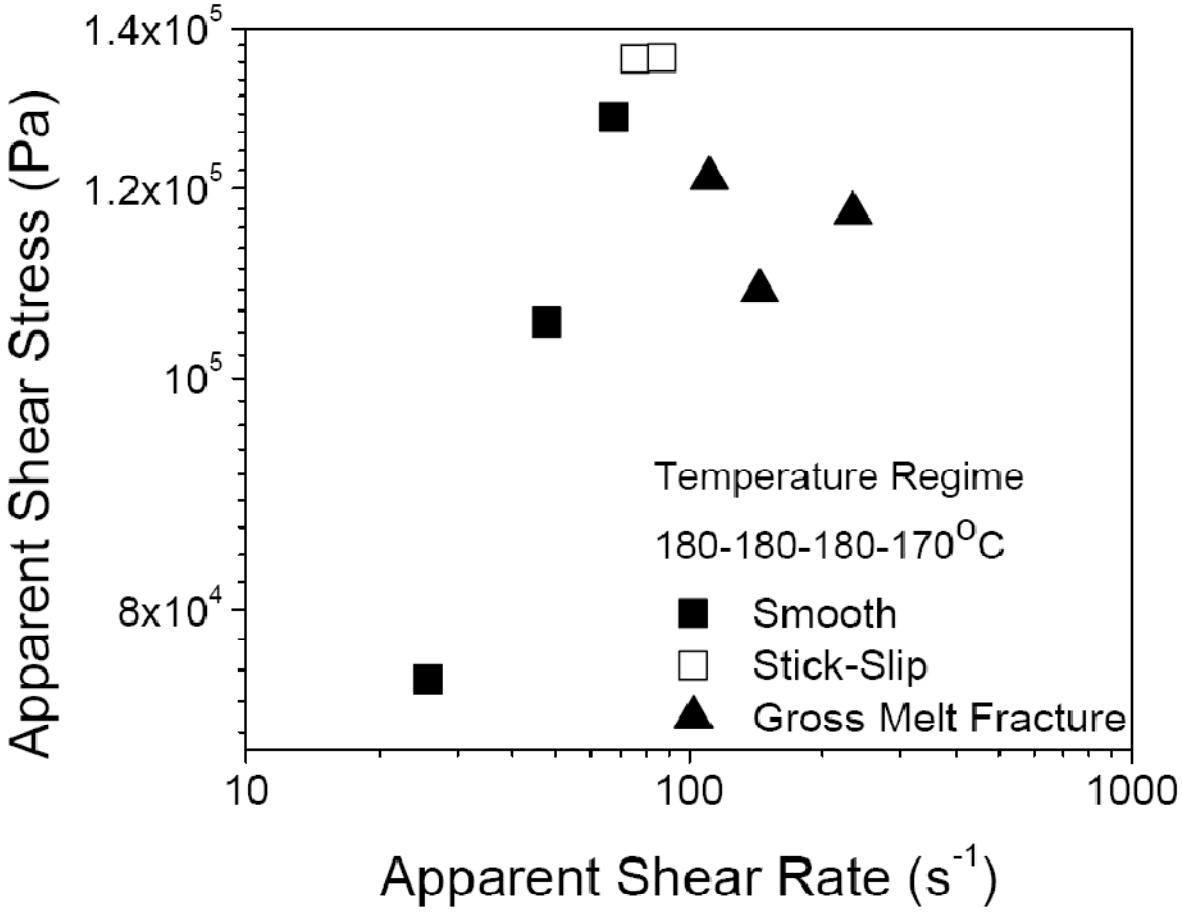

Figure 5.8: Flow curve of HDPE when the slit die temperature was 170^{o}C

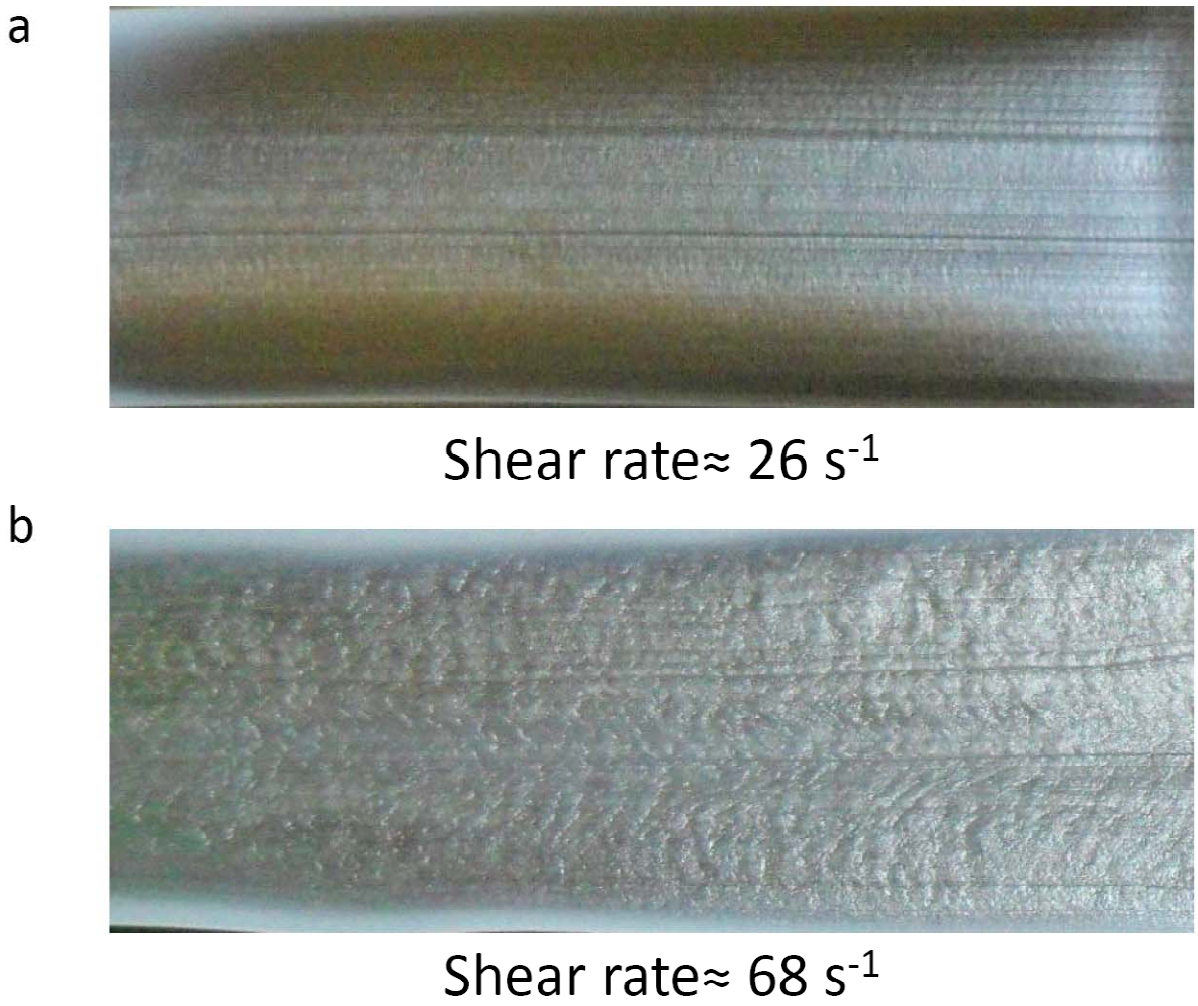

Figure 5. 9: HDPE extrudate at a shear rate of 26 s^{-1} and (b) at a shear rate of 68 s^{-1}

Figure 5.10 shows the extrudate at the stick-slip and gross melt fracture regimes. The stick-slip is characterized by high pressure fluctuation and mean pressure. However, a pressure drop occurred at the onset of gross melt fracture before gradual increase in the pressure as depicted in Figure 5.8.

a

Shear rate≈ 87 s^{-1}

b

Shear rate≈ 144 s^{-1}

Figure 5.10: HDPE extrudate (a) at a shear rate of 87 s^{-1} (stick-slip region) and (b) at a shear rate of 144 s^{-1} (Gross melt fracture region)

The effect of the different processing aids on HDPE was studied at three apparent shear rates. The shear rates were selected from the three regions. This was done because of material consumption during the experiment. At each shear rate, the experiment was conducted to last for about 30 minutes to attain stable flow and collect data for Fourier Transform analysis. The addition of the processing additives had effect on the appearance of the HDPE extrudate. It was visually observed that all the processing additives made the HDPE extrudate smoother at apparent shear rate of 67 s^{-1}.

At apparent shear rate of 87 s^{-1} (stick slip regime), all the processing aids eliminated the stick-slip instabilities in HDPE except when the fluoropolymer was used alone. It was observed that the fluoropolymer made the sample smooth until after about 15 minutes, when the instability reappeared. At this time, the melt instability was not stick-slip but gross-melt fracture. The reason for the reappearance of the fracture might be due to the fact that the fluoropolymer concentration used in this work was not optimal. A typical result for all other processing additives was as shown in Figure 5.11a.

At apparent shear rate of 144 s^{-1}, none of the processing additive eliminated the gross-melt fracture. The extrusion line was purged with pure HDPE before the commencement of any extrusion involving additives. At the beginning of extrusion when shear rate was 144 s^{-1}, the extrudates were smooth but the melt instability set in after a period of time. The time before the set-in of the gross-melt fracture varied depending on the additives. When the organoclay and fluoropolymer were combined together, it took about 20 minutes before the onset of the gross-melt fracture. This was found to be the longest time length. Figure 5.11b shows what happened to the HDPE-C15A extrudate after about 8 minutes from the start of the experiment.

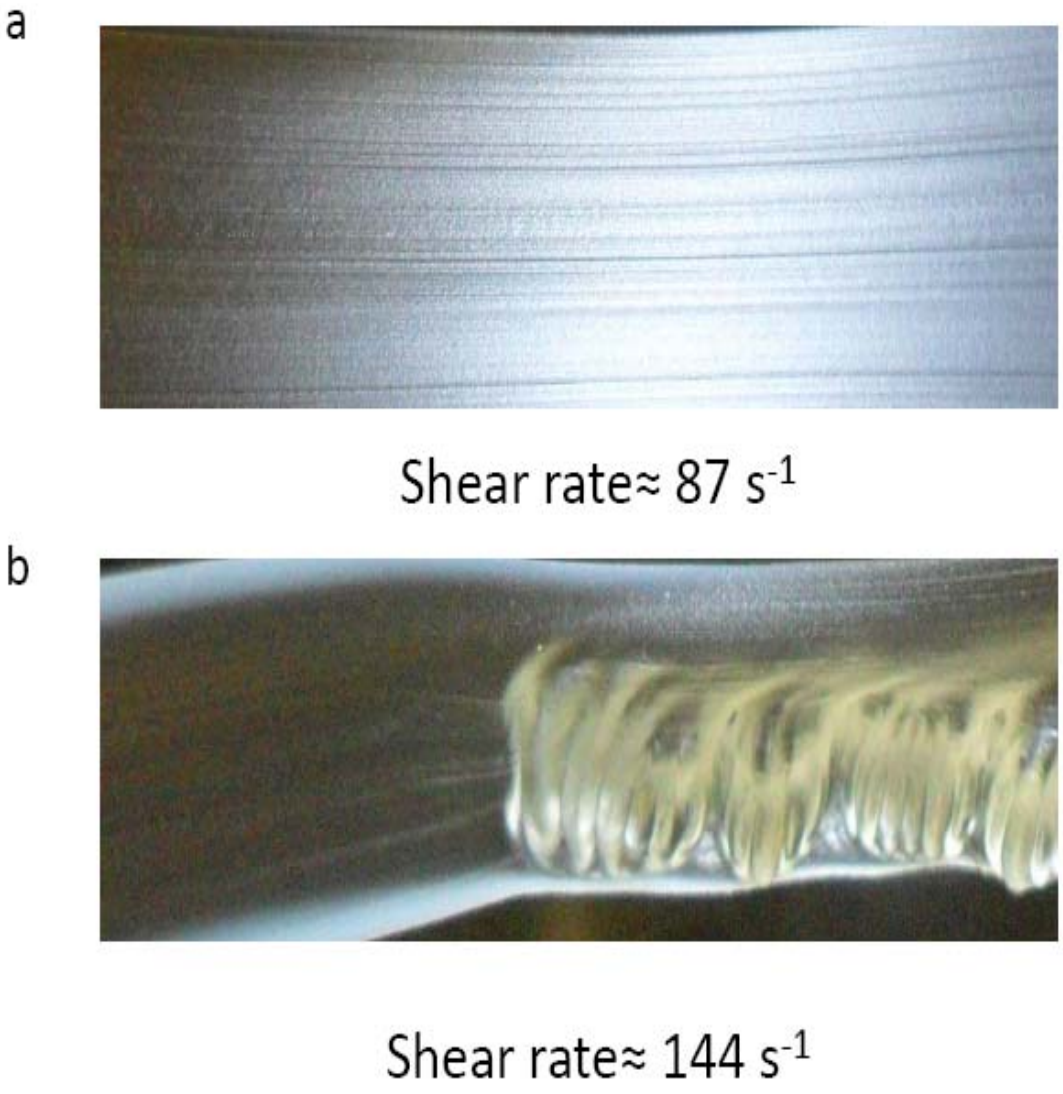

Figure 5.11: Extrudate of HDPE-C15A at apparent shear rate of (a) 87 s^{-1} (stick-slip region) and (b) 144 s^{-1} (gross melt fracture region)

The pressure fluctuations along the die characterized with moment and Fourier Transform analyses were presented in Figures 5.12 to 5.14. Figure 5.12 shows that the pressure fluctuation of HDPE is the highest at apparent shear rate of 67 s^{-1}. This result support the visual presentation presented earlier in Figure 5.9b. At apparent shear rate of 87 s^{-1}, both Moment and DF analyzes show that all the samples had similar values

except HDPE-Fluoro-C15A (Figure 5.12a) and HDPE-BN (Figure 5.12b). As the polymer melt flew down the slit die, all samples except HDPE-Fluoro relaxed faster than HDPE. As a result, the fluctuations in HDPE-BN, HDPE-C15A and HDPE-Fluoro-C15A were less as shown in Figures 5.13 and 5.14. These results also confirm the visual observations at stick-slip regime when all the additives remove the stick-slip instability except fluoropolymer.

At apparent shear rate of 114 s^{-1}, the difference between the moment and DF analyzes of all the samples was insignificant. This is in agreement with the observation that none of the processing additives eliminated the gross-melt fracture at this apparent shear rate. There is a need for further optimization with respect to the concentration of the processing aids. It was noted that the addition of fluoropolymer to HDPE containing organoclay (HDPE-C15A-Fluoro) further reduced the DF and S_D/P_{mean} of HDPE-C15A as shown in Figures 5.13 and 5.14.

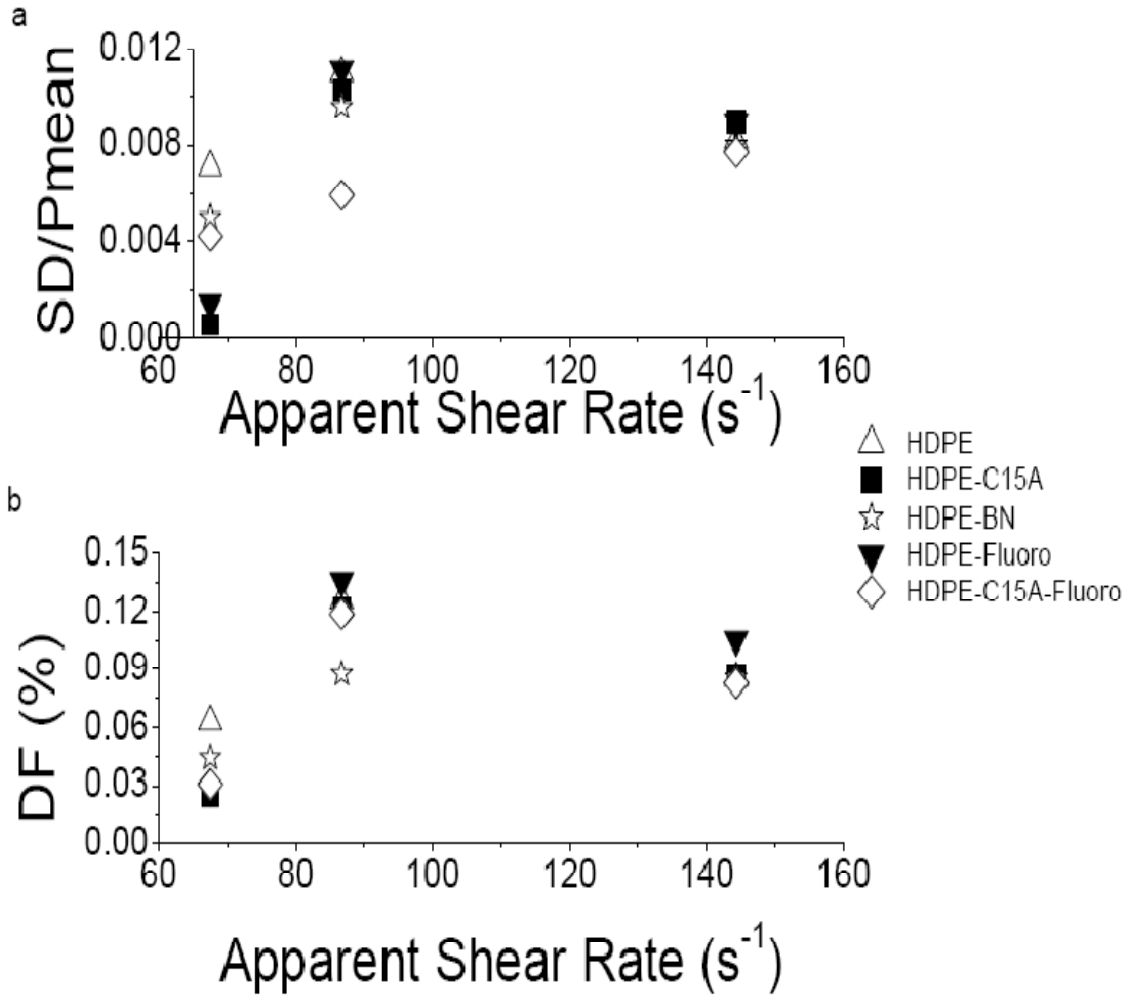

Figure 5.12: (a) Ratio of standard deviation and the mean pressure (b) Distortion factor as a function of apparent shear rate for HDPE, HDPE-C15A, HDPE-BN, HDPE-Fluoro and HDPE-C15A-Fluoro at transducer 1 position.

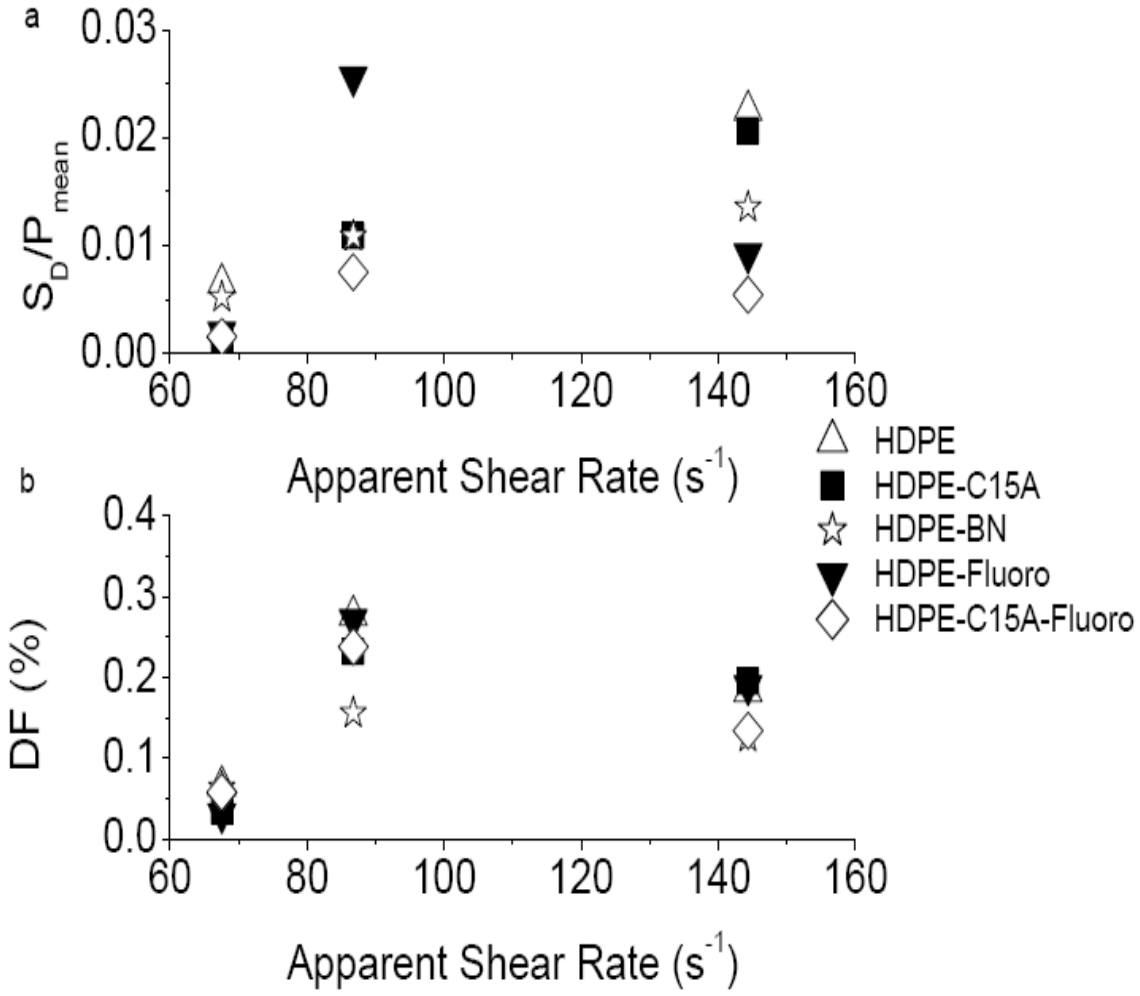

Figure 5.13: (a) Ratio of standard deviation and the mean pressure (b) Distortion factor as a function of apparent shear rate for HDPE, HDPE-C15A, HDPE-BN, HDPE-Fluoro and HDPE-C15A-Fluoro at transducer 2 position.

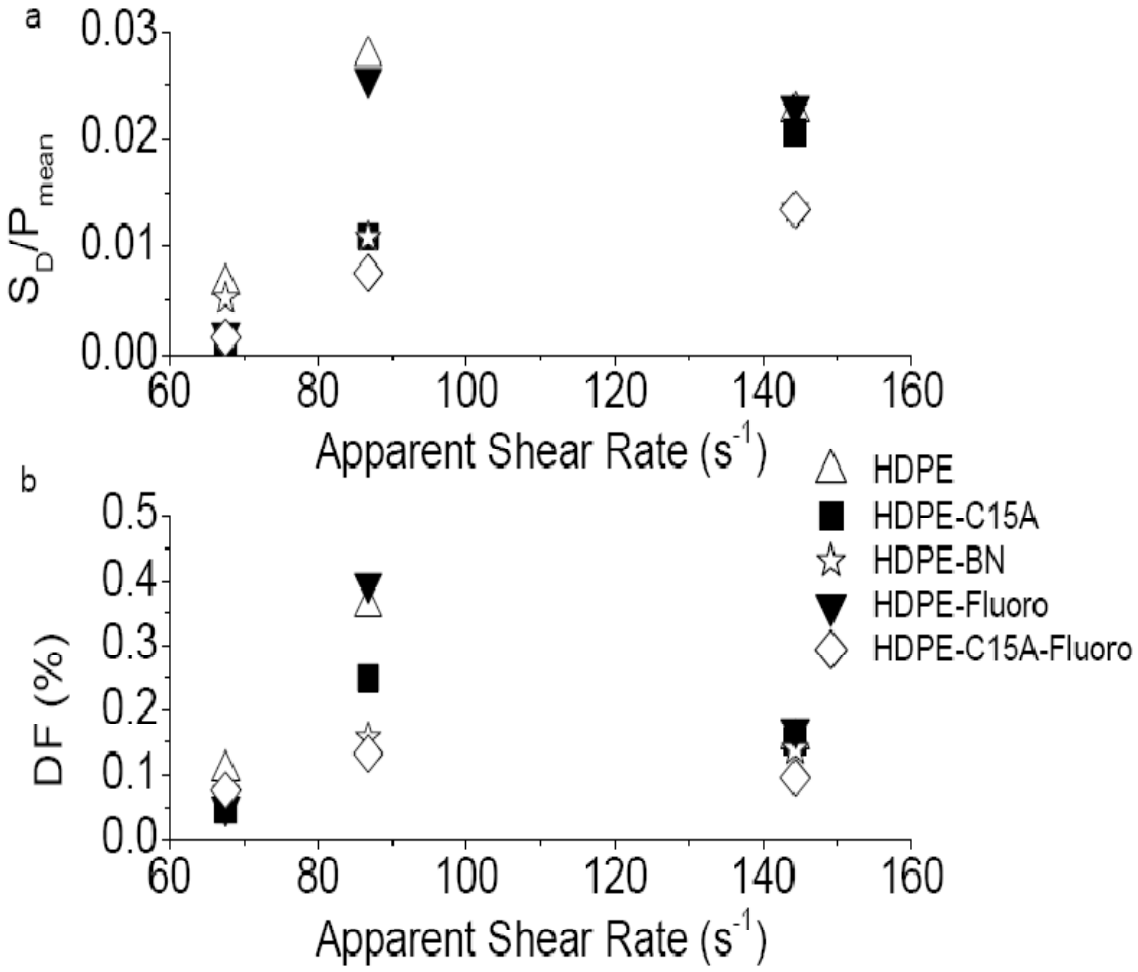

Figure 5.14: (a) Ratio of standard deviation and the mean pressure (b) Distortion factor as a function of apparent shear rate for HDPE, HDPE-C15A, HDPE-BN, HDPE-Fluoro and HDPE-C15A-Fluoro at transducer 3 position.

5.4 Conclusion

Different processing additives were considered in this work. Organoclay, boron nitride and fluoropolymer had effect on the phase angle of HDPE below the crossover frequency. Generally, at this region, the elastic modulus was reduced. Despite the effect of the additives on the phase angle of HDPE, the additives have no effect on the higher harmonics of HDPE as shown by FT-rheology. Organoclay and boron nitride reduced the transient shear viscosity and extensional stress growth of HDPE. Fluoropolymer also did the same. Furthermore, addition of fluoropolymer to HDPE containing organoclay reduced the transient shear viscosity and extensional stress growth.

Three different flow regimes were noticed during HDPE extrusion: smooth, stick slip and gross- melt fracture regimes. A weak and sharkskin-like extrudate was observed towards the end of the smooth regime. All the processing aids eliminated the weak sharkskin-like instability. Also, the stick-slip fracture was eliminated by all processing additives except fluoropolymer. The concentration of fluoropolymer used in this work was probably not optimal for this polymer. Furthermore, boron nitride and organoclay did not eliminate the gross-melt fracture at apparent shear rate of 114 s^{-1}. The combined organoclay and fluoropolymer did not as well. However, both moment and distortion factor analyzes were able to quantify the visual trends observed in the extrudates. The quantifying tools (Moment and DF Analyzes) indicated that the combined organoclay and fluoropolymer as processing aids acted better in the reduction of the pressure fluctuation as compared to when both were used individually.

5.5 References

Achilleos EC, Georgiou G, Hatzikiriakos SG (2002) Role of processing aids in the extrusion of molten polymers. Journal of Vinyl and Additive Technology 8 (1):7-24. doi:10.1002/vnl.10340

Adesina AA, Hussein IA (Accepted) Impact of Organoclay and Maleated Polyethylene on the Rheology and Instabilities in the Extrusion of High Density Polyethylene. Journal of Applied Polymer Science

Adesina AA, Hussein IA (Submitted) Rheology and Enhancement of Extrusion of linear and branched Polyethylenes using low amount of Organoclay. Journal of Applied Polymer Science

Adesina AA, Marques PN, Teixeira P, Hilliou L, Covas JA, Hussein IA (Submitted) Rheology and organoclay assisted slip in the extrusion of HDPE using Particle Image Velocimetry. Macromolecules

Anastasiadis SH, Hatzikiriakos SG (1998) The work of adhesion of polymer/wall interfaces and its association with the onset of wall slip. Journal of Rheology 42 (4):795-812

Barone JR, Plucktaveesak N, Wang SQ (1998) Interfacial molecular instability mechanism for sharkskin phenomenon in capillary extrusion of linear polyethylenes. Journal of Rheology 42 (4):813-832

Fujiyama M, Kawasaki Y (1991) Rheological properties of polypropylene/high-density polyethylene blend melts. I. Capillary flow properties. Journal of Applied Polymer Science 42 (2):467-480. doi:10.1002/app.1991.070420219

Guadarrama-Medina TdJ, Pérez-González J, de Vargas L (2005) Enhanced melt strength and stretching of linear low-density polyethylene extruded under strong slip conditions. Rheologica Acta 44 (3):278-286. doi:10.1007/s00397-004-0409-0

Hatzikiriakos SG, Hong P, Ho W, Stewart CW (1995) The effect of teflon™ coatings in polyethylene capillary extrusion. Journal of Applied Polymer Science 55 (4):595-603. doi:10.1002/app.1995.070550406

Hatzikiriakos SG, Kazatchkov IB, Vlassopoulos D (1997) Interfacial phenomena in the capillary extrusion of metallocene polyethylenes. Journal of Rheology 41 (6):1299-1316

Hatzikiriakos SG, Migler KB (2005) Polymer Processing Instabilities Control and Understanding Marcel Dekker, New York

Hatzikiriakos SG, Rathod N, Muliawan EB (2005) The effect of nanoclays on the processibility of polyolefins. Polymer Engineering & Science 45 (8):1098-1107. doi:10.1002/pen.20388

Hill DA, Hasegawa T, Denn MM (1990) On the apparent relation between adhesive failure and melt fracture. Journal of Rheology 34 (6):891-918

Hong Y, Coombs SJ, Cooper-White JJ, Mackay ME, Hawker CJ, Malmström E, Rehnberg N (2000) Film blowing of linear low-density polyethylene blended with a novel hyperbranched polymer processing aid. Polymer 41 (21):7705-7713

Hong Y, Cooper-White JJ, Mackay ME, Hawker CJ, Malmstrom E, Rehnberg N (1999) A novel processing aid for polymer extrusion: Rheology and processing of

polyethylene and hyperbranched polymer blends. Journal of Rheology 43 (3):781-793

Hussein IA, Ho K, Goyal SK, Karbashewski E, Williams MC (2000) Thermomechanical degradation in the preparation of polyethylene blends. Polymer Degradation and Stability 68 (3):381-392

Kazatchkov IB, Hatzikiriakos SG, Stewart CW (1995) Extrude distortion in the capillary/slit extrusion of a molten polypropylene. Polymer Engineering & Science 35 (23):1864-1871. doi:10.1002/pen.760352305

Kazatchkov IB, Yip F, Hatzikiriakos SG (2000) The effect of boron nitride on the rheology and processing of polyolefins. Rheologica Acta 39 (6):583-594. doi:10.1007/s003970000113

Kharchenko SB, McGuiggan PM, Migler KB (2003) Flow induced coating of fluoropolymer additives: Development of frustrated total internal reflection imaging. Journal of Rheology 47 (6):1523-1545

Larson RG (1992) Instabilities in viscoelastic flows. Rheologica Acta 31 (3):213-263. doi:10.1007/bf00366504

Migler KB, Lavallee C, Dillon MP, Woods SS, Gettinger CL (2001) Visualizing the elimination of sharkskin through fluoropolymer additives: Coating and polymer--polymer slippage. Journal of Rheology 45 (2):565-581

Migler KB, Son Y, Qiao F, Flynn K (2002) Extensional deformation, cohesive failure, and boundary conditions during sharkskin melt fracture. Journal of Rheology 46 (2):383-400

Pruss EA, Randa SK, Lyle SS, Clere TM (2002) Properties of m-LLDPE blown films extruded utilizing boron nitride based polymer process aids. Paper presented at the Proc. ANTEC, Tech. Pap. , San Francisco, CA,

Rodríguez-González F, Pérez-González J, de Vargas L, Marín-Santibáñez B Rheo-PIV analysis of the slip flow of a metallocene linear low-density polyethylene melt. Rheologica Acta 49 (2):145-154. doi:10.1007/s00397-009-0398-0

Rosenbaum EE, Randa SK, Hatzikiriakos SG, Stewart CW, Henry DL, Buckmaster M (2000) Boron nitride as a processing aid for the extrusion of polyolefins and fluoropolymers. Polymer Engineering & Science 40 (1):179-190. doi:10.1002/pen.11151

Seth M, Hatzikiriakos SG (2001) Combining boron nitride with a fluoroelastomer: An enhanced polymer processing additive. Journal of Vinyl and Additive Technology 7 (2):90-97. doi:10.1002/vnl.10273

Seth M, Hatzikiriakos SG, Clere TM (2002) Gross melt fracture elimination: The role of surface energy of boron nitride powders. Polymer Engineering & Science 42 (4):743-752. doi:10.1002/pen.10986

Shih CK (1976) Rheological properties of incompatible blends of two elastomers. Polymer Engineering & Science 16 (11):742-746. doi:10.1002/pen.760161106

Stewart CW (1993) Wall slip in the extrusion of linear polyolefins. Journal of Rheology 37 (3):499-513

Vogel R, Hatzikiriakos SG, Brünig H, Tändler B, Golzar M (2003) Improved Spinnability of Metallocene Polyethylenes by Using Processing Aids. International Polymer Processing (2):67-73

Xing KC, Schreiber HP (1996) Fluoropolymers and their effect on processing linear low-density polyethylene. Polymer Engineering & Science 36 (3):387-393. doi:10.1002/pen.10425

Yip F, Diraddo R, Hatzikiriakos SG (2000a) Effect of combining boron nitride with fluoroelastomer on the melt fracture of HDPE in extrusion blow molding. Journal of Vinyl and Additive Technology 6 (4):196-204. doi:10.1002/vnl.10253

Yip F, Hatzikiriakos SG, Clere TM (2000b) A new processing aid for the extrusion of polyolefins. Journal of Vinyl and Additive Technology 6 (2):113-118. doi:10.1002/vnl.10234

Yip K, Rozenbaum EE, Randa SK, Hatzikiriakos SG, Stewart CW (1999) The effect of boron nitride type and concentration on the rheology and processability of molten polymers. Paper presented at the Proc. ANTEC, New York, NY, USA,

CHAPTER SIX

Conclusions, Future Works and Significance of this Work

6.1 General Conclusion

The results obtained in this thesis work confirmed the use of organoclay as a processing aid in polyolefins. The work studied the effect of organoclay on the rheology and extrusion of polyolefins. The interaction between different processing aids was also investigated.

The work first considered the effect of organoclay on the linear polyethylene to establish the mechanism through which organoclay impact the extrusion of polyethylene. High density polyethylene was chosen for this preliminary study. Different polyethylenes were then used to generalize the effect of organoclay. In addition, other processing additives were compared with organoclay and possible synergy between them was discussed.

The organoclay used in this work was Cloisite 15A because of its high thermal stability and compatibility with polyolefins compared to others. The polymers investigated in this work included high density polyethylene and linear low density polyethylene of different branch content and catalyst of production. Oleamide and fluoropolymer were used as conventional slip agent and processing additives. Boron nitride, another promising processing aid was used in this work as well. Polyethylene grafted maleic anhydride was used as a compatibilizer.

The characterization tools including different rheometers, scanning electron microscopy, X-ray diffractometer, Particle image velocimetry, single and twin screw extruders with slit dies were used in this work.

At clay loadings between 0.05-0.1 wt percent, the shear and extensional rheology of HDPE were impacted. The elasticity, normal stress differences and extensional stress growth and strain of HDPE were reduced. All these contributed to the ability of the organoclay to act as a good processing aid during HDPE extrusion. The gross melt fracture was eliminated with organoclay in a single-screw extruder at slit die temperature of 145^{o}C. Both moment analysis and distortion factor showed that organoclay reduced the intensity of pressure fluctuations along the die. Extrusion pressure was reduced as well.

At low organoclay loading (0.05 -0.1 wt %), addition of a compatibilizer was found not to be necessary in the dispersion of organoclay when using a combination of master batching and dilution in the preparation of the polyolefin- organoclay nanocomposites.

Wall slip is an important phenomenon in rheology and processing. The work considered the effect of organoclay at low clay loading on the slip of HDPE at the wall during extrusion. The decrease in shear rate dependent viscosity of HDPE was as a result of shear thinning and not wall slip. Such reduction came out of disruption organoclay caused within HDPE hence less disentanglement.

PIV results showed that organoclay induced more wall slip in HDPE at all the shear rates. Based on all the aforementioned results, a possible mechanism was proposed to explain how organoclay affect the HDPE during continuous extrusion. In

the presence of strong flow, organoclay aligns in the direction of flow and migrate to the surface. Such alignment and migration resulted in dual effects on bulk and surface properties of HDPE.

The study on the interaction between organoclay and polyethylenes of different branch content showed that organoclay had effect only on linear viscoelastic properties of linear polyethylene. The transient stress overshoot and normal stress difference were reduced when 0.05 wt % organoclay was added to the polyethylenes. Extensional stresses became dissipated in the presence of organoclay as well. However, such effect became reduced as the branch content increases. The trend is independent of the type of flow.

Organoclay, boron nitride and fluoropolymer had effect on the phase angle of HDPE below the cross over frequency. Generally, at this region, the elastic modulus was reduced. Similar trend was observed during transient shear growth and extensional tests. Organoclay and boron nitride reduced the transient shear viscosity as well as the extensional stress growth of HDPE. Fluoropolymer also did the same. Addition of fluoropolymer to HDPE containing organoclay reduced the transient shear viscosity and extensional stress growth. The reduction was less than the decrease attained when both were used individually.

Higher shear rates were obtained when the slit die temperature was increased from 145^{o}C to 170^{o}C. At 170^{o}C, three different flow regimes were noticed during HDPE extrusion: smooth, stick slip and gross melt fracture regimes. The extrudate became weak sharkskin -like towards the end of the smooth regime. All the processing aids eliminated the weak sharkskin-like instability. However, the fluoropolymer did not

succeed in eliminating the stick-slip fracture. The concentration of fluoropolymer use was probably not optimal for this polymer. Boron nitride and organoclay did not eliminate the gross melt fracture at apparent shear rate of 114 s^{-1}. The combined organoclay and fluoropolymer did not as well. However, both moment and distortion factor analyzes were able to quantify the visual trends observed in the extrudates. The quantifying tools indicated that combined organoclay and fluoropolymer as processing aids acted better in the reduction of the pressure fluctuation compared to when both were used individually.

6.2 Future Work

The focus of this research work was very interesting and promising. However, there are some areas yet to be investigated. Some of these are discussed in this section.

The single screw extruder with the specially designed slit die for instability study had limitation of low shear rate. The possible reason for this was the size of the die, especially the slit die gap, is big. For this reason, it was high density polyethylene that was investigated. Future efforts should be on how to re-design the slit die so that high shear rate can be attained. For example, Professor Wilhelm and his group (Germany) proposed the redesign of the slit die inlay as shown in the figure below:

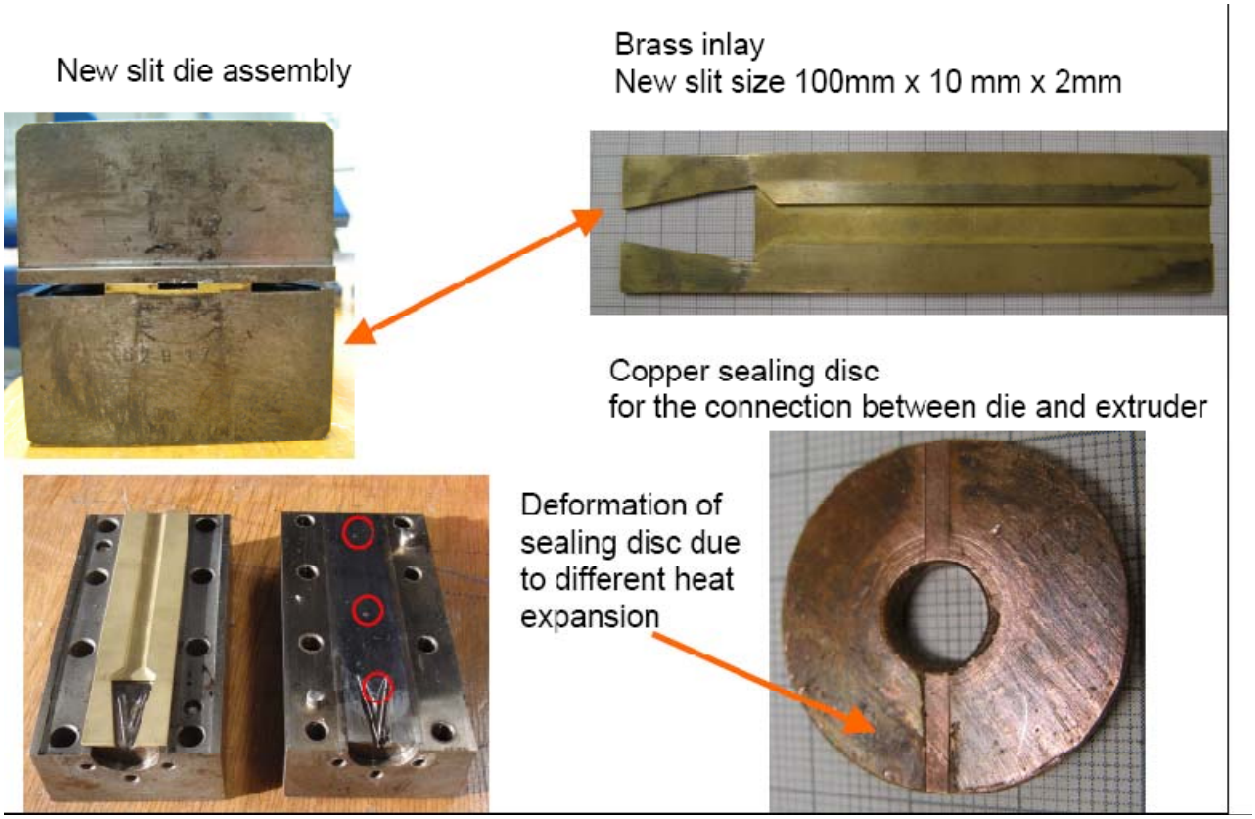

Figure 6.1: Design of a new slit die inlay to increase the polymer melt flowrate

It should be noted that different temperature setting between the single screw region and slit die has long term effect on the sealing disc used as a coupling device between the die head and screw region. Unfortunately, the temperature regime used in this work violated the condition of equal temperature along the extruder and the die. So, it will be a better option to modify the slit inlay as shown in Figure 6.1 to attain higher shear rate. However, this may also result in an increase in the pressure head. There should be a compromise between the competing factors during the redesign.

The PIV experiment was very useful in unfolding the underlying mechanism between high density polyethylene during extrusion and organoclay at low concentration (0.05-0.1 wt %). However, there is a need to extend the work to measure the wall slip at higher shear rates. In addition, other polyolefins should be considered.

6.3 Significance of the work

The work further confirmed the use of organoclay as a processing aid during extrusion of polyolefins. The mechanism through which organoclay interacted with polyolefins during extrusion was suggested.

The use of a slit die containing highly sensitive piezoelectric transducer combined with advanced data analysis is a right step towards evolving an “intelligent extruder”. Further enhancement of the work can lead to an automation of the extrusion in the wake of melt instabilities.

This work finds applicability in all polymer-based industries that use extruder. Saudi Arabia Basic Industries Corporation (SABIC) and SIPCHEM can benefit immensely from this research to enhance their product throughput and better automation of extrusion during polymer processing.

REFERENCES

1 Giannelis, E.P. Polymer Layered Silicate Nanocomposites. *Advanced Materials*, 1996, 8(1), 29-35.

2 Sinha Ray, S. and Okamoto, M. Polymer/layered silicate nanocomposites: a review from preparation to processing. *Progress in Polymer Science*, 2003, 28(11), 1539-1641.

3 Vaia, R.A., Ishii, H. and Giannelis, E.P. Synthesis and properties of two-dimensional nanostructures by direct intercalation of polymer melts in layered silicates. *Chemistry of Materials*, 1993, 5(12), 1694-1696.

4 Chen, J.-S., Poliks, M.D., Ober, C.K., Zhang, Y., Wiesner, U. and Giannelis, E. Study of the interlayer expansion mechanism and thermal-mechanical properties of surface-initiated epoxy nanocomposites. *Polymer*, 2002, 43(18), 4895-4904.

5 Mohanty, A.K., Wibowo, A., Misra, M. and Drzal, L.T. Development of renewable resource–based cellulose acetate bioplastic: Effect of process engineering on the performance of cellulosic plastics. *Polymer Engineering & Science*, 2003, 43(5), 1151-1161.

6 Hiroi, R., Ray, S.S., Okamoto, M. and Shiroi, T. Organically Modified Layered Titanate: A New Nanofiller to Improve the Performance of Biodegradable Polylactide. *Macromolecular Rapid Communications*, 2004, 25(15), 1359-1364.

7 Mitchell, C.A., Bahr, J.L., Arepalli, S., Tour, J.M. and Krishnamoorti, R. Dispersion of Functionalized Carbon Nanotubes in Polystyrene. *Macromolecules*, 2002, 35(23), 8825-8830.

8 Sinha Ray, S. and Bousmina, M. Biodegradable polymers and their layered silicate nanocomposites: In greening the 21st century materials world. *Progress in Materials Science*, 2005, 50(8), 962-1079.

9 Aranda, P. and Ruiz-Hitzky, E. Poly(ethylene oxide)-silicate intercalation materials. *Chemistry of Materials*, 1992, 4(6), 1395-1403.

10 Vaia, R.A. and Giannelis, E.P. Polymer Melt Intercalation in Organically-Modified Layered Silicates:â€‰ Model Predictions and Experiment. *Macromolecules*, 1997, 30(25), 8000-8009.

11 Hotta, S. and Paul, D.R. Nanocomposites formed from linear low density polyethylene and organoclays. *Polymer*, 2004, 45(22), 7639-7654.

12 Chang, J.-H., An, Y.U., Cho, D. and Giannelis, E.P. Poly(lactic acid) nanocomposites: comparison of their properties with montmorillonite and synthetic mica (II). *Polymer*, 2003, 44(13), 3715-3720.

13 Paul, M.-A., Alexandre, M., Degée, P., Henrist, C., Rulmont, A. and Dubois, P. New nanocomposite materials based on plasticized poly(-lactide) and organo-modified montmorillonites: thermal and morphological study. *Polymer*, 2003, 44(2), 443-450.

14 Shah, R.K. and Paul, D.R. Organoclay degradation in melt processed polyethylene nanocomposites. *Polymer*, 2006, 47(11), 4075-4084.

15 Hatzikiriakos, S.G., Rathod, N. and Muliawan, E.B. The effect of nanoclays on the processibility of polyolefins. *Polymer Engineering & Science*, 2005, 45(8), 1098-1107.

16 Carreras E., N. Kissi, J.-M. Piau, F. Toussaint, and S. Nigen, *Rheologica Acta*, 45, 209 (2006).

17 Evdokia A., C. G. Georgios, and S. G. Hatzikiriakos, *Applied Rheology* 88 (2002).

18 Hatzikiriakos S. G. and K. B. Migler, *Polymer Processing Instabilities Control and Understanding*, Marcel Dekker, New York (2005).

19 Delgadillo-Velázquez O., G. Georgiou, M. Sentmanat, and S. G. Hatzikiriakos, *Polymer Engineering & Science*, **48,** 405 (2008).

20 Mitsuyoshi F. and I. Hitoshi, *Journal of Applied Polymer Science*, **84,** 2111 (2002).

21 Mitsuyoshi F. and I. Hitoshi, *Journal of Applied Polymer Science*, **84,** 2120 (2002).

22 Palza H., S. Filipe, I. F. C. Naue, and M. Wilhelm, *Polymer*, **51,** 522 (2010).

23 Anastasiadis S. H. and S. G. Hatzikiriakos, *Journal of Rheology*, **42,** 795 (1998).

24 Kolnaar J. W. H. and A. Keller, *Journal of Non-Newtonian Fluid Mechanics*, **69,** 71 (1997).

25 Pudjijanto S. and M. M. Denn, *Journal of Rheology*, **38,** 1735 (1994).

26 Perez-Gonzalez J. and M. M. Denn, *Industrial & Engineering Chemistry Research*, **40,** 4309 (2001).

27 Hatzikiriakos S. G., H. Peter, H. Wally, and W. S. Charles, *Journal of Applied Polymer Science*, **55,** 595 (1995).

28 Kazatchkov I. B., S. G. Hatzikiriakos, N. Bohnet, and S. K. Goyal, *Polymer Engineering & Science*, **39,** 804 (1999).

29 Filipe S., A. Becker, C. V. Barroso, and M. Wilhelm, *Appl. Rheology* 12 (2009).

30 Hong Y., J. J. Cooper-White, M. E. Mackay, C. J. Hawker, E. Malmstrom, and N. Rehnberg, *Journal of Rheology*, **43,** 781 (1999).

31 Hong Y., S. J. Coombs, J. J. Cooper-White, M. E. Mackay, C. J. Hawker, E. Malmström, and N. Rehnberg, *Polymer*, **41,** 7705 (2000).

32 Hatzikiriakos S. G., I. B. Kazatchkov, and D. Vlassopoulos, *Journal of Rheology*, **41,** 1299 (1997).

33 Xing K. C. and H. P. Schreiber, *Polymer Engineering & Science*, **36,** 387 (1996).

34 Migler K. B., C. Lavallee, M. P. Dillon, S. S. Woods, and C. L. Gettinger, *Journal of Rheology*, **45,** 565 (2001).

35 Kharchenko S. B., P. M. McGuiggan, and K. B. Migler, *Journal of Rheology*, **47,** 1523 (2003).

36. Franky Y., S. G. Hatzikiriakos, and M. C. Thomas, *Journal of Vinyl and Additive Technology*, **6,** 113 (2000).

37 Eugene E. R., K. R. Stuart, S. G. Hatzikiriakos, W. S. Charles, L. H. Donald, and B. Marlin, *Polymer Engineering & Science*, **40,** 179 (2000).

38 Manish S., S. G. Hatzikiriakos, and M. C. Thomas, *Polymer Engineering & Science*, **42,** 743 (2002).

39 Kazatchkov I. B., F. Yip, and S. G. Hatzikiriakos, *Rheologica Acta*, **39,** 583 (2000).

40 Palza H., B. Reznik, M. Kappes, F. Hennrich, I. F. C. Naue, and M. Wilhelm, *Polymer*, **51,** 3753 (2010).

41 Kharchenko S. B., J. F. Douglas, J. Obrzut, E. A. Grulke, and K. B. Migler, *Nat Mater*, **3,** 564 (2004).

42 Hatzikiriakos S. G., R. Nimish, and B. M. Edward, *Polymer Engineering & Science*, **45,** 1098 (2005).

43 Manish S. and S. G. Hatzikiriakos, *Journal of Vinyl and Additive Technology*, **7,** 90 (2001).

44 Kim Y. C. and K. S. Yang, *Polymer Journal*, **31,** 579 (1999).

45 Muliawan E. B., N. Rathod, S. G. Hatzikiriakos, and M. Sentmanat, *Polymer Engineering & Science*, **45,** 669 (2005).

46 Lee S. M. and J. W. Lee, in *Proceeding ANTEC, Technical Paper* New York, USA, (2001).

47 Seth M., F. Yip, and S. G. Hatzikiriakos, in *Proceeding ANTEC, Technical Paper* pp. 2649, Dallas, TX, (2000).

48 Yip F., R. Diraddo, and S. G. Hatzikiriakos, *Journal of Vinyl and Additive Technology*, **6,** 196 (2000).

49 Kim Y. C., S. J. Lee, J. C. Kim, and H. Cho, *Polymer Journal*, **37,** 206 (2005).

50 Hotta S. and D. R. Paul, *Polymer*, **45,** 7639 (2004).

51 Százdi L., Á. Ábrányi, B. Pukánszky, and J. G. Vancso, *Macromolecular Materials and Engineering*, **291,** 858 (2006).

52 Macosko C. W., *Rheology Principles, Measurements, and Applications*, Wiley-VCH, New York (1994).

53 Filipe S., I. Vittorias, and M. Wilhelm, *Macromolecular Materials and Engineering*, **293,** 57 (2008).

54 Sentmanat M. and S. G. Hatzikiriakos, *Rheologica Acta*, **43,** 624 (2004).

55 Larson R. G., *Rheologica Acta*, **31,** 213 (1992).

56. Kissi N. E., L. Léger, J. M. Piau, and A. Mezghani, *Journal of Non-Newtonian Fluid Mechanics*, **52,** 249 (1994).

57 Mooney, M. *Journal of Rheology* **1931,** 2, (2), 210-222.

58 Reiner, M. *Journal of Rheology* **1931,** 2, (4), 337-350.

59 Denn, M. M. *Annual Review of Fluid Mechanics* **2001,** 33, (1), 265-287.

60 Schowalter, W. R. *Journal of Non-Newtonian Fluid Mechanics* **1988,** 29, 25-36.

61 Granick, S.; Binder, K.; de Gennes, P. G.; Giannelis, E.; Grest, G.; Hervet, H.; Krishnamoorti, R.; Léger, L.; Manias, E.; Raphaël, E.; Wang, S. Q.; Wang, S.-Q., Molecular Transitions and Dynamics at Polymer / Wall Interfaces: Origins of Flow Instabilities and Wall Slip. In *Polymers in Confined Environments*, Springer Berlin / Heidelberg: 1999; Vol. 138, pp 227-275.

62 Joshi, Y. M.; Lele, A. K.; Mashelkar, R. A. *Journal of Non-Newtonian Fluid Mechanics* **2000,** 89, (3), 303-335.

63 Done, D. S.; Baird, D. G.; Everage, A. E. *Chemical Engineering Communications* **1983,** 21, (4), 293 - 309.

64 Ghanta, V. G.; Riise, B. L.; Denn, M. M. *Journal of Rheology* **1999,** 43, (2), 435-442.

65 Perez-Gonzalez, J.; Denn, M. M. *Industrial & Engineering Chemistry Research* **2001,** 40, (20), 4309-4316.

66. Piau, J. M.; El Kissi, N.; Tremblay, B. *Journal of Non-Newtonian Fluid Mechanics* **1988,** 30, (2-3), 197-232.

67. Piau, J. M.; Nigen, S.; El Kissi, N. *Journal of Non-Newtonian Fluid Mechanics* **2000,** 91, (1), 37-57.

68 Kalika, D. S.; Denn, M. M. *Journal of Rheology* **1987,** 31, (8), 815-834.

69 Ramamurthy, A. V. *Journal of Rheology* **1986,** 30, (2), 337-357.

70. Perez-Gonzalez, J. *Journal of Rheology* **2001,** 45, (4), 845-853.

71 Piau, J. M.; El Kissi, N. *Journal of Non-Newtonian Fluid Mechanics* **1994,** 54, 121-142.

72 Piau, J. M.; Kissi, N.; Mezghani, A. *Journal of Non-Newtonian Fluid Mechanics* **1995,** 59, (1), 11-30.

73 Hatzikiriakos, S. G.; Dealy, J. M. *Journal of Rheology* **1991,** 35, (4), 497-523.

74 Reimers, M. J.; Dealy, J. M. *Journal of Rheology* **1996,** 40, (1), 167-186.

75 Yoshimura, A.; Prud'homme, R. K. *Journal of Rheology* **1988,** 32, (1), 53-67.

76 Henson, D. J.; Mackay, M. E. *Journal of Rheology* **1995,** 39, (2), 359-373.

77 Archer, L. A., Wall Slip: Measurement and Modeling Issues. In *Polymer Processing Instabilities: Control and Understanding* Hatzikiriakos, S. G.; Migler, K. B., Eds. Marcel Dekker: U.S.A, 2005; pp 73-120.

78 Black, W. B.; Graham, M. D. *Physical Review Letters* **1996,** 77, (5), 956.

79 Dhori, P. K.; Giacomin, A. J.; Slattery, J. C. *Journal of Non-Newtonian Fluid Mechanics* **1997,** 71, (3), 215-229.

80 Dao, T. T.; Archer, L. A. *Langmuir* **2002,** 18, (7), 2616-2624.

81 Barone, J. R.; Wang, S. Q. *Journal of Rheology* **2001,** 45, (1), 49-60.

82 Hay, G.; Mackay, M. E.; McGlashan, S. A.; Park, Y. *Journal of Non-Newtonian Fluid Mechanics* **2000,** 92, (2-3), 187-201.

83 Mackay, M. E.; Henson, D. J. *Journal of Rheology* **1998,** 42, (6), 1505-1517.

84 Hay, G.; Mackay, M. E.; Awati, K. M.; Park, Y. *Journal of Rheology* **1999,** 43, (5), 1099-1116.

85 Yang, X.; Ishida, H.; Wang, S.-Q. *Journal of Rheology* **1998,** 42, (1), 63-80.

86 Migler, K. B.; Hervet, H.; Leger, L. *Physical Review Letters* **1993,** 70, (3), 287.

87 Kraynik, A. M.; Schowalter, W. R. *Journal of Rheology* **1981,** 25, (1), 95-114.

88 Lim, F. J.; Schowalter, W. R. *Journal of Rheology* **1989,** 33, (8), 1359-1382.

89 Mhetar, V.; Archer, L. A. *Macromolecules* **1998,** 31, (19), 6639-6649.

90 Rodríguez-González, F.; Pérez-González, J.; de Vargas, L.; Marín-Santibáñez, B. *Rheologica Acta* **2010,** 49, (2), 145-154.

91 Munstedt, H.; Schmidt, M.; Wassner, E. *Journal of Rheology* **2000,** 44, (2), 413-427.

92 Robert, L.; Demay, Y.; Vergnes, B. *Rheologica Acta* **2004,** 43, (1), 89-98.

93 Mitsoulis, E.; Schwetz, M.; Münstedt, H. *Journal of Non-Newtonian Fluid Mechanics* **2003,** 111, (1), 41-61.

94 Fournier, J. E.; Lacrampe M. F. ; Krawczak, P. *eXPRESS Polymer Letters* **2009,** 3, 569-578.

95 Mackley, M. R.; Moore, I. P. T. *Journal of Non-Newtonian Fluid Mechanics* **1986,** 21, (3), 337-358.

96 Nigen, S.; El Kissi, N.; Piau, J. M.; Sadun, S. *Journal of Non-Newtonian Fluid Mechanics* **2003,** 112, (2-3), 177-202.

97. Rodríguez-González, F.; Pérez-González, J.; Marín-Santibáñez, B. M.; de Vargas, L. *Chemical Engineering Science* **2009,** 64, (22), 4675-4683.

98 Buscall, R. *Journal of Rheology* **2010,** 54, (6), 1177-1183.

99 Hristov, V.; Takács, E.; Vlachopoulos, J. *Polymer Engineering & Science* **2006,** 46, (9), 1204-1214.

100 Li, T. Q.; Wolcott, M. P. *Polymer Engineering & Science* **2005,** 45, (4), 549-559.

101 Hatzikiriakos, S. G.; Dealy, J. M. *International Polymer Processing* **1993,** 1, 36-43.

102 Kharchenko, S. B.; McGuiggan, P. M.; Migler, K. B. *Journal of Rheology* **2003,** 47, (6), 1523-1545.

103 Migler, K. B.; Lavallee, C.; Dillon, M. P.; Woods, S. S.; Gettinger, C. L. *Journal of Rheology* **2001,** 45, (2), 565-581.

104 Rosenbaum, E. E.; Randa, S. K.; Hatzikiriakos, S. G.; Stewart, C. W.; Henry, D. L.; Buckmaster, M. D., A New Processing Additive Eliminating Surface and Gross Melt Fracture in the Extrusion of Polyolefins and Fluoropolymers. In *ANTEC'98*, Atlanta, 1998; Vol. 44.

105 Hatzikiriakos, S. G.; Rathod, N.; Muliawan, E. B. *Polymer Engineering & Science* **2005,** 45, (8), 1098-1107.

106 Adesina, A. A.; Hussein, I. A. *Journal of Applied Polymer Science* **in press**.

107 Adesina, A. A.; Hussein, I. A. **submitted**.

109 Hussein, I. A.; Ho, K.; Goyal, S. K.; Karbashewski, E.; Williams, M. C. *Polymer Degradation and Stability* **2000,** 68, (3), 381-392.

110 Vittorias, I.; Parkinson, M.; Klimke, K.; Debbaut, B.; Wilhelm, M. *Rheologica Acta* **2007,** 46, (3), 321-340.

111 Neidhofer, T.; Wilhelm, M.; Debbaut, B. *Journal of Rheology* **2003,** 47, (6), 1351-1371.

112 Hilliou, L.; Wilhelm, M.; Yamanoi, M.; Gonçalves, M. P. *Food Hydrocolloids* **2009,** 23, (8), 2322-2330.

113 Michael, D. G. *Journal of Rheology* **1995,** 39, (4), 697-712.

114 Klein, C. O.; Spiess, H. W.; Calin, A.; Balan, C.; Wilhelm, M. *Macromolecules* **2007,** 40, (12), 4250-4259.

115 Hyun, K.; Baik, E. S.; Ahn, K. H.; Lee, S. J.; Sugimoto, M.; Koyama, K. *Journal of Rheology* **2007,** 51, (6), 1319-1342.

116 Mackay, M. E.; Dao, T. T.; Tuteja, A.; Ho, D. L.; Van Horn, B.; Kim, H.-C.; Hawker, C. J. *Nat Mater* **2003,** 2, (11), 762-766.

117 Tuteja, A.; Mackay, M. E.; Hawker, C. J.; Van Horn, B. *Macromolecules* **2005,** 38, (19), 8000-8011.

118 Emmanuel PG: Polymer Layered Silicate Nanocomposites. *Adv. Mat.*, 1996, 8(1), 29-35.

119 Krishnamoorti R, Vaia RA, Giannelis EP: Structure and Dynamics of Polymer-Layered Silicate Nanocomposites. *Chem. Mater.* , 1996, 8(8), 1728-1734.

120 Wang KH, Chung IJ, Jang MC, Keum JK, Song HH: Deformation Behavior of Polyethylene/Silicate Nanocomposites As Studied by Real-Time Wide-Angle X-ray Scattering. *Macromolecules*, 2002, 35(14), 5529-5535.

121 Wang KH, Xu M, Choi YS, Chung IJ: Effect of aspect ratio of clay on melt extensional process of maleated polyethylene/clay nanocomposites. *Polym. Bull.*, 2001, 46(6), 499-505.

122 Susteric Z, Kos T: Rheological Idiosyncrasies of Elastomer/Clay Nanocomposites. *Appl. Rheol.*, 2008, 18 ,54894.

123 Katsikis N, Koniger T, Munstedt H,: Elongational viscosities of polymethylmethacrylate / nano-clay composites. *Appl. Rheol.*, 2007, 17, 52751.

124 Solomon MJ, Almusallam AS, Seefeldt KF, Somwangthanaroj A, Varadan P: Rheology of Polypropylene/Clay Hybrid Materials. *Macromolecules*, 2001, 34(6), 1864-1872.

125 Hatzikiriakos SG, Rathod N, Muliawan EB: The effect of nanoclays on the processibility of polyolefins. *Polym. Eng. Sci.*, 2005, 45(8), 1098-1107.

126 Adesina AA, Hussein IA: Impact of Organoclay and Maleated Polyethylene on the Rheology and Instabilities in the Extrusion of High Density Polyethylene. *J. Appl. Polym. Sci.*, in press.

127 Lee YH, Wang KH, Park CB, Sain M: Effects of clay dispersion on the foam morphology of LDPE/clay nanocomposites. *J. Appl. Polym. Sci.*, 2007, 103(4), 2129-2134.

128 Krishnamoorti R, Ren J, Silva AS: Shear response of layered silicate nanocomposites. *J. Chem. Phys.*, 2001, 114(11), 4968-4973.

129 Rosenbaum EE, Randa SK, Hatzikiriakos SG, Stewart CW, Henry DL, Buckmaster M: Boron nitride as a processing aid for the extrusion of polyolefins and fluoropolymers. *Polym. Eng. Sci.*, 2000, 40(1), 179-190.

130 Wissbrun KF, Dealy JM: *Melt Rheology and Its Role in Plastics Processing - Theory and Applications* (Springer, 1999).

131 Gu, SY, Ren J, Wang QF: Rheology of poly(propylene)/clay nanocomposites *J. Appl. Polym. Sci.*, 2004(91), 2427-2434.

132 Jin Z, Alexander BM, Joseph DH: Rheological characterization of polystyrene–clay nanocomposites to compare the degree of exfoliation and dispersion *Polymer*, 2005, 46, 8641- 8660.

133 Treece MA, Oberhauser JP: Processing of polypropylene-clay nanocomposites: Single-screw extrusion with in-line supercritical carbon dioxide feed versus twin-screw extrusion. *J. Appl. Polym. Sci.*, 2007, 103(2), 884-892.

134 Ren J, Krishnamoorti R: Nonlinear Viscoelastic Properties of Layered-Silicate-Based Intercalated Nanocomposites. *Macromolecules*, 2003, 36(12), 4443-4451.

135 Jian L, Cixing Z, Gang W, Zhao D: Study on rheological behavior of polypropylene/clay nanocomposites *J. Appl. Polym. Sci.*, 2003, 89(13), 3609-3617.

136 Thierry A, Tolotrahasina R, Médéric P: Rheological investigation of the melt state elastic and yield properties of a polyamide-12 layered silicate nanocomposite *J. Rheol.*, 2005, 49(2), 425- 440.

137 Filipe S, Vittorias I, Wilhelm M: Experimental Correlation between Mechanical Non-Linearity in LAOS Flow and Capillary Flow Instabilities for Linear and

Branched Commercial Polyethylenes. *Macromol. Mater. Eng.*, 2008, 293(1), 57-65.

138 Hussein IA: Melt miscibility and mechanical properties of metallocene linear low-density polyethylene blends with high-density polyethylene: influence of comonomer type. *Polym. Int.*, 2005, 54(9), 1330-1336.

139 Hussein IA, Hameed T, Sharkh BFA, Mezghani K: Miscibility of hexene-LLDPE and LDPE blends: influence of branch content and composition distribution. *Polymer*, 2003, 44(16), 4665- 4672.

140 Usami T, Gotoh Y, Takayama S: Generation mechanism of short-chain branching distribution in linear low-density polyethylenes. *Macromolecules*, 1986, 19(11), 2722-2726.

141 Vittorias I, Wilhelm M: Application of FT Rheology to Industrial Linear and Branched Polyethylene Blends. *Macromol. Mater. Eng.*, 2007, 292(8), 935-948.

142 Filipe S, Becker A, Barroso V, Wilhelm, M: Evaluation of melt flow instabilities of high-density polyethylenes via an optimised method for detection and analysis of the pressure fluctuations in capillary rheometry. *Appl. Rheol.*, 2009, 19, 23345.

143 Klein C, Venema P, Sagis L, van Dusschoten D, Wilhelm M, Spiess H, van der Linden E, Rogers S, Donald A: Rheo-optical Measurements using Fast Fourier Transform and Oversampling. *Appl. Rheol.*, 2007, 17, 45210.

144 Wilhelm M, Reinheimer P, Ortseifer M, Neidhöfer T, Spiess HW: The crossover between linear and non-linear mechanical behaviour in polymer solutions as detected by Fourier-transform rheology. *Rheol. Acta*, 2000, 39(3), 241-246.

145 Hameed T, Hussein IA: Rheological study of the influence of Mw and comonomer type on the miscibility of m-LLDPE and LDPE blends. *Polymer*, 2002, 43(25), 6911-6929.

146 Palza H, Filipe S, Naue IFC, Wilhelm M: Correlation between polyethylene topology and melt flow instabilities by determining in-situ pressure fluctuations and applying advanced data analysis. *Polymer*, 2010, 51(2), 522-534.

147 Vittorias I, Parkinson M, Klimke K, Debbaut B, Wilhelm M: Detection and quantification of industrial polyethylene branching topologies via Fourier-transform rheology, NMR and simulation using the Pom-pom model. *Rheol. Acta*, 2007, 46(3), 321-340.

148 Neidhofer T, Wilhelm M, Debbaut B: Fourier-transform rheology experiments and finite-element simulations on linear polystyrene solutions. *J. Rheol.*, 2003, 47(6), 1351-1371.

149 Wilhelm M: Fourier-Transform Rheology. *Macromol. Mater. Eng.*, 2002, 287(2), 83-105.

150 Bourgeois JR, Peter WB: HDPE. In Epel JN, Margolis JM , Newman S eds. *Engineeered Materials Handbook*, pp. 163 (Metal Park, Ohio USA, 1988).

150 Lohse DJ, Milner ST, Fetters LJ, Xenidou M, Hadjichristidis N, Mendelson RA, Garca Franco CA, Lyon MK: Well-Defined, Model Long Chain Branched Polyethylene. 2. Melt Rheological Behavior. *Macromolecules*, 2002, 35(8), 3066-3075.

151 Chen YL, Larson RG, Patel SS: Shear fracture of polystyrene melts and solutions. *Rheol. Acta*, 1994, 33(4), 243-256.

152 Hatzikiriakos SG, Dealy JM: Role of slip and fracture in the oscillating flow of HDPE in a capillary. *J. Rheol.*, 1992, 36(5), 845-884.

153 Hatzikiriakos SG, Migler KB: *Polymer Processing Instabilities Control and Understanding*. (Marcel Dekker, New York, 2005).

154 Hristov V, Takács E, Vlachopoulos J: Surface tearing and wall slip phenomena in extrusion of highly filled HDPE/wood flour composites. *Polym. Eng. Sci.*, 2006, 46(9), 1204-1214.

155 Becraft ML, Metzner AB: The rheology, fiber orientation, and processing behavior of fiber-filled fluids. *J. Rheol.*, 1992, 36(1), 143-174.

156 Knutsson BA, White JL, Abbas KB: Rheological and extrusion characteristics of glass fiber- reinforced polycarbonate. *J. Appl. Polym. Sci.*, 1981, 26(7), 2347-2362.

157 Schlatter G, Fleury G, Muller R: Fourier Transform Rheology of Branched Polyethylene: Experiments and Models for Assessing the Macromolecular Architecture. *Macromolecules*, 2005, 38(15), 6492-6503.

158 Vega JF, Santamar ÃA, MuÃoz EA, Lafuente P: Small-Amplitude Oscillatory Shear Flow Measurements as a Tool To Detect Very Low Amounts of Long Chain Branching in Polyethylenes. *Macromolecules*, 1998, 31(11), 3639-3647.

159 Michael, DG: J Rheol 1995, 39, 4, 697-712.

160 Achilleos EC, Georgiou G, Hatzikiriakos SG (2002) Role of processing aids in the extrusion of molten polymers. Journal of Vinyl and Additive Technology 8 (1):7-24. doi:10.1002/vnl.10340

161 Adesina AA, Hussein IA (Submitted) Rheology and Enhancement of Extrusion of linear and branched Polyethylenes using low amount of Organoclay. Journal of Applied Polymer Science

162 Adesina AA, Marques PN, Teixeira P, Hilliou L, Covas JA, Hussein IA (Submitted) Rheology and organoclay assisted slip in the extrusion of HDPE using Particle Image Velocimetry. Macromolecules

163 Anastasiadis SH, Hatzikiriakos SG (1998) The work of adhesion of polymer/wall interfaces and its association with the onset of wall slip. Journal of Rheology 42 (4):795-812

164 Barone JR, Plucktaveesak N, Wang SQ (1998) Interfacial molecular instability mechanism for sharkskin phenomenon in capillary extrusion of linear polyethylenes. Journal of Rheology 42 (4):813-832

165 Fujiyama M, Kawasaki Y (1991) Rheological properties of polypropylene/high-density polyethylene blend melts. I. Capillary flow properties. Journal of Applied Polymer Science 42 (2):467-480. doi:10.1002/app.1991.070420219

166 Guadarrama-Medina TdJ, Pérez-González J, de Vargas L (2005) Enhanced melt strength and stretching of linear low-density polyethylene extruded under strong slip conditions. Rheologica Acta 44 (3):278-286. doi:10.1007/s00397-004-0409-0

167 Hatzikiriakos SG, Hong P, Ho W, Stewart CW (1995) The effect of teflon™ coatings in polyethylene capillary extrusion. Journal of Applied Polymer Science 55 (4):595-603. doi:10.1002/app.1995.070550406

168 Hatzikiriakos SG, Kazatchkov IB, Vlassopoulos D (1997) Interfacial phenomena in the capillary extrusion of metallocene polyethylenes. Journal of Rheology 41 (6):1299-1316

169 Hatzikiriakos SG, Migler KB (2005) Polymer Processing Instabilities Control and Understanding Marcel Dekker, New York

170 Hatzikiriakos SG, Rathod N, Muliawan EB (2005) The effect of nanoclays on the processibility of polyolefins. Polymer Engineering & Science 45 (8):1098-1107. doi:10.1002/pen.20388

171 Hill DA, Hasegawa T, Denn MM (1990) On the apparent relation between adhesive failure and melt fracture. Journal of Rheology 34 (6):891-918

172 Hong Y, Coombs SJ, Cooper-White JJ, Mackay ME, Hawker CJ, Malmström E, Rehnberg N (2000) Film blowing of linear low-density polyethylene blended with a novel hyperbranched polymer processing aid. Polymer 41 (21):7705-7713

173 Hong Y, Cooper-White JJ, Mackay ME, Hawker CJ, Malmstrom E, Rehnberg N (1999) A novel processing aid for polymer extrusion: Rheology and processing of polyethylene and hyperbranched polymer blends. Journal of Rheology 43 (3):781-793

174 Hussein IA, Ho K, Goyal SK, Karbashewski E, Williams MC (2000) Thermomechanical degradation in the preparation of polyethylene blends. Polymer Degradation and Stability 68 (3):381-392

175 Kazatchkov IB, Hatzikiriakos SG, Stewart CW (1995) Extrude distortion in the capillary/slit extrusion of a molten polypropylene. Polymer Engineering & Science 35 (23):1864-1871. doi:10.1002/pen.760352305

176 Kazatchkov IB, Yip F, Hatzikiriakos SG (2000) The effect of boron nitride on the rheology and processing of polyolefins. Rheologica Acta 39 (6):583-594. doi:10.1007/s003970000113

177 Kharchenko SB, McGuiggan PM, Migler KB (2003) Flow induced coating of fluoropolymer additives: Development of frustrated total internal reflection imaging. Journal of Rheology 47 (6):1523-1545

178 Larson RG (1992) Instabilities in viscoelastic flows. Rheologica Acta 31 (3):213-263. doi:10.1007/bf00366504

179 Migler KB, Lavallee C, Dillon MP, Woods SS, Gettinger CL (2001) Visualizing the elimination of sharkskin through fluoropolymer additives: Coating and polymer--polymer slippage. Journal of Rheology 45 (2):565-581

180 Migler KB, Son Y, Qiao F, Flynn K (2002) Extensional deformation, cohesive failure, and boundary conditions during sharkskin melt fracture. Journal of Rheology 46 (2):383-400

181 Pruss EA, Randa SK, Lyle SS, Clere TM (2002) Properties of m-LLDPE blown films extruded utilizing boron nitride based polymer process aids. Paper presented at the Proc. ANTEC, Tech. Pap. , San Francisco, CA,

182 Rodríguez-González F, Pérez-González J, de Vargas L, Marín-Santibáñez B Rheo-PIV analysis of the slip flow of a metallocene linear low-density polyethylene melt. Rheologica Acta 49 (2):145-154. doi:10.1007/s00397-009-0398-0

183 Rosenbaum EE, Randa SK, Hatzikiriakos SG, Stewart CW, Henry DL, Buckmaster M (2000) Boron nitride as a processing aid for the extrusion of

polyolefins and fluoropolymers. Polymer Engineering & Science 40 (1):179-190. doi:10.1002/pen.11151

184 Seth M, Hatzikiriakos SG (2001) Combining boron nitride with a fluoroelastomer: An enhanced polymer processing additive. Journal of Vinyl and Additive Technology 7 (2):90-97. doi:10.1002/vnl.10273

185 Seth M, Hatzikiriakos SG, Clere TM (2002) Gross melt fracture elimination: The role of surface energy of boron nitride powders. Polymer Engineering & Science 42 (4):743-752. doi:10.1002/pen.10986

186 Shih CK (1976) Rheological properties of incompatible blends of two elastomers. Polymer Engineering & Science 16 (11):742-746. doi:10.1002/pen.760161106

187 Stewart CW (1993) Wall slip in the extrusion of linear polyolefins. Journal of Rheology 37 (3):499-513

188 Vogel R, Hatzikiriakos SG, Brünig H, Tändler B, Golzar M (2003) Improved Spinnability of Metallocene Polyethylenes by Using Processing Aids. International Polymer Processing (2):67-73

189 Xing KC, Schreiber HP (1996) Fluoropolymers and their effect on processing linear low-density polyethylene. Polymer Engineering & Science 36 (3):387-393. doi:10.1002/pen.10425

190 Yip F, Diraddo R, Hatzikiriakos SG (2000a) Effect of combining boron nitride with fluoroelastomer on the melt fracture of HDPE in extrusion blow molding. Journal of Vinyl and Additive Technology 6 (4):196-204. doi:10.1002/vnl.10253

191 Yip F, Hatzikiriakos SG, Clere TM (2000b) A new processing aid for the extrusion of polyolefins. Journal of Vinyl and Additive Technology 6 (2):113-118. doi:10.1002/vnl.10234

192 Yip K, Rozenbaum EE, Randa SK, Hatzikiriakos SG, Stewart CW (1999) The effect of boron nitride type and concentration on the rheology and processability of molten polymers. Paper presented at the Proc. ANTEC, New York, NY, USA,

VITAE

Name	Ayuba Adegoke Adesina
Date of Birth	April 20, 1973.
Place of Birth	Lagos, Nigeria.
Nationality	Nigerian.
Education	Bachelor of Science in Chemical Engineering University of Lagos, Lagos, Nigeria, **February, 1998.** Master of Science in Chemical Engineering University of Lagos, Lagos, Nigeria, **May, 2002.** Doctor of Philosophy in Chemical Engineering King Fahd University of Petroleum & Minerals, Dhahran, Saudi Arabia**. May, 2011.**
Permanent Address	14, Temidire Street Dopemu Agege, Lagos State, Nigeria
Email Address	ayub_adesina@yahoo.co.uk